# STABILIZATION OF AQUEOUS TWO-PHASE SYSTEMS USING CHARGED NANOPARTICLES

*A Thesis Submitted*

*in Partial Fulfilment of the Requirements*

*for the Degree of*

## DOCTOR OF PHILOSOPHY

*by*


**Chandra Shekhar**

**(2018chz0002)**




**DEPARTMENT OF CHEMICAL ENGINEERING**

**INDIAN INSTITUTE OF TECHNOLOGY ROPAR**


**July, 2023**

## ***Dedication***

*To My father,* ***Mr. Subhash Chandra Shrivastav***

*To My mother,* ***Mrs. Rani Devi***

*To My motherland,* ***Aonla, Bareilly, Uttar Pradesh, India***

*This would have never been possible without their extreme support, trust and love*

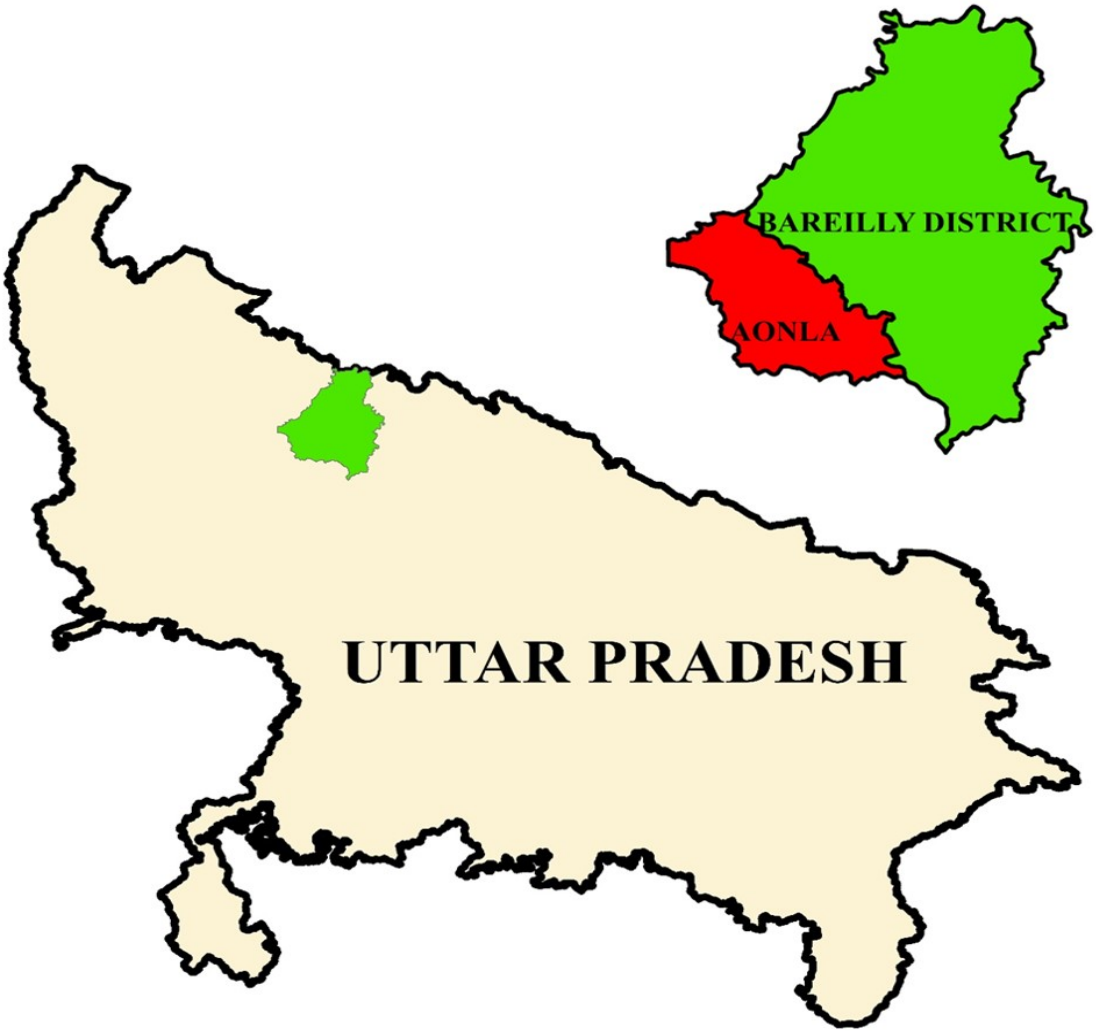


उत्तर प्रदेश; उत्तम प्रदेश...

# Declaration of Originality

I hereby declare that the work which is being presented in the thesis entitled **STABILIZATION OF AQUEOUS TWO-PHASE SYSTEMS USING CHARGED NANOPARTICLES** has been solely authored by me. It presents the result of my independent investigation/research conducted from **July 2018 to July 2023** under the supervision of **Dr. S. Manigandan, Assistant Professor, Department of Chemical Engineering, IIT Ropar**. To the best of my knowledge, it is an original work, both in terms of research content and narrative, and has not been submitted or accepted elsewhere, in part or in full, for the award of any degree, diploma, fellowship, associateship, or similar title of any university or institution. Further, due credit has been attributed to the relevant state-of-the-art collaborations with appropriate citations and acknowledgements in line with established ethical norms and practices. I also declare that any idea/data/fact/source stated in my thesis has not been fabricated/ falsified/ misrepresented. All the principles of academic honesty and integrity have been followed. I fully understand that if the thesis is found to be unoriginal, fabricated, or plagiarized, the Institute reserves the right to withdraw the thesis from its archive and revoke the associated Degree conferred. Additionally, the Institute also reserves the right to appraise all concerned sections of society of the matter for their information and necessary action. If accepted, I hereby consent for my thesis to be available online in the Institute's Open Access repository, inter-library loan, and the title & abstract to be made available to outside organizations.


Signature

Name: **Chandra Shekhar**
Entry Number: **2018chz0002**
Program: **PhD (Doctor of Philosophy)**
Department: **Chemical Engineering**
**Indian Institute of Technology Ropar**
**Rupnagar, Punjab 140001**

**Date: 25 July 2023**

# Acknowledgement

Another chapter and dream of my life are about to be complete with the submission of my PhD thesis, numerous helping hands and genuine advice behind the completion of this thesis work. Firstly, I express my heartfelt gratitude and admiration to my thesis supervisor **Dr Manigandan Sabapathy**, Assistant Professor, Department of Chemical Engineering, IIT Ropar, for his admired guidance, constant cheering throughout the study and tireless help, without which this research work would not have attained its shape. The ocean of his knowledge can not be defined in words, and I feel blessed to have had guidance and command from him during this research work. I am also thankful to **Dr Mamatha**, BDS, for her parental advice and support that helped me grow as a researcher and a better individual.

I thank **Prof. Sarit Kumar Das**, former director of IIT Ropar, and **Prof. Rajeev Ahuja**, Director of IIT Ropar, for their magnificent administration and research environment provided to me during my work at IIT Ropar.

I feel fortunate to have interacted with various heads of the department; **Prof. R.P. Chhabra**, former Head of the Department, IIT Ropar, followed by **Dr Vishwajeet Mehandia**, current Head of the Department, chemical engineering, IIT Ropar, and chairperson of my DC committee, **Dr Venkateshwar Rao Dugyala**, Head of the chemical engineering department, IISER Bhopal. I am grateful to them for their valuable suggestion and evaluation of my work. Additionally, I extend my gratitude to **Dr Vishwajeet Mehandia** and **Dr Venkateshwar Rao Dugyala** for providing valuable inputs as mentors and collaborators of our research group.

It would not be good if I proceed without thanking my DC committee members **Dr Chandi Sasmal, Dr Himanshu Paliwal, Dr Saikat Roy** Assistant Professor, Department of Chemical Engineering, **Dr L. Vijay Anand** Assistant Professor, Department of Civil Engineering, for sharing their inputs and feedback during the DC meetings. They have patiently attended all the DC meetings and allowed me to complete my views by giving me adequate time.

I am sincerely thankful to all the Chemical Engineering department staff members, IIT Ropar - Ms Sunpreet Kaur, Mr Rishabh Semwal, and Mr Sachin, for helping me with all the office-related work.

In this life, I can't forget my friends and colleagues who make our life enjoyable. I am very fortunate to have friends as **Dr Akshar Tripathi**, Assistant Professor, Department of Civil Engineering, IIT Patna, India, **Dr Hreetabh Kishore Shri Vastav**, Visiting Professor, Department of Mechanical Engineering, TTU, USA, and **Ms Sugra Khatoon** Research fellow, ONGC Energy Center, Delhi, India whose cheerful presence always gave

me the energy to face all the challenges in the research and life. I am also very thankful to **Dr Abhimanyu Kiran, Mr Bilal Khan, Mr Faizan Khan, Mr Varun Katiyar, Mr Sahil Rana, Mr Vishal Singh Pawak, Mr Ashin V.K., Mr Abhishek Sri Vastav, Mr Vankar Parnav Vinubhai** and all my lab members (Ms Richa Ranjan, Ms Sangeeta Kumari, Ms Priyanka Saini) for helping to achieve this moment.

Most importantly, I thank my beloved parents for their continuous support and encouragement, especially elder sister **Ms Ruchi Srivastava** and brother **Mr Hari Shanker**.

Last but not least, I extend my gratitude to **"Lord Krishna"** and his almighty for giving me the power to fulfil my dreams and guidance throughout my life.

Kindly excuse me if I missed anyone who contributed to my success due to my low memory.

# Certificate

This is to certify that the thesis entitled **Stabilization of Aqueous Two-Phase Systems Using Charged Nanoparticles**, submitted by **Chandra Shekhar (2018chz0002)** for the award of the degree of **Doctor of Philosophy** of Indian Institute of Technology Ropar, is a record of bonafide research work carried out under my guidance and supervision. To the best of my knowledge and belief, the work presented in this thesis is original and has not been submitted, either in part or full, for the award of any other degree, diploma, fellowship, associateship or similar title of any university or institution. In my opinion, the thesis has reached the standard of fulfilling the requirements of the regulations relating to the Degree.

Signature of the Supervisor

**Dr Manigandan Sabapathy**
Assistant Professor
Deparment of Chemical Engineering
Indian Institute of Technology Ropar
Rupnagar, Punjab 140001

Date: 25 July 2023

# Abstract

Aqueous two-phase system (ATPS) is a liquid-liquid separation technique. This technique represents a mixture of two polymers in an aqueous medium that separates into two clear phases. Interestingly, the interfacial tension between these two separated phases is very low, typically 3 to 4 orders lower than any alkane-water systems. This template-based route finds several applications in various fields such as extraction, separation, drug delivery, cosmetics and bio-medical as purification and enrichment of proteins and membranes. Water-in-Water (w/w) emulsion is a well-known example system of ATPS. In this thesis, an attempt has been made to understand the physics of two-phase systems and the equilibrium structures that can be derived from the stabilized products. The commercial grade positively charged (CL-30) and negatively charged (HS-40) nanoparticles have been utilized as stabilizers. Chapter 3 and Chapter 5 focus on stabilizing thermodynamically incompatible systems such as PEO and dextran mixtures using oppositely charged nanoparticles (OCNPs), while Chapter 4 employed pure nanoparticles of type HS-40 to stabilize w/w emulsions. When the stabilization is achieved using OCNPs, the self-assembly phenomenon is exploited to generate clusters or aggregates of varying sizes and compositions. Therefore, it is envisaged that one can easily tune not just the interfacial area but also the contact angle, as these parameters are linked to the size and composition of the aggregates being adsorbed at the respective water-water interface. This additional flexibility provides more advantages in tuning the Gibbs detachment energy. Apart from stabilizing w/w emulsion droplets, this thesis reports a unique pathway to generate a few novel structures, such as bijels (), emulsion-filled gels, and double emulsions formed due to self-assembly and several other underlying factors.

Chapter 3 illustrates a simple yet straightforward methodology of stabilizing aqueous two-phase systems (ATPS) using OCNPs. When these OCNPs are mixed using an emulsifier, they are known to self-assemble to form aggregates of varying sizes with net positive, net negative, and neutral charges. The interplay of this size and charge nature promotes stronger adsorption by increasing Gibbs detachment energy and yields exciting 3d bi-continuous network channels, i.e., bijels, depending on the nature of charged aggregates at a particular experimental regime. It will be shown later in Chapter 3 that the resulting clusters with net zero charge will give rise to the formation of such bijels, while the net positive and negative clusters favour the formation of droplets. A detailed phase diagram has been constructed to demonstrate the influence of nanoparticles' and polymers' composition on the structural transformation from droplet-bijel-droplet. Therefore, creating such a phase diagram based on the empirical study using turbidity and zeta potential measurements to identify a suitable experimental regime for generating bijels without performing any complicated surface modifications is a noteworthy contribution. Several experimental studies reveal that the formation of bijels will be most likely when the parameter M (ratio of weight fraction of positively

charged nanoparticles to negatively charged nanoparticles) is chosen between 0.7-4. Nevertheless, the w/w droplets stabilized by OCNPs showed good resilience under high centrifugal action irrespective of M, while bijels produced in this route remained stable for a long time. The proposed route offers a simple pathway to fabricate the bijels with three-dimensional hierarchical-bicontinuous network channels.

Chapter 4 demonstrates the simple yet straightforward procedure to generate stable w/w emulsions and emulsion-filled gels stabilized by pure HS-40 silica nanoparticles. The rheological studies well support the hypothesis presented in this section. The focus of this chapter slightly shifts to altering the molecular weight of one of the polymers in the emulsion mixtures, i.e., PEO. It will be shown later in this chapter that the increase in the molecular weight of PEO increases the stability of the resulting emulsions owing to a synergistic effect. Like the droplet-bijel-droplet transition shown in Chapter 3 at different M, Chapter 4 also captures a distinct sol-gel transition in a particular experimental regime through repeated experimental studies at different variables such as molecular weights, storage times, and polymer compositions. The phase diagram created using the combination of these variables helps identify the distinct regimes for generating the emulsion-filled gels and w/w emulsion droplets. The time evolution of shear-induced structures reveals that the viscoelastic properties of these emulsion-filled gels correlate directly with storage time, molecular weight, and polymer compositions.

Chapter 5 describes a single-step approach for synthesizing Water-in-Water-in-Water (W/W/W) Pickering double emulsions. The proposed method involves varying both 'M' and the molecular weight of the polymers in both phases. The results indicate that the molecular weight of the PEO and dextran used in the aqueous phase is a crucial parameter in deciding the structural formation of the emulsion and the generation of stable double emulsions. Additionally, this chapter discusses the effect of scalability by batch size on the generation of double emulsions. The findings reiterate that the formation of double emulsions is independent of size (volume of the batch) and dependent on the concentration of nanoparticles used. The proposed method offers a unique methodology of generating double emulsions in single-step with excellent stability for at least 30 days.

This thesis thoroughly investigates the stability and diverse morphological characteristics of aqueous two-phase systems (ATPS) stabilized by charged nanoparticles, unveiling their extensive applications in drug delivery, cosmetics, and other industries. The primary objective was to synthesize and meticulously characterize intricate structures, including bijels, emulsion-filled gels, and double emulsions. These unique structures possess exceptional properties that position them as highly promising candidates for various applications.

**Keywords**: ATPS; OCNPs; Bijels; Emulsion-filled-gel; dobule emulsions; W/W/W

emulsion; W/W emulsion; nanoparticles

# List of Publications

**List of Published Journals Based on Thesis**

1. Droplet-Bijel-Droplet Transition in Aqueous Two-Phase Systems Stabilized by Oppositely Charged Nanoparticles: A Simple Pathway to Fabricate Bijels.
   **Chandra Shekhar, Abhimanyu Kiran, Vishwajeet Mehandia, Venkateshwar Rao Dugyala, and Manigandan Sabapathy***
   Langmuir 2021, 37, 7055-7066.

2. Probing emulsion-gel transition in aqueous two-phase systems stabilized by charged nanoparticles: A simple pathway to fabricate water-in-water emulsion-filled gels.
   **Chandra Shekhar, Sai Geetha Marapureddy, Vishwajeet Mehandia, Venkateshwar Rao Dugyala, Manigandan Sabapathy***
   Colloids and Surfaces A: Physicochemical and Engineering Aspects 670 (2023) 131474.

3. Single-step generation of double emulsions in aqueous two-phase systems.
   **Chandra Shekhar, Vishwajeet Mehandia, Manigandan Sabapathy***
   Physics of fluids (Accepted for Publication). https://doi.org/10.1063/5.0153788

**List of Presentations in Confrences**

1. Delivered an oral talk on "Rheological characterization of aqueous two-phase emulgels" at the **36th European Colloid and Interface Society Conference, Greece (ECIS 2022)** (Mode: Online).

2. Delivered an oral talk on "Emulsion to Emulsion-Filled Gel Transition in Charged Nanoparticles Stabilized Water-in-Water Emulsion" at the **4th National Conference on Advances in Chemical Engineering and Science, Indian Institute of Science Education and Research Bhopal, India (ACES 2023)** (Mode: Offline).

3. Pressented a poster "Droplet-Bijel-Droplet Transition in Aqueous Two-Phase Systems Stabilized by Oppositely Charged Nanoparticles: A Simple Pathway to Fabricate Bijels" at the **36th European Colloid and Interface Society Conference, Greece (ECIS 2022)** (Mode: Online).

4. Pesented a poster "Building Nano-capsules via Nano-particles stabilized water-in-water emulsion route" at the **National Technology Day 2022, Indian Institute of Technology Ropar, India** (Mode: Offline).

# Contents

# List of Figures

# List of Tables

# Chapter 1

# Introduction

## 1.1 Aqueous two-phase systems

Aqueous two-phase systems (ATPS) involve the separation of solutions into distinct liquid phases through phase separation, which is determined by their compositions (Iqbal et al. [1], Hatti-Kaul [2]). This technique emerged as a highly desirable technology for separation processes due to its ability to provide cost-effective and non-toxic isolation, along with fast and large-scale purification capabilities. ATPS offer a one-step process wherein both contaminant components can be removed, simultaneously separating the relevant targeted products. The separation occurs by selectively partitioning the desired products into two separate phases (Tang et al. [3], Rosa et al. [4]). The efficiency of ATPS separation relies on various parameters associated with the properties of the system. By manipulating the intricate physicochemical aspects involved in the partitioning process, ATPS has been effectively utilized in the downstream recovery of biopharmaceutical products.
ATPS phenomenon was accidentally discovered by M. W. Beijerinck in 1896 at the time of mixing starch and gelatin aqueous solutions during some laboratory experiments. In 1950, Per-Åke Albertsson made groundbreaking discoveries regarding the practical applications of ATPS, employing them to accumulate and separate various types of biological materials (Albertsson [5]). ATPS, known for their simplicity, rapidity, and relatively affordable nature, find applications across diverse fields. They can separate smaller particulate matter streams and large volumes, operating continuously with short contact times (Iqbal et al. [1], Yau et al. [6]). From a thermodynamic perspective, the phase separation of an aqueous mixture occurs when the entropic contribution that promotes mixing diminishes compared to the enthalpic penalty opposing it (Gustafsson et al. [7]). However, the mixture undergoes spontaneous phase separation into two immiscible phases once it reaches a critical or high solute concentration (Chao and Shum [8]).

The phase diagram presents a visual representation of the formation of two phases in a mixture and defines the operational range of a specific two-phase system. It acts as a distinctive "fingerprint" for the system under conditions like pH, temperature, and salt concentration. This phase or state diagram offers valuable information, such as the necessary component concentrations to establish a system with two equilibrium phases, the resulting concentrations of these components in the bottom and top phases, and the ratio of fluid volumes (Hatti-Kaul [2]). A phase diagram illustrates a binodal curve that separates

the region of component concentrations capable of forming two immiscible aqueous phases (above the curve) from those that result in a single phase (at and below the curve), as depicted in Figure 1.1. The coordinates along a tie-line represent all possible system compositions, connecting two points on the binodal curve. These points indicate the final concentrations of components in the bottom and top phases. Moving along the tie-line coordinates separates the systems with different final compositions of the respective fluid phases while maintaining the same final concentration of polymers in the bottom and top phases. Furthermore, the binodal curve includes a critical point where the composition and volume of both phases, including the partitioned material, are nearly equal. Notably, three common methods exist for preparing a phase diagram. (Hatti-Kaul [2]),

1. Turbidometric Titration
2. Cloud Point Method
3. Node Determination

Turbidometric titration is an efficient method to determine the binodal curve. When different phases of a mixture cannot mix uniformly, the resulting mixture exhibits turbidity, which allows for a visual measurement of the binodal. A series of systems with known total concentration and mass are prepared. The mixture becomes less turbid when one phase is formed after diluting with the appropriate solvent. The composition of the mixture at the point of transition is calculated and corresponds to a point on the binodal. The cloud-point method adopts a similar methodology. A solution of component 1 is introduced slowly to a known quantity of a concentrated solution containing component 2. At a critical point called the cloud point, the mixture undergoes turbidity, indicating the formation of two phases. The composition before the appearance of two phases is calculated, providing a data point on the binodal. The mixture is subsequently diluted below the cloud point, and the process is repeated. Another method involves determining the nodes for a series of systems, resulting in data points on the binodal. However, these methods have limitations in accuracy when applied to polydisperse polymers. Such polymers exhibit a gradual decrease or increase in turbidity instead of a sharp change, making it challenging to calculate the transition point precisely.

The aqueous two-phase systems contain a more significant amount of water, typically over 80-90% by weight, yielding some unique properties to ATPS than traditional water-alkane systems. ATPS formed with hydrosoluble additives can exhibit high biocompatibility since the two solution phases do not contain organic solvents. Phase separation in ATPS is influenced by factors such as pH, temperature, hydrophobicity, molecular weight and concentration of polymers or salt. However, the impact of salt concentration on ATPS and its underlying mechanisms in phase separation remain poorly explored (Zafarani-Moattar et al. [9]). During phase separation, a drop typically experiences three forces: frictional force, flotation force, and gravitational force. The equilibrium between these forces

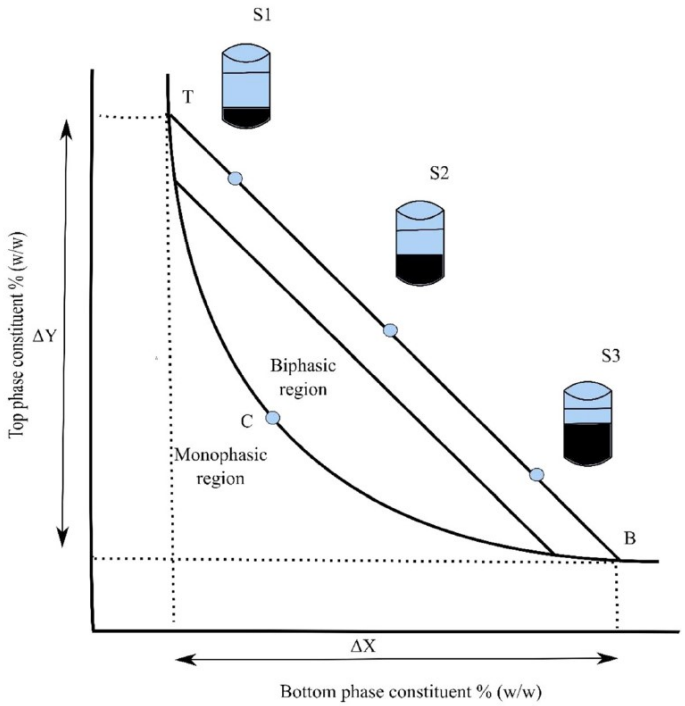


Figure 1.1: Schematic representation of Phase diagram. Reproduce from [(Iqbal et al.2016)] under creative common licence (CCC)

determines the positioning of the drop within the system. The system's density influences the gravitational force, whereas the other two forces are influenced by the flow properties of the phases (Asenjo and Andrews [10], Salamanca et al. [11]). Aqueous two-phase systems can be categorized into various types, including (Iqbal et al. [1]):

1. Polymer-Polymer aqueous two-phase system
2. Polymer-Salt aqueous two-phase system
3. Alcohol-Salt aqueous two-phase system
4. Ionic-Liquid based aqueous two-phase system

### 1.1.1 Polymer-Polymer aqueous two-phase system

Polymer-polymer aqueous two-phase systems (ATPS) are versatile liquid-liquid phase separation systems comprising two distinct polymer-rich phases in an aqueous environment, as depicted in Figure 1.2. In this system, two polymers, often possessing opposite charges or different molecular weights, are mixed in water, resulting in phase separation driven by the thermodynamic incompatibility of the polymers. This mixing leads to forming polymer-rich phases that can be easily separated. These systems have been extensively studied in various scientific domains, including biotechnology, biocatalysis, and protein purification. They offer several advantages for product recovery and purification processes. By creating a favourable and biocompatible environment for biomolecules, polymer-polymer ATPS enable selective partitioning of these molecules

or recovery of valuable products between the two phases based on their affinity for the polymers without requiring extensive downstream processing steps. Moreover, polymer-polymer ATPS can be modulated and optimized by controlling a few parameters, such as polymer types, concentrations, molecular weights, and pH. The partitioning behaviour can be modulated by precisely controlling these factors, enhancing the separation efficiency of specific target molecules or products. Using polymer-polymer ATPS holds great potential in various applications, including protein recovery, enzyme purification, nucleic acid isolation, and other biomolecular separations. Additionally, these systems have been explored for their ability to create advanced materials, such as microencapsulation, nanoparticle synthesis, and drug delivery systems.

### 1.1.2 Polymer-Salt aqueous two-phase system

Polymer-salt aqueous two-phase systems (ATPS) are liquid-liquid phase separation systems with polymer-rich and salt-rich phases in an aqueous environment, as depicted in Figure 1.2. In this system, a water-soluble polymer and a salt are combined, resulting in two distinct phases with varying compositions and properties. Adding salt to the polymer solution induces phase separation through the salting-out effect, reducing the polymer's solubility and forming immiscible phases. The polymer-rich phase typically contains a higher concentration of polymer, while the salt-rich phase contains a higher concentration of salt. These systems have extensive applications in diverse scientific fields, including biotechnology, separation processes, and biocatalysis. They offer several advantages for separating and purifying biomolecules and other compounds. The aqueous-based environment provided by these systems is compatible with many biological materials. Moreover, phase separation can be easily controlled by adjusting the concentrations of the polymer and salt and the solution conditions such as pH and temperature. Polymer-salt ATPS has been widely used to separate and purify enzymes, nucleic acids, proteins, and other biomolecules. The selective partitioning of target compounds between the two phases allows for efficient separation without the need for complex downstream processing steps. Additionally, these systems have shown promise in extracting bioactive compounds from natural sources, such as plant extracts or fermentation broths.

### 1.1.3 Alcohol-Salt aqueous two-phase system

Alcohol-salt aqueous two-phase systems (ATPS) are liquid-liquid phase separation systems in which alcohol-rich and salt-rich phases are formed in an aqueous environment, as illustrated in Figure 1.2. These systems combine alcohol (such as ethanol or isopropanol) with salt, resulting in two distinct phases with unique compositions and properties. Adding salt to the alcohol solution induces phase separation through the salting-out effect, which reduces the solubility of the alcohol. This type of separation leads to two immiscible phases, with the alcohol-rich phase containing a higher alcohol concentration and the salt-rich phase containing a higher salt concentration. Alcohol-salt ATPS has found extensive applications, including extraction, separation, and purification processes. These

systems provide a relatively mild and non-toxic environment, making them compatible with various organic compounds and biomolecules. They are beneficial for extracting bioactive compounds from natural sources, such as plants, algae, or microbial cultures. The selective partitioning of target compounds between the two phases allows for efficient extraction without complex and energy-intensive procedures. The composition and properties of the ATPS can be adjusted by varying the concentrations of the alcohol and salt, as well as the solution conditions like temperature and pH. This flexibility enables the optimization of the system to suit specific applications and desired separation efficiencies.

### 1.1.4 Ionic-Liquid based aqueous two-phase system

Ionic liquid-based aqueous two-phase systems (IL-ATPS) are liquid-liquid phase separation systems that utilize ionic liquids as components that form the phases. As depicted in Figure 1.2, these systems consist of ionic liquid and aqueous phases. In recent years, IL-ATPS have garnered significant attention due to their unique properties and wide range of potential applications in fields such as separation processes, biotechnology, and extraction. Incorporating ionic liquids in ATPS offers several advantages over traditional systems based on polymers or salts. Ionic liquids possess tunable properties such as hydrophobicity, polarity, and viscosity. This tunability allows for precise control of the phase behaviour and selectivity of IL-ATPS, making them suitable for specific separation processes or target compounds. IL-ATPS have been successfully utilized to separate and purify various biomolecules, including enzymes, nucleic acids, and proteins. The distinct solvation properties of ionic liquids enable the selective partitioning of target compounds between the two liquid phases, facilitating extraction and separation without the need for complex downstream processing steps. Moreover, IL-ATPS offer a greener alternative to conventional solvent extraction methods. Ionic liquids are often regarded as environmentally friendly solvents due to their non-flammability, low volatility, and recycling potential. They provide a sustainable and efficient approach to extracting and recovering valuable compounds. The design and optimization of IL-ATPS involve selecting suitable combinations of ionic liquids and aqueous solutions and adjusting factors such as pH, concentration, and temperature. Ongoing research on the thermodynamics and molecular interactions in IL-ATPS continues to expand our understanding, leading to developing of more efficient and tailored systems for specific applications.

## 1.2 Water-in-water emulsion

An emulsion refers to a mixture of two liquids that are immiscible with each other, where one liquid is dispersed in the form of droplets within the other liquid. The emulsion consists of two main components: the dispersed phase and the continuous phase. The dispersed phase is the substance that exists as droplets or particles within the emulsion. It typically represents the minority component and is usually immiscible with the continuous phase (Israelachvili [12]). Take the water-in-oil (w/o) emulsion, where water serves as the

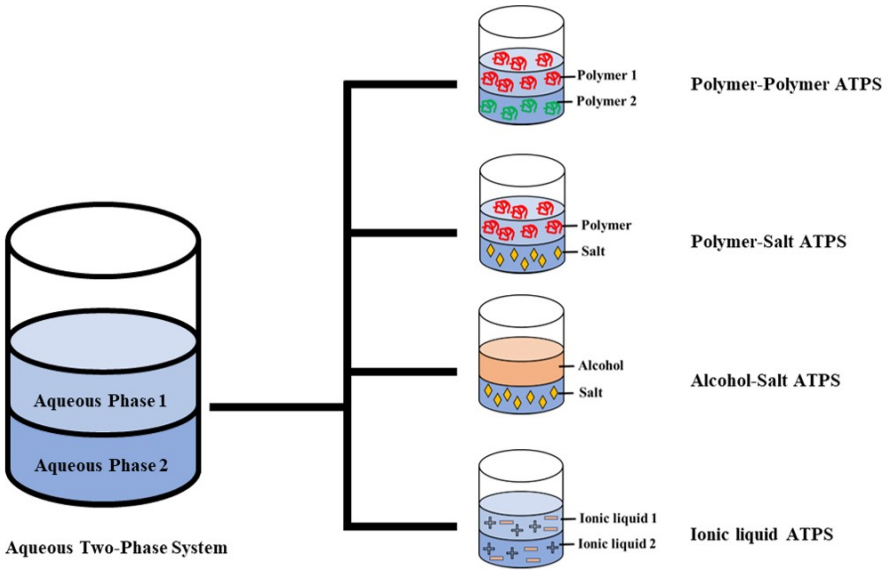


Figure 1.2: Classification of Aqueous Two-Phase Systems

dispersed phase and oil acts as the continuous phase. The continuous phase encompasses and suspends the dispersed phase within it. It represents the predominant component and forms the medium in which the dispersed phase is distributed. In the case of w/o emulsion, the continuous phase comprises oil. Emulsions require an emulsifying agent or emulsifier to form and maintain stability, as Figure 1.3 depicts. Emulsifiers possess both hydrophilic (water-loving) and lipophilic (oil-loving) properties. They function by reducing the surface tension between the two immiscible phases, preventing their separation. Emulsifiers commonly include surfactants, proteins, and specific food additives (Israelachvili [12], Bibette et al. [13]). Emulsions have diverse applications across industries such as food, pharmaceuticals, cosmetics, and painting. They play a crucial role in achieving uniform ingredient distribution, enhancing product stability, and facilitating the delivery of substances that are challenging to mix or administer otherwise (Israelachvili [12], Bibette et al. [13], Tadros et al. [14]). Diverse varieties of stabilizers are available for the stabilization of different types of emulsions. Generally, surface-active compounds or surfactants are widely recognized for their ability to stabilize oil/water or water/oil emulsions.

In 1903, W. Ramsden initially observed that particles could stabilize emulsions in oil-water systems (Ramsden [15]). In 1907, S.U. Pickering proposed the concept of particle-stabilized emulsions in oil-water systems (Pickering [16]). The emulsion mentioned here is called a Pickering or Ramsden emulsion, named after one of the co-discoverers. The phenomenon of particles accumulating at the interface and their stabilizing effect in o/w emulsions has been recognized for over a century and extensively documented in the literature (Aveyard et al. [17], Binks and Horozov [18], Chevalier and Bolzinger [19], Dickinson [20]). Figure 1.3 depicts the stabilization of oil droplets using surfactants and particles. Pickering emulsions maintain the fundamental characteristics of conventional emulsions that rely on surfactants for stabilization. Consequently, Pickering emulsions can be viable alternatives

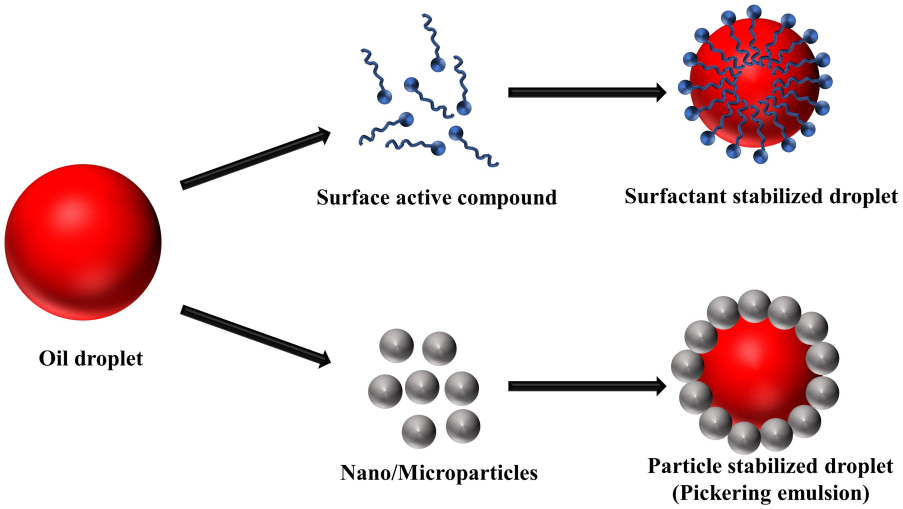


Figure 1.3: Schematic representation of emulsion stabilization

for traditional emulsions in most application scenarios. Their unique attribute lies in the stabilization achieved through solid particles, endowing them with distinctive properties. Notably, their exceptional resistance to coalescence stands out as a significant advantage. The absence of surfactants, rendering them "surfactant-free," makes Pickering emulsions particularly appealing in various fields of application, especially within the domains of cosmetics and pharmaceuticals. Surfactants often exhibit undesirable effects such as irritation and hemolytic behaviour, making Pickering emulsions a preferable alternative route (Albert et al. [21], Melle et al. [22]). Following the remarkable discovery of Pickering emulsion, stabilizing aqueous two-phase systems (ATPS) in water-water emulsion has gained considerable attention. The water-in-water emulsion is a classic example of ATPS and can be formed using polymer-polymer or polymer-salt systems.

Water-in-water (W/W) emulsions are colloidal systems that combine two aqueous solutions containing incompatible macromolecules. This mixture results in the formation of dispersed droplets of one aqueous phase within another aqueous phase. Notably, these emulsions lack an oil phase and rely on intermolecular forces and steric hindrance for stabilization (Frith [23]). Molecular surfactants are ineffective in stabilizing W/W emulsions because the interface between the two phases occurs at scales more significant than the correlation length surfactant molecule. This factor prevents the surfactants from effectively adsorbing and reducing the interfacial tension. Figure 1.4 illustrates the schematic representation of W/W emulsion and the stabilization of droplets using particles in a polymer-polymer emulsion.

In 2008, Poortinga observed that introducing microparticles into w/w emulsions, formed by combining polysaccharides, resulted in the complex aggregation of particles at the interface. This phenomenon enhanced emulsion stability (Poortinga [24]). Later this was confirmed by Firoozmand, Murray, and Dickinson in 2009, who demonstrated that the accumulation of particles at the interface delayed the coarsening process of w/w emulsions created by mixing starch and gelatin (Firoozmand et al. [25]). The stability of such

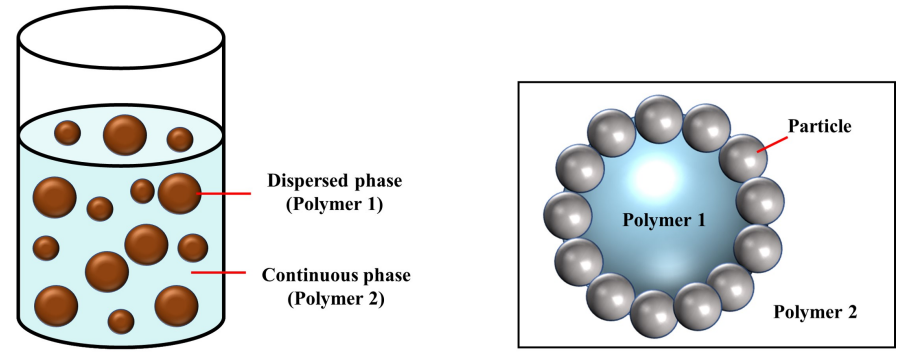


Figure 1.4: Schematic representation of w/w emulsion stabilization

emulsions is maintained by the increased free energy ($\Delta$G) that occurs when particles are present at the interface between two phases, typically liquid-liquid or liquid-gas. These particles become immobilized at the interface and resist coalescence or separation of the phases by increasing the interfacial area between the two phases, which would require the removal of the particles. The interfacial area of a particle located at the interface is in contact with both bulk phases. As a result, the decrease in Gibbs free energy ($\Delta$G) will only occur if the difference in interfacial tension ($\gamma$) between the particle and bulk phase A ($\gamma_{PA}$) and the particle and bulk phase B ($\gamma_{PB}$) is less than the interfacial tension between two fluid phases ($\gamma_{AB}$). This process can be understood using thermodynamic principles related to interfacial phenomena. The reduction of interfacial area upon adsorption of these particles can be used to deduce the change in Gibbs free energy ($\Delta$G) using the formula $\Delta G = \gamma.A$, where $\gamma$ is the interfacial tension, and A is the reduction in interfacial area. Therefore, the equation can be used to determine the free energy change associated with spherical particle adsorption with a given contact angle and radius. The equation describes the interfacial area occupied by spherical particles with a radius of R and a contact angle of $\theta$ with the interface. The area is given by $\pi R^2$(1-cos($\theta$))$^2$.

$$\Delta G = -\pi R^2 (1 - cos(\theta))^2. \tag{1.1}$$

The contact angle between a particle and a phase interface can be described by the balance of intermolecular forces at the interface. Precisely, it is calculated by deducing the difference in interfacial tension between the particle and the bulk phase A ($\gamma_{PA}$) or bulk phase B ($\gamma_{PB}$).

$$cos(\theta) = (\gamma_{PA} - \gamma_{PB})/\gamma_{AB} \tag{1.2}$$

It is assumed that the effects of gravitational forces can be disregarded or considered negligible.

In the context of nanoparticles in O/W emulsions, it has been observed that the difference in Gibbs free energy ($\Delta$G) is significantly larger than the thermal energy ($k_BT$) by several

orders of magnitude; This is true when the difference in interfacial tension ($\gamma_{PA}$-$\gamma_{PB}$) is smaller than the interfacial tension between the particle and the surrounding medium ($\gamma_{AB}$), which is usually the case. However, in W/W emulsions, this effect is less prominent. The lower $\Delta$G, in this case, is because the $\gamma_{A-B}$ between two aqueous polymer solutions is significantly less and ultimately approaches zero at the critical point. Therefore, Firoozmand et al. (2009) have suggested that the gathering of particles at the interface of W/W emulsions occurs as a result of particle depletion from the polymer solutions towards the interface where the solvent concentration is high (Firoozmand et al. [25]). However, practical values of the parameters in equation 1 demonstrate that even in the case of W/W emulsions, the difference in Gibbs free energy ($\Delta$G) can still be substantially more significant than the thermal energy (kT), provided that (i) the particles are of sufficient size and (ii) the mixtures are not close to the critical point. As a result of these unique characteristics, water-in-water emulsions find numerous applications across diverse industries (Yan et al. [26], Esquena [27], Wu and Ma [28]). For instances,

1. **Cosmetics**: W/W emulsions find applications in cosmetic formulations, particularly for products like creams, lotions, and moisturizers. They offer advantages such as enhanced stability, improved sensory properties, and controlled release of active ingredients.

2. **Food and Beverage**: W/W emulsions are used in the food and beverage industry for applications such as encapsulation and controlled release of flavours, aromas, and nutrients. They can create emulsified food products like dressings, sauces, and beverages.

3. **Pharmaceutical and Biomedical**: W/W emulsions have potential applications in drug delivery systems. They can be utilized for the encapsulation and targeted delivery of drugs, providing controlled release and improved bioavailability. They can also be employed in biomedical imaging and diagnostic techniques.

4. **Personal Care Products**: W/W emulsions are used to formulate personal care products like shampoos, conditioners, and hair treatments. They can improve the stability of these formulations and provide unique sensory characteristics.

5. **Agrochemicals**: W/W emulsions find application in the agricultural sector for formulating agrochemicals such as pesticides, herbicides, and fertilizers. They can improve the efficiency and targeted delivery of these substances.

In the following, **Chapter 2** of the study provides a comprehensive literature review on synthesizing water-in-water (W/W) emulsions, specifically focusing on utilizing particles of different shapes, sizes, and charges to achieve unique structures. The review explores the diverse applications of these emulsions in various fields and discusses their potential for future material advancements. **Chapter 3** shifts the focus to the transition of the emulsion to bijel formation. The main emphasis of this chapter is investigating the role

of in-situ self-assembly of oppositely charged nanoparticles (OCNPs) and their impact on morphology formation. A new straightforward approach is proposed to stabilize aqueous two-phase systems (ATPS), which involves commercial-grade Ludox OCNPs. These OCNPs promote self-assembly, forming 2D and 3D aggregates with various sizes and shapes that strongly adsorb at the water-water interface. The chapter highlights the interplay between the size and shape of these aggregates, which results in increased Gibbs detachment energy and modulation of cluster adsorption at the interface. This process enhances stability and provides control over the structural state of the emulsions. The influence of polymer compositions and particle characteristics on the structural transformation from droplet-bigger-droplet is also discussed. A phase diagram is presented to illustrate a single pathway leading to the production of stable bijels or colloidal capsules within the ATPS domain. The chapter concludes that the essential condition for bijel formation is a three-phase contact angle of 90°, which can be achieved by selecting suitable experimental conditions using the phase diagram. This strategy eliminates the need for complicated surface modification procedures reported in the literature. The mechanistic route favouring the formation of bijels and emulsion droplets under different experimental conditions is introduced based on empirical studies using turbidity and zeta potential measurements. **Chapter 4** presents a novel and straightforward synthesis methodology to prepare emulsion-filled gels stabilized by charged silica nanoparticles in aqueous two-phase systems (ATPS). Binary aqueous polymer solutions (polyethene oxide and dextran) are chosen to prepare the emulsion, which separates into two immiscible phases beyond specific concentrations. The rheological properties of these particle-stabilized gels are characterized by varying the concentrations of polymers and the molecular weight of the polymer used in the aqueous phase. Several repeated experimental studies show a distinct sol-gel transition in a specific experimental regime. The time evolution of shear-induced structures reveals that several parameters, such as storage time, molecular weight, and polymer compositions, directly influence the viscoelastic properties of these types of emulsions gels. The emulsion-filled gels prepared using this method exhibit excellent storage stability of up to 60 days. As this process involves an aqueous-based template route for the synthesis, it has numerous potential applications in various fields, including tissue engineering, wound dressing, drug delivery, and soft robotics. **Chapter 5** presents a straightforward, efficient method for producing water-in-water-in-water (W/W/W) Pickering double emulsions. It involves using oppositely charged nanoparticles (OCNPs) to induce the in-situ formation of aggregates that promote the Gibbs detachment energy of particles at the water-water interface. This chapter investigates the influence of polymer molecular weight and particle mass ratio (M) on double emulsion formation. The findings suggest that the interplay between the molecular weight of the polymers and the attachment of OCNP aggregates at the interface of the two-phase system influences the formation of double emulsions. It describes the synthesis of double emulsions using equal molecular weight polymer mixtures (polyethene oxide/dextran) and different M values. Moreover, the double emulsions synthesized using the proposed approach exhibit

excellent stability for up to 30 days. This study is the first reported method for the one-step synthesis of multiple emulsions in an aqueous two-phase system utilizing a Pickering emulsion template. Finally, **chapter 6** is concluded, consolidating the key results of chapters 3-5.

The future of W/W emulsions lies in their ability to enable the design of advanced materials and functional systems across various disciplines. Continued research and development in this area are expected to unlock new possibilities and applications, leading to advancements in diverse fields and addressing societal needs.

# Chapter 2

# Literature Review

This chapter discusses recent advancements in synthesizing different morphologies within water-in-water emulsions. As previously explained in Chapter 1, a water-in-water emulsion is a particle-stabilized aqueous two-phase system in a polymer-polymer mixture. These emulsions exhibit various morphologies, such as bijels, emulsion-filled gels, and double emulsions, which find applications across multiple fields. The reported methods for synthesizing water-in-water emulsions and their diverse morphologies include two approaches: 1) Microfluidics and 2) Mixing (Single-step or two-step processes).

The fortuitous identification of water-in-water emulsions was made by microbiologist Beijerinck in 1896 during his investigation into bacterial growth on starch (Beijerinck [29]). During his experimental investigations, Beijerinck employed hydrolysis with hydrochloric acid to produce water-soluble starch, which was subsequently utilized for bacterial culturing. The observer experienced astonishment upon witnessing the emergence of droplets during the amalgamation of starch solutions and gelatin. Beijerinck, renowned for his inquisitiveness, conducted rudimentary experiments employing iodine dye to examine the emulsions' composition. The user accurately discerned that the emulsions comprised two separate aqueous solutions. In addition, Beijerinck observed that emulsions consisting of starch-in-gelatin or gelatin-in-starch could be obtained, with the specific composition of the emulsion depending on the ratio of the polymers. Furthermore, it was determined by the researcher that the manipulation of both polymers in a solution could effectively regulate the size of the droplets. Interestingly, the author also documented the existence of multiple emulsions, characterized by the encapsulation of tiny starch droplets within bigger gelatin droplets dispersed throughout the starch medium, continuous phase. Beijerinck's publication in 1896 is recognized as the initial scientific documentation of water-in-water emulsions, despite the need for explicit usage of the term in his work. In 1898, Bütschli conducted investigations on a comparable system comprising water, gelatin, and hydrolyzed starch a mere two years after the aforementioned event. Bütschli effectively replicated the process of generating stable liquid droplets; however, he did not extensively explore the intricacies of this phenomenon (Bütschli [30]). In a subsequent scholarly publication in 1910, Beijerinck documented droplet formation within aqueous agar and gelatin mixtures. The user accurately distinguished one phase as abundant in agar but with a limited quantity of starch. In contrast, the other phase exhibited a high starch content but was deficient in agar. Phase separation was observed over a broad spectrum of polymer concentrations. The process of droplet coalescence exhibited a

sluggish rate, thereby facilitating the creation of droplets that maintained their dispersion state (Beijerinck [31]).

In 1907, S. U. Pickering, along with Ramsden in 1903, made a significant discovery by demonstrating that particles can serve as effective stabilizers for emulsions, surpassing the stability provided by traditional surface-active compounds (Ramsden [15], Pickering [16]). After that, the particle-stabilized emulsion was sequenced as Pickering or Ramsden emulsion in honour of them. This remarkable beginning brought attention to water-in-water emulsions for various applications. There is growing interest in utilizing particles of different shapes and sizes to enhance stability and achieve diverse structures within water-in-water emulsions (Esquena [32, 27]). Although several approaches have been reported in the literature for the efficient stabilization of water-in-water emulsions, there still needs to be a simple yet straightforward method to ensure the stability and scalability of the system.

## 2.1 Synthesis of water-in-water emulsion

In the context of the w/w emulsion stabilization, Poortinga [24] (2008) proposed the first particle-stabilized w/w emulsion with the mixture of incompatible polysaccharides. Furthermore, these authors noted that it increases the stability of the formed emulsion. They also reported that the low interfacial tension favours the formation of the tubular structure of the emulsion. Firoozmand et al. [25] (2009) first proposed the bijel structure formation in gelatin and oxidized starch system; the particles tend to concentrate at the interface between the liquid phases and affect the coarsening process of the microstructure. The interfacial regions with a high concentration of particles exhibit significant variations in local curvature, indicating the presence of a viscoelastic boundary between the two liquids. Firoozmand et al. [33] (2009) conducted small-deformation rheology and confocal microscopy experiments on high-sugar gel samples composed of gelatin and oxidized starch, which exhibit thermodynamic incompatibility. The experiments were conducted by manipulating the heating duration and temperature during the gel preparation. As a result, the produced gels exhibited distinct storage modulus ($G'$) values and varying degrees of phase separation. The relationship between the $G'$ and the degree of gelatin crosslinking was observed to be affected by the thermal processing conditions. Increasing the starch content resulted in gels with lower $G'$ and increased phase separation. Van den Berg et al. [34] (2009) demonstrated the first soft gel synthesis in the protein and polysaccharide system using a cold gelation process. The resulting gel structure exhibited heterogeneity, comprising protein beads enveloped by serum pools that contained spherical domains enriched in proteins, referred to as protein beads.

Jansen and Harting [35] (2011) introduced a simulation algorithm that integrates a multi-component "lattice Boltzmann" model and molecular dynamics. This algorithm

was employed to examine the impact of microscopic particle-particle and fluid-particle interactions on the macroscopic rheology of particle-stabilized emulsions. The model presented in their study accommodates a diverse set of fluid properties and allows for the consideration of arbitrary contact angles on the surfaces of particles. Through the examination of the transformation process from a "bicontinuous interfacially jammed bijel" to a "Pickering emulsion", this study aims to gain a deeper understanding of the underlying mechanisms and dynamics involved in this transition. The researchers investigated the influence of particle concentration, solvent ratio, and contact angle ($\theta$) on this transition. After that, Balakrishnan et al. [36] (2012) determined the particles' $\theta$ at the interface of dextran and PEO droplets using latex particles as the stabilizer for w/w emulsion. He reported that the particle trapped at the interface showed a $\theta$ around $145^o$ at the interface of a dextran-formed droplet in the PEO continuous medium using a microscopic approach. They also reported that the fusion of droplets leading eventually to macroscopic phase separation. Buzza et al. [37](2013) demonstrated the formation of polymersome-like structures by employing triblock block copolymers to stabilize w/w emulsions within the context of PEG-dextran ATPS. They observed that the stabilized emulsion droplets exhibited sizes ranging from 5 to 200 $\mu$m and remained stable for extended periods.

Further, Nguyen et al. [38] (2013) demonstrated the utilization of protein particles in the form of a monolayer at the interface between dextran/PEO to stabilize the w/w emulsion. These authors found that native proteins, due to their small size, were unable to stabilize the emulsion effectively. Also, the droplet size decreased with increasing particle concentration but reached saturation at approximately 30%. Firoozmand and Rousseau [39] (2014) demonstrated the utilization of unicellular microorganisms as micron-sized colloidal particles within biopolymer solutions to create innovative morphologies/structures, such as edible bijel-like structures. The rheological properties of gelatin-maltodextrin gels are altered by these microbes, which mitigates the decrease in storage modulus ($G^{'}$) commonly observed during phase separation and salt addition. Through the manipulation of the relative quantities of these microorganisms, it becomes feasible to generate gels exhibiting a wide range of microstructural characteristics and adjustable rheological attributes. Including cell-containing gels in the repertoire of food gel types introduces novel microstructures and customizable rheological properties. Dewey et al. [40] (2014) demonstrated the bioreactors with semipermeable and size-controlled interiors using liposome-stabilized all-aqueous emulsions. These bioreactors were achieved through the implementation of liposome-stabilized all-aqueous emulsions. Within this particular system, aqueous droplets rich in dextran are dispersed throughout a continuous aqueous phase rich in polyethylene glycol (PEG). The PEGylated and negatively charged liposomes exhibit adsorption at the interface, impeding droplet coalescence. They confirmed the stability and integrity of the liposomes at the interface. The emulsion is electrostatically stabilized due to inter-droplet repulsion, even with submonolayer

liposome coatings. The permeability of the droplets allows the diffusion of RNA and DNA molecules, with their concentrations regulated by partitioning.

Murray and Phisarnchananan [41] (2014) demonstrated that the addition of silica nanoparticles in polysaccharide-polysaccharide systems affects phase separation. The nanoparticles preferentially interact with starch domains rather than the gum phase. As the hydrophobicity and concentration of the particles increase, aggregation occurs within the starch domains and possibly at the water-in-water (W/W) interface between the phases. Vis et al. [42](2015) demonstrated that thin plate-like particles are capable of stabilizing w/w emulsions, which is challenging due to low interfacial tension between the water phases. These particles can effectively block the interface with their strong surface activity. Interestingly, the amount of interface blocked by the nanoplates is not affected by the equilibrium contact angle ($\theta$) at which the water interface contacts the nanoplates, except when $\theta$ is 90°. It comes to say that nanoplates have stronger adsorption than spheres of the same size, except under specific conditions.

Nguyen et al. [43] (2015) conducted a study on the topic mentioned. The study indicated that microgels with pH sensitivity could enhance the stability of water-in-water (W/W) emulsions within a defined pH range, thereby enabling the manipulation of emulsion stability through pH adjustments. The microgels exhibit inherent interface coverage between the dextran and PEO phases over a broad pH range ranging from 5 to 8. Nevertheless, they successfully stabilize the water-in-water emulsions within a limited pH range close to the physiological pH. It should be noted that the stability range of these emulsions shifts towards lower pH values when a small quantity of monovalent salt is introduced. The microgels experience substantial swelling beyond a critical pH value, although the alterations in emulsion stability cannot be exclusively ascribed to the fluctuations in size. The potential influence of the interplay between microgels at the interface and the mechanical characteristics of the microgel layer is expected to be significant. Moreover, a variation in stability was observed between emulsions of PEO-in-dextran and dextran-in-PEO, which emphasizes the importance of interface curvature. In addition, changes in pH or the introduction of electrolytes can induce the spontaneous migration of nonadsorbed microgel particles from the polyethylene oxide (PEO) phase to the dextran phase. Cacace et al. [44] (2015) demonstrated the utilization of liposomes to stabilize all-aqueous emulsion droplets as artificial mineralizing vesicles (AMVs). The functionality of these biomimetic microreactors is achieved by allowing the introduction of precursors while preserving a protein catalyst. This biomimetic functionality is accomplished by separating the protein catalyst between internal and external polymer-rich phases, facilitated by utilizing small molecule chelators with moderate binding affinity. Significantly, the process of mineral deposition took place solely within the interior of the AMV, with the assistance of compartmentalized urease. The entire population of AMVs exhibited uniform particle formation of multiple

submicrometer amorphous $CaCO_3$ particles. The present study showcased a novel technique involving an all-aqueous emulsion-based methodology to produce biomimetic vesicles capable of facilitating substantial mineral deposition. This approach can be customised further to enable enzyme-catalyzed synthesis of diverse materials through metal ion, enzyme, and chelator alterations.

de Freitas et al. [45] (2016) found that the phenomenon of segregative phase separation takes place in mixtures comprising amylopectin (AMP) and xyloglucan (XG). In this system, protein particles could stabilize water-in-water emulsions within the pH range of $\leq$ 5.0. At elevated pH levels, the affinity of $\beta$-lactoglobulin ($\beta$-LG) microgels towards the AMP phase was more pronounced than the XG phase. As a result, the microgels were hindered from entering the interface between the two polysaccharide solutions. Nevertheless, when the pH level drops below 5.5, XG exhibits an affinity for $\beta$-LG microgels, impeding their extensive aggregation near the protein's isoelectric point. This phenomenon enhances the microgels' attraction to the XG phase, facilitating their penetration into the interface and subsequent stabilization of the emulsions. When the volume fraction of AMP is elevated, there is a tendency to form sizable droplets of AMP, which subsequently settle into a densely arranged stratum, interspersed by thin layers of XG. Adding a 50 mM sodium chloride (NaCl) electrolyte exerts negligible influence on the characteristics of the mixtures. The ability of particles to stabilize w/w emulsions can be modified through the adsorption of polysaccharides onto their surfaces, forming core-shell particles. This alteration results in a modification of the interplay between particles and their interaction with both phases, consequently modifying the properties exhibited by particle-stabilized emulsions. Peddireddy et al. [46] (2016) were the first to provide evidence that nanorod-shaped cellulose nanocrystals (CNCs) can serve as an effective stabilizer for water-in-water (W/W) emulsions. The surface coverage of CNCs was determined through confocal microscopy and static light scattering techniques. The researchers observed that adding a concentration of 50 mM NaCl and an excess of CNCs in the continuous phase resulted in the formation of weak gels. These gels effectively prevented the creaming of the dispersed phase. According to their report, the non-toxic properties, sustainability, and affordability of CNCs, in conjunction with the ample availability of cellulose, render them exceptionally well-suited for the formulation of water-in-water emulsions. Gonzalez Jordan et al. [47] (2016) studied the effect of different morphologies of the protein on the w/w emulsion stabilization, including rod-like fibrils, homogeneous spheres, and fractal aggregates. In this study, it was observed that fibrils exhibited a higher degree of efficacy in stabilizing PEO droplets within a continuous dextran phase at a pH of 7.0, whereas fractals demonstrated comparatively lower effectiveness. In contrast, the coalescence of dextran droplets within a continuous medium, i.e., the PEO-rich phase, occurred rapidly, irrespective of the type of protein particles employed. Coalescence was observed to be inhibited at a pH of 3.0, except in the case of emulsions containing fibrils. The emulsions, which were stabilized by fractals,

exhibited a reduced rate of creaming or sedimentation at a pH of 3.0. This deficiency can be attributed to minuscule droplets forming within the emulsions. According to their report, the efficacy of stabilization is influenced by factors such as particle morphology, phases, and the system's pH. The distribution of proteins between the two phases, which is significantly influenced by the pH, is likely a crucial determinant.

Soltani and Madadlou [48] (2016) conducted a study on the enrichment of zein particle-based materials. The utilization of pectin at elevated concentrations in Pickering emulsions resulted in prolonged stability for the emulsions. The process of cross-linking pectin resulted in the conversion of emulsions into self-supporting gels, which have the potential to serve as effective vehicles for delivering fish oil and calcium. Welch et al. [49] (2017) employed mean-field theory and a Landau-Ginzburg model to obtain a self-sustenance expression for the particle density at the jammed interface in bijels. This expression facilitates an approximate quantitative analysis of the necessary conditions for forming bijels. The findings are consistent with empirical observations and intuitive comprehension, highlighting the significance of overall particle concentration in influencing dynamics and morphology. Gonzalez-Jordan et al. [50] (2017) demonstrated the formation of soft gels in a system consisting of dextran and polyethylene oxide (PEO). This gelation process was achieved by incorporating minute quantities (0.5 wt%) of fractal aggregates or microgels derived from $\beta$-lg protein. The protein particles undergo aggregation and subsequently assemble into a compact, gelatinous film when exposed to a pH range of 6 to 3.5 in the presence of 0.3 M NaCl. The process of aggregation results in the coalescence of droplets, thereby causing the creaming of PEO droplets or the settling of dextran droplets. The surplus protein particles primarily accumulate within the dextran phase, forming substantial clusters or a network that extends across the continuous dextran phase, encapsulating the PEO droplets. The network formation process in this context impedes the phenomenon of creaming in PEO droplets, resulting in the formation of weak gels that can sustain their weight.

Collini et al. [51] (2018) reported the shake gel synthesis with PEO and silica particles at higher concentrations of the particles (25 wt%) in the system. They observed that the gelation time showed a wide range, ranging from seconds to over an hour, and was greatly influenced by shear rate. A peak in gelation time was observed at polymer concentrations in the range between 0.35-0.40% and a temperature around 20°C. Elevated temperatures significantly expedited the gelation time, as kinetic effects became more dominant over thermodynamic and structural resistances to gel formation. Singh et al. [52] (2018) shows the NaCMC-gelatin system and investigated as a potential matrix for encapsulating probiotic bacteria. The results indicate that at certain polymer concentrations, a separate phase forms, allowing the creation of W/W emulsions. Notably, stable emulsion droplets were observed without significant sedimentation. Although slow sedimentation may occur due to the system's low-density difference and high viscosity in these w/w emulsions.

Liu et al. [53] (2018) devised a straightforward and effective approach to generate W/W droplets through the utilization of an integrated microfluidic platform. This methodology facilitates the facile production of aqueous droplets containing varying concentrations and molecular weights of dextran and PEG, obviating the requirement for pre-mixing. Droplet size control can be achieved by manipulating flow rates for both phases and the valve switch cycle. Zhang et al. [54] (2018) conducted a study on the utilization of polydopamine nanoparticles (PDP) as stabilizers in aqueous emulsions composed of dextran and poly(ethylene glycol) (PEG). These biocompatible materials can generate stable emulsions that can be disrupted through dilution or the introduction of surfactants. The stability of emulsion droplets is enhanced by cross-linking polydopamine (PDP) with poly(acrylic acid) and carbodiimide, forming a structure resembling colloidosomes. Following the cross-linking process, the emulsions exhibit enhanced resistance to demulsification when subjected to dilution or the addition of surfactants. The formation of aqueous emulsions through the use of PDP (phase separation-induced demulsification) can be utilized in a wide range of water-in-water emulsions containing diverse polymers. This diversity presents novel opportunities for surface modification and microencapsulation. Gonzalez-Jordan et al. [55] (2018) demonstrated that the preference for particles could be modified to significantly favour the polyethylene oxide (PEO) phase when protein is absent but can shift to favour the dextran phase when there is an excess of protein. The particles demonstrate optimal emulsion stabilization when they prefer the continuous phase, resulting in outward protrusion from the droplets. Intermediate coverage enables the stabilization of both dextran-in-PEO emulsions and PEO-in-dextran emulsions. Ben Ayed et al. [56] (2018) conducted a study on w/w emulsion gel. Gels can be formed by inducing particle aggregation, which imparts stability to prevent droplet coalescence. The manipulation of particle concentration allows for the modulation of the elasticity of gels. Weak gels that hinder the separation of droplets but still exhibit flow under the influence of gravity are observed at lower concentrations. Increased concentrations result in the formation of more robust gels capable of providing structural support for their mass. A network is established in the presence of a slight surplus of particles, wherein thin layers of particles interconnect droplets. Particle aggregates form a network structure in which droplets are embedded when there is a greater surplus. Droplets exert a notable influence on the stiffness of gels, particularly in the case of weak gels characterized by a lower abundance of surplus particles. The control of particle aggregation can be modulated by introducing salt, a critical factor in attaining the intended gel characteristics.

Binks and Shi [57] (2019) conducted a study in which W/W emulsions were synthesized, both with and without the incorporation of conventional emulsifiers. Various surfactants, including ionic and nonionic varieties, were examined alongside a polymer and various solid particles, such as hydrophilic calcium carbonate particles and wax microspheres.

However, a stable emulsion could not be successfully formed despite these efforts. Nonetheless, dichlorodimethylsilane-modified nano-sized silica particles were effectively utilized to create stable W/W emulsions of both polymer-in-salt and salt-in-polymer types. The utilization of partially hydrophobic fumed silica as an emulsifier resulted in the maintenance of complete stability in the emulsions for a duration exceeding one year. Furthermore, the degree of particle hydrophobization was correlated with the emulsions' properties, as determined by contact angle measurements. Furthermore, a series of systematic investigations were carried out to examine various overall compositions, with the aim of correlating alterations in emulsion type and stability with the phase diagram. The decrease in emulsion stability and subsequent coalescence were observed as the conditions approached phase inversion.

Pavlovic et al. [58] (2020) introduced a novel approach to produce temperature-responsive W/W emulsions through the utilization of custom-designed block copolymers. The copolymers are composed of two constituents, namely PDMA and PDEA. The PDEA block exhibits a response to variations in temperature. The researchers observed that the copolymers demonstrated effective stabilization of W/W emulsions composed of PEG (with a molecular weight of 35000 Da) and dextran (with a molecular weight of 40000 Da) at temperatures exceeding a specific critical temperature ($T_{cp}$). Nevertheless, the emulsions rapidly underwent phase separation when the temperature fell below the critical temperature ($T_{cp}$). Tea et al. [59] (2020) examined the viscous and rheological properties of the w/w emulsions. The authors indicated that the viscosity of w/w emulsions becomes less significant at a particular shear rate due to droplet deformation and alignment. The droplets experience rupture and subsequent coalescence at elevated shear rates, forming thinner strands. Upon cessation of the flow, the aforementioned strands undergo fragmentation, forming smaller droplets that promptly merge to form larger droplets.

Wang et al. [60] (2021) proposed a novel microfluidic system capable of fabricating hydrogel fibres filled with equidistant aqueous droplets (ADHFs) in a single step. This system relies on carefully designed pump valve cycles and immiscible liquids with a stable aqueous interface. By adjusting the flow rates of the three phases and the valve switch cycle, the architecture of the ADHFs can be flexibly controlled. The resulting ADHFs demonstrate excellent controllability, uniformity, biocompatibility, and stability. Kulkarni and Mani [61] (2021) show the synthesis of w/w emulsion using dextran and PEO polymers and stabilized by the oppositely charged particles. They observed that positively (+) charged particles chose the dextran-rich phase, while negatively (-) charged particles were confined within the continuous phase, i.e., the PEO-rich phase. The interface revealed that the OCP aggregates were attached to the dextran droplet interface, but droplet coalescence and sedimentation occurred over time. The average droplet diameter decreased slightly, indicating that the destabilization was due to droplet

sedimentation. Zhang et al. [62] (2021) studied the stability of dextran/HPMC under different environmental conditions, focusing on the behaviour of interfacial protein microgels. The formed emulsions remained stable at pH $3-5$ but destabilized at higher pH values, causing the microgels to move into the continuous phase. The emulsions also maintained stability at high ionic strength levels, although incomplete coverage of microgels on HPMC droplet surfaces was observed at ionic strengths above 100 mM. The emulsions stabilized by protein microgels exhibited thermal stability, but heat treatment at 90°C partially fused protein particles on the droplet surface.

Wang et al. [63] (2022) proposed the use of w/w emulsions as stable sliding surface fluids (SSFs) stabilized by collagen nanofibrils. Formed emulsions demonstrate excellent stabilization due to strong surface activity and increased degree of surface coverage of the given nanofibrils. The superior lubrication performance is attributed to the viscosity of the W/W emulsion, absorption of emulsion droplets on interfaces, hydration layers of collagen, and contact pair deformation. Wang et al. [64] (2022) presented a multilayer-stabilized w/w emulsions consisting of PEG/dextran with the addition of DNA strands. The emulsions exhibit ring-like structures, which can be explained using a nanofluid film model. The behaviour of the emulsions, including stability and interfacial tension, can be controlled by the type and concentration of DNA strands and the volume fraction of the dispersed phase. These findings could expand the creation of novel emulsions for various applications, such as emulsion polymerization and DNA transport using w/w emulsion templates. Coudon et al. [65] (2022) demonstrated a stable and impenetrable w/w emulsions by forming bilayers at the interface of dextran-rich droplets using the surface active agents such as a mixture of sodium oleate/1-decanol. These impermeable and stable emulsions were achieved through segregative liquid-liquid phase separation with PEG. The lipids are self-assembled into multilamellar structures on the droplet surface. The lipid-based membrane prevented the passage of low molecular weight dyes, oligonucleotides, and proteins, enabling strict encapsulation of chemicals within the droplets prior to membrane formation. Machado et al. [66] (2022) prepared w/w emulsion by mixing pullulan (PUL) and amylopectin (AMP) solutions in the presence of whey-protein-microgels (MG) and demonstrated that decreasing the pH resulted in a shift in MG preference from the PUL-rich phase to the AMP-rich phase, causing MG binding at the interface. The emulsion morphology and stability varied with pH and the dispersion of AMP droplets in the PUL phase or vice versa. Some emulsions formed weak gels that flowed when tilted, while others had dispersed droplets stabilized by a gelled MG interface layer. Adding anionic polysaccharides, capable of forming complexes with MG below pH 5.6, influenced MG partitioning, emulsion stability, and morphology.

Merland et al. [67] (2022) demonstrated the importance of bis-hydrophilicity using thermoresponsive microgels on the stabilization of W/W emulsions with dextran and PEO. Using sensitive microgels allows for temperature-controlled stability in w/w

emulsions, offering exciting possibilities for encapsulation and release applications. This new class of emulsifiers shows promise for on-demand encapsulation and release of molecules. Plucinski and Schmidt [68] (2022) investigated a new ATPS composed of PDMA and pullulan, where the stability depends on polymer molar mass. The PDMA/pullulan ATPS was utilized to generate w/w emulsions stabilized by polystyrene (PS) nanoparticles or PDMAEMA-b-POEGMA block copolymers in the all-aqueous emulsion mixtures. The emulsion remained stable during and after emulsification, with pullulan occupied inside the droplets and PDMA distributed throughout. The PDMAEMA-b-POEGMA stabilized emulsion showed pH sensitivity, allowing for stabilization or destabilization depending on pH. Qian et al. [69] (2022) showed that the cross-linking of starch nanocrystals (SNCs) leads to increased particle size and improved emulsifying ability, while acetylation reduces particle size and enhances emulsifying efficiency. The two emulsion systems exhibit different phase inversion behaviours, with cross-linked SNCs following a depletion-stabilization mechanism and acetylated SNCs following a diffusion-controlled mechanism.

Lei et al. [70] (2022) synthesized w/w emulsion using dextran and maltodextrin and stabilized with bacterial cellulose (BC) nanofibrils. They observed that increasing the BC surface charge did not significantly affect the droplet size, but it reduced the emulsions' storage modulus ($G'$), loss modulus ($G''$), and viscosity ($\eta$). The stabilization mechanism relied on forming a viscoelastic network structure by BC nanofibrils. Increasing the BC content resulted in smaller droplet sizes, and the BC-stabilized emulsion exhibited excellent stability over seven days. Also, the formed emulsion was unaffected by changes in ionic strength or pH.

Cui et al. [71] (2023) demonstrated that the self-assembled chitosan colloidal particles (CSCPs) could be utilized as an underlying layer to deposit BSA/urease and as a surface-active agent to stabilize P/D emulsions, where BSA/urease was encapsulated at the interface. The prepared P/D emulsions were employed to fabricate drug-loaded nanofibers by spinning the solution. This novel approach allows encapsulating active compounds in w/w emulsions without requiring preferred solubility in the dispersed phase. The study conducted by Zhou et al. [72] (2023) reveals that an increase in the dextran (DEX) concentration reduces emulsion stability while increasing the polyethylene oxide (PEO) concentration results in improved stability. They utilized cellulose nanocrystals (CNCs) to prepare water-in-water emulsions. This CNCs-based DEX-in-PEO emulsion offered a new approach to high-density encapsulation and cultivation of probiotics.

You et al. [73] (2023) investigated the tribological properties of w/w emulsions generated with different combinations of gelatinized starch (GS) and $\kappa$-carrageenan ($\kappa$C), with/without added wheat protein microgels (WPM). The W/W emulsions exhibited shear thinning behaviour and higher viscosity than the individual components. The

morphology of the water droplets influenced the tribological and rheological performance. WPM-stabilized emulsions showed higher bulk viscosity compared to unstabilized mixtures.

Moutkane et al. [74] (2023) presented two methods for creating stable protein-based microcapsules in all-aqueous systems while capturing water-soluble ingredients. The first method utilizes protein-based microgels to stabilize w/w emulsions formed by droplets of a pullulan-rich phase dispersed in an amylopectin-rich phase. The microgels adsorb at the water-water interface, forming a monolayer that can be physically or covalently bonded through chemical treatments. Covalently bonded capsules show higher resistance to dilution, pH changes, and heating. The second method involves an aqueous three-phase system where dextran forms a layer around PEO droplets dispersed in the continuous phase. The protein-based microgels selectively partition to the dextran-rich phase and can be physically/covalently cross-linked. Covalently bonded microcapsules exhibit increased resistance to dilution, pH changes, and heating. Furthermore, this method allows for the formation of microcapsule shells with controlled thickness, enhancing their resistance to deformation.

## 2.2 Synthesis of water-in water-in-water (w/w/w) emulsions

Ziemecka et al. [75] (2011) have successfully developed a continuous method for generating w/w/w microdroplets using aqueous-based polymer solutions. This approach enables the efficient encapsulation of biomaterials in a biocompatible environment without organic solvents. It is a versatile platform for creating stable all-aqueous microstructured systems through the cross-linking of the shell, and the same facilitates the fabrication of complex multicompartment microstructured phases. Without a lipid bilayer as a physical barrier, these core-shell structures can significantly impact synthetic cell studies by allowing biomaterials to easily transfer from the core to the surrounding environment in these all-aqueous two-phase fluids. Sauret and Cheung Shum [76] (2012) developed a simple method to create w/w single emulsions directly. The method involves perturbing the pressure that drives the dispersed phase flow, causing the inner jet to break into droplets through Rayleigh-Plateau instability. This results in the formation of uniform droplets. Modifying a microfluidic device can form w/w/w double emulsions, controlling the number and size of encapsulated droplets. This approach allows for the application of droplet-based microfluidics in aqueous-based two-phase systems. Song and Shum [77] (2012) developed a method to create uniform w/w/w double emulsions via microfluidic devices. By extracting water from these droplets, the solute concentrations increase beyond their miscibility limit, causing the droplet to separate into two immiscible phases. This process leads to the formation of PEG-rich droplets within the initial emulsion.

These PEG-rich droplets merge, resulting in stable w/w/w double emulsions with acceptable consistency. These w/w/w double emulsions are solvent-free and well-suited for specific applications like protein purification, biomaterial fabrication, and biochemical reactions.

Mytnyk et al. [78] (2017) developed a method to continuously produce stable microcapsules consisting of an aqueous core and a permeable hydrogel shell. These capsules are generated by controlling photo-cross-linking of the shell in a w/w/w double emulsions. Unlike previous methods, this approach spontaneously generates double emulsion droplets at a three-dimensional flow-focusing junction using immiscible aqueous polyethylene glycol and dextran solution. The resulting capsules are free of lipids, organic solvents, and surfactants, and they exhibit excellent stability even under harsh conditions such as extreme pH levels and high salinity.

Hann et al. [79] (2017) prepared encapsulated double emulsions through interfacial complexation in aqueous two-phase systems (ATPS). This double emulsion occurs through the rapid formation of rigid membranes composed of polymerized nanoparticles (PE/NP), followed by osmotic pressure-driven water transfer between the phases. They observed the formation of these structures using PE/NP shells of different sizes. These double emulsions exhibit features similar to membrane-less organelles, such as selective compartmentalization, permeability, and compartmentalized reactions. They also incorporated lysozyme, an antibacterial protein, into the shell for encapsulation.

Cui et al. [80] (2017) developed complex emulsions with adjustable droplet shapes by utilizing polyethylene glycol (PEG), polyvinyl acetate (PVA) and dextran. By varying the mass ratio of these components and modifying PEG, one can form emulsion droplets with five different morphologies: single core-double shell, ellipsoid Janus, multicore-in-matrix, binary-core/shell, and core/shell-single-phase Janus. They established a geometry map to understand the formation of these shapes. Extended extraction times can lead to transitions between different morphologies. The formation and transition of complex emulsions are driven by changes in interfacial tensions between the components of the three-phase system caused by concentration changes due to water loss. Each compartment in the complex emulsion can be functionalized based on the specific affinities of PEG, PVA, and dextran to different materials.

Jeyhani et al. [81] (2020) developed a microfluidic hybrid device to form w/w/w double and triple emulsions. Their system combines a conventional flow-focusing geometry with a microneedle and a glass capillary in the given junctions. The proposed configuration enables the focusing of coaxial two-phase streams, eliminating channel-wetting issues commonly encountered. This approach demonstrated the synthesis of stable emulsions in a PDMS-based microfluidic device and offered control over the structure of w/w/w

emulsions. This microfluidic approach provides an easy way to create higher-order biocompatible emulsions, making it promising for various biotechnological applications.

## 2.3 Objectives:

Based on the literature survey conducted in the domain of aqueous two-phase systems or water-in-water Pickering single emulsions, double emulsions, and bijels, the following research gap has been identified as a centre of focus for further investigation:

1. To develop a generalized method for stabilizing water-in-water emulsions using commercially available oppositely charged nanoparticles.

2. To gain a comprehensive understanding of the impact of variables such as molecular weight, polymer compositions, and storage duration on the stability of emulsions and the underlying structural developments resulting from the emulsification of aqueous two-phase systems.

3. To perform systematic rheological investigations to probe structural transition at a particular experimental regime.

4. To systematically characterize the as-generated emulsion products stabilized by the charged nanoparticles.

# Chapter 3

# Droplet−Bijel−Droplet transition in aqueous two−phase systems stabilized by oppositely charged nanoparticles: A Simple pathway to fabricate bijels

This chapter demonstrates a simple pathway for the synthesis of bijel, showing the structural transition from droplets to bijel, using commercial-grade oppositely charged nanoparticles (OCNPs) as a ready-to-use approach for various applications. The emulsification using OCNPs leads to forming the self-assembly, which subsequently produces 2d and 3d clusters of aggregates of more significant sizes. Since the resulting clusters are bigger than the individual nanoparticles, they promote strong adsorption at the water-water interface. By tuning the mass ratio (M) of these nanoparticles, the size and shape of the formed clusters can be changed, promoting stability due to increased interfacial area and, thereby, the Gibbs detachment energy. Eventually, this strategy helps promote the adsorption and the desired state of microstructures formed at the interface. For instance, the tuning of M changes the interfacial area and the three-phase contact angle ($\theta$), as these two aspects are linked to the size and composition of resulting clusters formed due to self-assembly. Therefore, one can modulate the stability and, simultaneously, the $\theta$ to obtain desired microstructures such as droplets and bijels depending on M. It can be shown later in this chapter that at a suitable M, one can quickly achieve the essential condition, i.e., $\theta = 90°$, for generating bijels. Moreover, this chapter predicts the mechanistic route favouring the bijel and droplet formation at respective M based on empirical studies using turbidity and zeta potential measurements. It will be shown later in this chapter that the formation of bijels will be favoured when M (ratio of weight fraction of positively and negatively charged nanoparticles) is chosen between 0.7-4. The emulsification in these regimes of M favours the formation of bijels. At the same time, the droplets emerge at the rest of M. It should also be noted that the droplets and bijels stabilized by OCNPs remained stable for at least 30 days. Also, although the droplets became slightly elongated, the formed droplets displayed good mechanical stability when subjected to high centrifugal force. Thus, this chapter proposes a single-step

yet straightforward approach for synthesizing bijels (a hierarchical network structure) and droplets in w/w emulsion.

## 3.1 Introduction

Phase separation in an aqueous solution containing polymer mixtures is a common phenomenon. Most hydrophilic polymers are found to be incompatible, yielding two coexisting phases in aqueous solutions such that each of the phases would be rich in one of the polymer types, in addition to water. Such two-phase systems are called aqueous two-phase systems (ATPS). It is important to emphasize that the two-phase separation under discussion does not fall within the category of separations induced by complex coacervation or the presence of salts. These ATPS are often used to fabricate particle-stabilized water-in-water (w/w) emulsion droplets. The use of particle adsorption at fluid-fluid interfaces has been considered to be one of the traditionally adopted approaches to stabilize oil-in-water (O/W) or water-in-oil (W/O), thanks to the discovery of particle-stabilized emulsion droplets by Ramsden [82] (1903), and Pickering [83] (1907), and produce drug carriers such as colloidosomes or microcapsules (Dinsmore et al. [84]). In many situations, such as the encapsulation of oil-sensitive active ingredients and the development of sustainable next-generation low-calorie food products, the oil phase is known to cause deleterious effects. Hence, replacing the oil phase with another suitable aqueous phase is desirable.

Despite the unique challenges offered by w/w emulsion systems, i.e., ultra-low interfacial tension ($1\mu$N/m) and large interfacial zone thickness, several researchers have reported the stabilization of w/w droplets using various types of spherical and non-spherical colloidal particles. Among several studies that involve w/w emulsions, the particles employed for the stabilization are proteins (Nguyen et al. [38]), silica (Murray and Phisarnchananan [41]), and polystyrene (PS) (Firoozmand et al. [25], Balakrishnan et al. [36]). Apart from spherical particles, studies have been conducted to show the stabilization abilities of non-spherical particles such as rod-like (Peddireddy et al. [46]), and plate-like (Vis et al. [42]) particles as well. In general, when the field of emulsion study is considered, the manipulation of particle's size and shape are the major factors in tuning the stability of droplets as they fundamentally affect the magnitude of Gibbs detachment energy of particles (Eq. 3.1), which is the essential requirement for the particles to remain trapped at the interface. Since the interfacial tension ($\gamma_{w-w}$) reported in this case is 3 to 4 orders of magnitude lesser than any conventional o/w or w/o emulsion system, it is imperative to employ fairly larger size particles to compensate for the energy loss. For instance, if we set the required adsorption energy to be $\geq$ 20 $k_BT$ to achieve stronger adsorption at the interface, we need to employ the particles with a diameter minimum of 160 nm for stabilizing w/w emulsions (Vis et al. [42]). However, one has to overcome a few challenges when using larger particles. They include (i) Rapid sedimentation of the particles due to gravity, which leads to early break-down of droplets, and (ii) Rapid exchange of solvent

ions from one phase to another due to large interstitial sites, resulting in the destabilization of emulsion droplets at the early stage.

$$\Delta G_d = \pi r^2 \gamma_{w-w}(1 \pm cos\theta)^2 \tag{3.1}$$

Where $r$ is the radius of the colloidal particle trapped at the interface of two immiscible fluids and $\gamma_{w-w}$ is the aqueous phase 1 - aqueous phase 2 interfacial energy and $\theta$ is the three-phase contact angle, given by Young-Dupre equation (Eq.3.2)(Binks and Horozov [18]).

$$cos\theta = \frac{\gamma_{pw1} - \gamma_{pw2}}{\gamma_{w-w}} \tag{3.2}$$

Wherein $\gamma_{pw1}$ and $\gamma_{pw2}$ are the particle-aqueous phase 1 and particle-aqueous phase 2 interfacial energies, respectively. Besides making colloidosomes, bijels can also be fabricated using the w/w emulsion route, as discussed later. As far as the fabrication of bijels is concerned, various groups have developed several methodologies for preparing bi-continuous structures. Bijels are defined as bi-continuous network-like structures formed when the stabilizer's wettability is nearly the same between the two fluid phases, i.e., $\theta \approx 90°$. In short, bijels can be prepared using one of the following routes: 1) by inducing phase separation in oil-water mixtures and stabilizing the fluid-fluid interfaces using neutrally wetting colloidal particles, 2) by quenching partially immiscible liquids such as alcohol-alkane, 2,6-lutidine-water to induce phase separation via spinodal decomposition. Stratford et al. [85] (2005)have shown for the first time the large-scale computer simulations pertaining to the demixing of binary mixtures containing the densely jammed colloidal particles. Using the lattice Boltzmann method, These authors demonstrated a new class of gels, i.e., bijels, with high tunability in elasticity and pore size. Cai and Clegg [86] (2015) demonstrated a methodology of stabilizing bijels utilizing a mixture of fumed silica nanoparticles. A pair of partially miscible binary liquids, Ethylene carbonate and p-xylene, have been used for the study. This mixture was first heated to 100°C and allowed to quench to induce phase separation. For stabilizing bijels, these authors have shown the use of the secondary clusters obtained by mixing R972 or R812 (more hydrophobic) and H30 (less hydrophobic) fumed silica nanoparticles as stabilizers. In yet another work, Cai et al. [87] (2017) reported another strategy using nanoparticles and molecular surfactants for stabilizing bijels.

The strategy based on the combinations of colloidal particles and surfactants for stabilizing emulsions has been known for many years (Haase et al. [88], Toor et al. [89], Forth and Clegg [90], Huang et al. [91]). The method reported by Cai et al. [87] differs from the work of Cui et al. [92] as the phase separation is induced via spinodal decomposition. In the method reported by Cai et al. [87], the molecular surfactant (CTAB) is used to adjust the hydrophobicity of silica nanoparticles to achieve contact angle 90° at the interfaces between silicone oil and glycerol. Recently, Herzig et al. [93] (2007) reported a mechanism of arresting bicontinuous structures made up of 2,6-lutidine-water mixtures using colloidal particles. Thermally-induced demixing follows two kinetic pathways: 1) nucleation and

growth, where droplets of the dispersed phase become frozen once they exceed a certain threshold size, 2) spinodal decomposition, wherein a thoroughly mixed liquid mixture phase separates into two coexisting phases resulting in a bicontinuous arrangement of domains. In work demonstrated by Herzig et al. [93] (2007) group, the phase separation follows the kinetic pathway induced by spinodal decomposition. The FITC labelled silica particles, dried at 70°C overnight under vacuum, were used to obtain neutrally wetting conditions. The study carried out by these authors reveals that the domain size is linearly scaled with the inverse of the volume fraction of the particles.

Although several methodologies have been reported in the literature for stabilizing bijels, they share a common protocol, such as tuning surface chemistry to make particles neutrally wetting followed by rapid quenching or mixing. It is important to note that the hydrophilic or hydrophobic particles having $\theta < 90^\circ$ or $> 90^\circ$ favor formation of droplets. However, we devised an alternative route to achieve stable emulsions with better storage and mechanical stability by employing commercial-grade (Ludox®) nanoparticle colloidal dispersions. Our proposed methodology deals with a straightforward technique to stabilize w/w emulsions by devising self-assembly phenomena induced by oppositely charged commercial-grade silica nanoparticles. Further, we show the structural transformation from droplet-bijel-droplet using a phase diagram. By tuning the mass ratio (M) of OCNPs, a desired wetting condition, i.e. $\theta < 90^\circ$ or $\approx 90^\circ$, is achieved. Bijels have been identified as the new class of soft materials in which the self-assembly of colloidal particles creates a novel bi-continuous structure (Stratford et al. [85], Herzig et al. [93], Kim et al. [94], Macmillan et al. [95], Welch et al. [49]). Unlike emulsion droplets, since the $\theta$ established by the particles at the interface is nearly 90°, these bijels stabilized by OCNPs exhibit strong attachment energy, making them suitable for applications that involve multi-component or multiphase flows. The resulting bijels could be potentially used as cross-flow microreactors (Stratford et al. [85], Reeves et al. [96], Gabelman and Hwang [97], Cates and Clegg [98], Li et al. [99]) wherein two-immiscible reactants can be brought into intimate contact through interstitial sites, scaffolds for tissue engineering (Lee et al. [100]), porous materials (Lee and Mohraz [101]), electrodes for batteries and fuel cells (Witt et al. [102]). Since bijels are formed based on the aqueous two-phase systems without performing any sequential surface modification and rapid thermal cycle, the proposed study offers a simple yet novel pathway.

## 3.2 Experimental Section

### 3.2.1 Materials and Methods

To produce aqueous two-phase systems (ATPS), the thermodynamically incompatible hydrophilic polymers such as polyethylene oxide (PEO) and dextran, purchased from Sigma Aldrich Chemicals Pvt. Ltd., India, were used without any further modification. As reported by the manufacturer, the average molecular weight of PEO and dextran are 100000 and 40000 g/mol, respectively. Fluorescently labelled dextran procured from

Table 3.1: ATPS prepared at 9 different concentrations of PEO and dextran

| S.No. | Dextran (wt%) | PEO (wt%) | Observation |
|---|---|---|---|
| 1 | 1 | 9 | Single phase |
| 2 | 2 | 8 | Single phase |
| 3 | 3 | 7 | Two-phase |
| 4 | 4 | 6 | Two-phase |
| 5 | 5 | 5 | Two-phase |
| 6 | 6 | 4 | Two-phase |
| 7 | 7 | 3 | Two-phase |
| 8 | 8 | 2 | Two-phase |
| 9 | 9 | 1 | Two-phase |

Sigma Aldrich Chemicals Pvt. Ltd., India, was used to visualize the emulsion type. To stabilize the emulsion droplets or bijels, commercially available Ludox® grade HS-40 (-) (40 wt%) and CL-30 (+) (30 wt%) spherical silica nanoparticles, purchased from Sigma Aldrich Chemicals Pvt. Ltd., India, were used. The average size of hydrophilic HS-40 (-) and CL-30 (+) nanoparticles measured based on a transmission electron microscope (TEM) were 16 ± 2 nm and 16 ± 2 nm, respectively. The measurement of the size of type HS-40 (-) and CL-30 (+) nanoparticles are in agreement with the values reported by Koroleva et al. [103]. An electrophoretic study was carried out using DLS to determine the particles' potential at the shear plane (zeta ($\zeta$), potential). The $\zeta$ potential of the nanoparticles determined for HS-40 (-) and CL-30 (+) in 1 mM NaCl electrolyte medium were -55 ± 1.8 mV and 51 ± 2.1 mV, respectively. Deionized water (18.2 MΩ) obtained from a Milli-Q™was used for all experiments.

### 3.2.2 Preparation of two-phase mixtures

The Preparation of a two-phase mixture begins with adding PEO into a dextran solution. Several PEO/Dextran aqueous mixtures were prepared by fixing the total weight, 5 g, of the solution constant and varying the concentration (wt%) of PEO and dextran. Table 3.1 describes the samples prepared at various compositions of PEO and dextran. These samples were left undisturbed overnight before being processed further. Visual examination of these samples revealed that they had been confined to a two-phase regime throughout the observation time except for samples 1 & 2, i.e., a mixture containing 9% PEO and 1% dextran & 8% PEO and 2% dextran. Hence, we choose to work with the samples corresponding to the concentration range from 3% to 9% dextran (Please refer to entries no. 3 to 9 in Table 3.1) to make bijels or emulsion droplets.

### 3.2.3 Preparation of emulsion droplets and bijels

Initially, the aqueous solutions of dextran and PEO were prepared in 2 X 7 glass vials separately and left undisturbed for a brief period. Subsequently, the Ludox® grade colloidal solutions of oppositely charged nanoparticles were introduced into a respective polymer solution at a known concentration such that CL-30 (+) was suspended in PEO and

HS-40 (-) in dextran solution, respectively. After that, the solutions of PEO and dextran containing nanoparticles, weighing 2.5 g each, were allowed to mix with their counterparts, i.e., 1% PEO solution with 9% dextran, 2% PEO with 8% dextran, etc., using a vortex mixer for 2 min and then left undisturbed for 48 h at 25°C. In all these experiments, it has been ensured that the total concentration of nanoparticles in the mixture did not exceed 1 wt.%, and the entire solution weight was kept constant. It is important to note that a total of 210 experiments were performed to construct the phase diagram at different polymers and particle concentrations, including three repeat experiments to ensure the consistency of the results. Subsequently, the samples were analyzed using a suitable characterization technique. MATLAB programming was used to compute the average diameter of the emulsion droplets. For analysis, a sample size of about 300 representative droplets at each M was considered to ensure consistency in the measurements for calculation. The volume fraction of the dispersed phase was measured based on the image analysis using ImageJ software. Figure 3.1 shows the schematic description of making droplets and bijels. As explained in Figure 3.1, HS-40 (-) and CL-30 (+) silica nanoparticles were first suspended in dextran and PEO solution, respectively, and then allowed to equilibrate for 30 min before mixing between PEO solution containing CL-30 (+) nanoparticles and dextran solution containing HS-40 (-) nanoparticles were initiated using a vortex mixture for up to 2 min. To prepare bijels, the aqueous polymer solutions containing oppositely charged nanoparticles at a suitable mixing ratio (M), i.e., the ratio of weight fraction of positively charged nanoparticles to negatively charged nanoparticles, were processed using the vortex mixer. It has been observed that the formation of bijels is favoured at a desired range of M, i.e., M = 0.7-4, the results of which are discussed in the subsequent section.

### 3.2.4 Characterization

The zeta potential of hetero-aggregates and pure nanoparticles of type HS-40 (-) and CL-30 (+) were measured based on electrophoretic light scattering (ELS) technique using Zetasizer procured from Malvern Instruments, Model: Zetasizer Nano ZSP. Nephelometric turbidity units (NTU) of aggregates were measured using a turbidity meter procured from Cole-Parmer (Oakton), Model: T-100. The size of HS-40 (-) and CL-30 (+) nanoparticles were determined using a high-resolution transmission electron microscope (HRTEM), Make: FEI Company, Model: Tecnai G2 20. Inverted light microscope (Make: Carl Zeiss, Model: AxioVert.A1), high-resolution scanning electron microscope (HRSEM), Make: Hitachi, Model: SU8000, and scanning electron microscope (SEM), Make: JEOL, Model: JSM-6610, were used to carry out the structural characterization of droplets and bijels. The fluorescent microscope (Make: Leica Microsystems, Model: DMI 6000B) was used to visualize the arrangement of bi-continuous domains and to probe the type of emulsions, whether PEO-in-dextran or dextran-in-PEO.

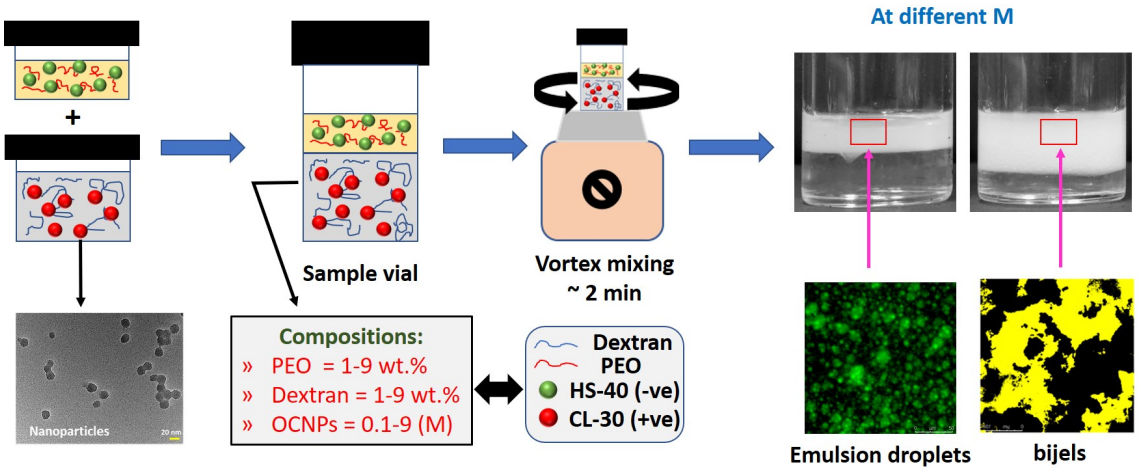


Figure 3.1: Schematic description showing the process of making bijels or emulsion droplets.

## 3.3 Results and Discussion

Before employing colloidal nanoparticles as a stabilizer, the binodal phase diagram was established first using a titration method followed by centrifugation to determine the single-two phase boundary for a given PEO-Dextran mixture to check the consistency of our thermodynamic data. The binodal diagram reported by Nguyen et al. [38] (2013) is analogous to our results. To identify a clear boundary, two-phase solutions were prepared by adding a solution of PEO to the solution of dextran dropwise until two phases were observed. Subsequently, centrifugation was performed to assert that the solution formed is a two-phase mixture. This step was necessary to visualize a single-to-two-phase solution in the glass vial. A similar procedure was repeated for several concentrations of PEO-Dextran solutions. Figure 3.2 displays the plot of the binodal diagram. The representative two-phase systems prepared at several data points above the single-two phase boundary line in Figure 3.2 were chosen to study the particle-laden emulsion systems in the rest of the manuscript. The concentration ranges were selected such that they fall on the same tie line to eliminate the variability in $\gamma$. The critical point for this PEO/dextran mixture is situated at $C_{PEO} = 1.5\%$ and $C_{dex} = 3\%$.

Next, stabilizing two-phase systems using commercial-grade nanoparticles of type CL-30 (+) or HS-40 (-) is discussed. For this study, the required colloidal dispersions were obtained by diluting the known amount from the original stock solution using DI water. For stabilizing the emulsion, a known concentration of nanoparticles of type HS-40 (1 wt%) or CL-30 (1 wt%), as well as the polymer solution containing 5% dextran and 5% PEO, were considered. However, preliminary experiments based on HS-40 (-) or CL-30 (+) type nanoparticles alone revealed that the stabilizing ability of these systems was insufficient to prevent the coalescence of droplets. In other words, the destabilization of the entire emulsion phase was observed within 72 hr of preparation of the samples stabilized by pure HS-40 (-) or CL-30 (+) nanoparticles. This destabilization could be attributed to droplets'

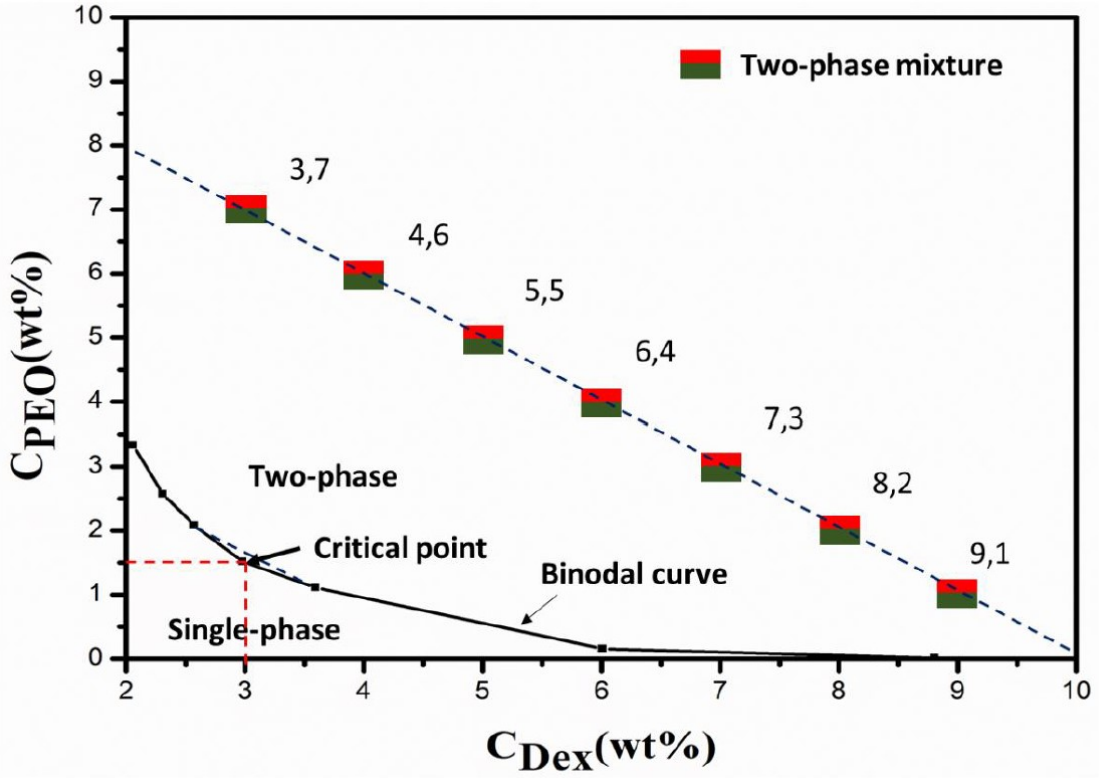


Figure 3.2: Plot showing the single-two phase boundary line for the polymer solutions containing PEO and dextran.

early breakdown and coalescence due to nanoparticles' weak adsorption at the interface. This weak adsorption could be linked to less detachment energy. For instance, if one assumes the radius and $\theta$ of nanoparticles as 10 nm and 80°, respectively, then, according to Eq.3.1, the energy required to detach the particles is just about 0.1 $k_BT$ which is sufficient to be pulled away from the interface by even a tiny thermal fluctuation. Figure 3.3 displays the surface morphology of HS-40 (-) and CL-30 (+) nanoparticles obtained by high-resolution transmission electron microscope (HRTEM), and Figure 3.4 vial images of samples stored up to 24 h and 72 h. By referring to Figure 3.4, it is clear that the emulsion phase of the samples corresponding to 72 h of storage at 25°C led to rapid breakdown of emulsions stabilized by pure HS-40 (-) or CL-30 (+) nanoparticles. The destabilization can be quantitatively evaluated by measuring % Volume of the emulsion phase, details of which are provided in the subsequent section.

Further, by taking a note from Nallamilli et al. [104] (2017) and connecting our ideas, it has been decided to employ OCNPs to produce 2D and complex clusters at the interface to arrest coalescence and promote stability. In this connection, a self-assembly phenomenon using OCNPs was devised to induce heteroaggregation in a polymer solution containing 5% dextran and 5% PEO. It has been found that the emulsions stabilized by OCNPs were stable even beyond 72 h. This enhanced stability motivated us further to prolong our study using these nanoparticles. It is envisaged that the self-assembly induced by attractive interaction potential between the nanoparticles' positive and negative surface

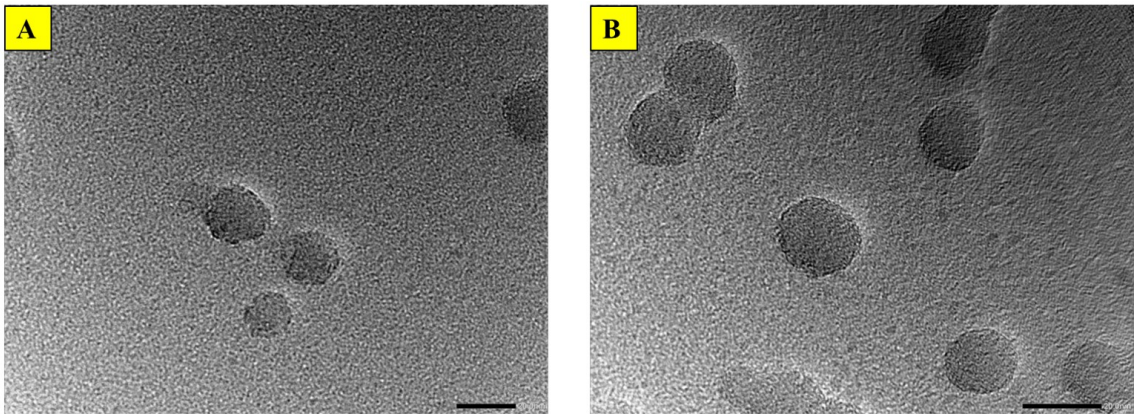


Figure 3.3: Representative TEM images of surface morphology of A) HS-40 (-), and B) CL-30 (+) nanoparticles. Scale bar given in the images correspond to 20 nm.

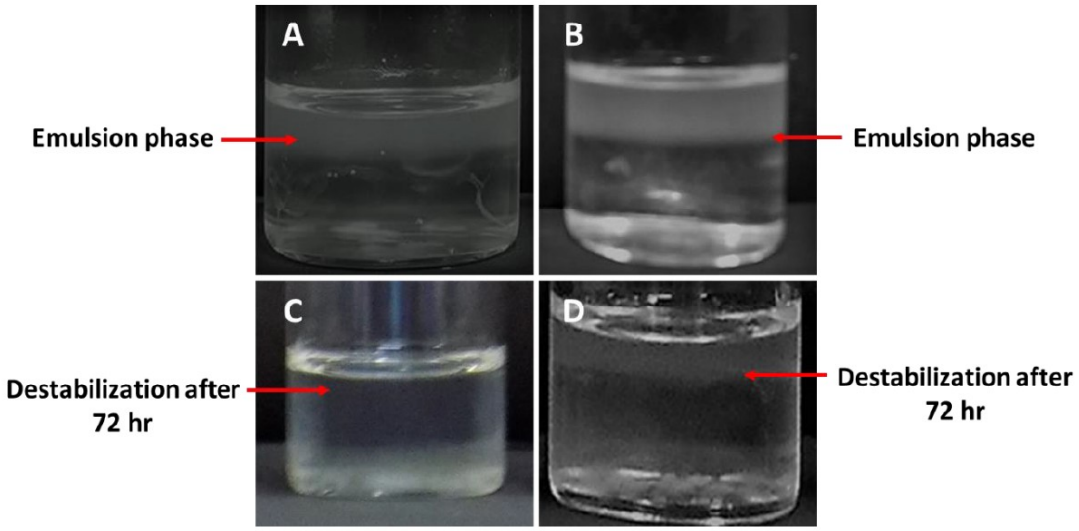


Figure 3.4: Vial images to present visual appearance of destabilization of emulsions stabilized by pure nanoparticles of type HS-40 (-) and CL-30 (+). A & C) State of emulsions stabilized by pure CL-30 (+) nanoparticles after 24 hr, and 72 hr, respectively. B & D) State of emulsions stabilized by pure HS-40 (-) nanoparticles after 24 hr, and 72 hr, respectively.

charge leads to complex clusters of varying sizes, shapes, and compositions. These self-assembled clusters are more significant than the size of the individual nanoparticle itself, so it is expected to raise the Gibbs detachment energy. This increase in detachment energy is necessary to enhance the stability of droplets. It is envisaged that the droplets' deformation rate can easily be tuned by modulating the size and the $\theta$ as it is directly linked to the composition. Exploiting the self-assembly of oppositely charged nanoparticles to stabilize w/w emulsions has received much less attention in the domain of w/w Pickering emulsions or ATPS. This phenomenon provides additional variability to study the physical characteristics of emulsion-based products. For instance, consider the influence of nanoparticles' concentration and size ratio on the structure and quality

of the desired outcomes. Hence, the effect of mass ratio (M) on the structural state of emulsions stabilized by the OCNPs was probed by keeping the concentration of polymers in the solution constant, details of which are described below.

A systematic study has been carried out to understand the variation in the structural state of emulsions by varying the M of nanoparticles. In our study, since we have observed that the droplets stabilized by OCNPs at some known M remained stable for up to 30 days, it intrigued us to know whether the wettability of self-assembled clusters could be modulated by just tuning the ratio of nanoparticles of different type without modifying the particle surface chemistry using any external agent. This idea drove us to build a phase diagram for different combinations of polymers and particles. Figure 3.5 depicts the structural transformation from droplet-bijel-droplet to varying PEO-dextran compositions and OCNPs of a two-phase mixture stabilized using a vortex mixer. As shown in Figure 3.5, the ratio of weight fraction of CL-30 (+) to HS-40 (-), M, plays a crucial role in establishing an appropriate pathway for fabricating bijel and droplet from any given combination of the two-phase mixture. Note: A similar droplet-bijel-droplet transition trend was obtained when a different emulsifying device such as a homogenizer (Make: IKA, Model: T 25 digital ULTRA-TURRAX®) was employed at a programmed speed of 10000 RPM, which imparts more mechanical energy as compared to the vortex mixer. This study helped us conclude that the emergence of various structural states was not affected by the emulsification path chosen, revealing that the structures obtained at a particular M are unique and correspond to an equilibrium state, similar to the microstructure depicted in Fig. 3.9.

Interestingly, the structural transition from droplet-bijel-droplet has been observed at a different mass ratio ranging from M=0.7 to M=4 depending on the concentration of PEO/dextran used in the solution. This structural transition could be attributed to the self-assembly of OCNPs and subsequent formation of the colloidal clusters. Three types of clusters could be formed as a result of self-assembly:

1. Clusters with a net negative charge
2. Clusters with a net positive charge
3. Neutral clusters

Figure 3.6 displays the representative microscopic images corresponding to different mass ratios (M) of OCNPs and polymer compositions. Unlike the droplets stabilized by the pure nanoparticles of type CL-30 (+) or HS-40 (-), the droplets stabilized by OCNPs did not visually show any destabilization of the emulsion phase as they remained stable for up to 30 days. To comment on the stability of these droplets, the droplet size variation for the samples corresponding to the storage time of 2 and 30 days was probed. From Figure 3.7, it is clear that there is no significant variation in the average diameter of the droplets measured at different M for the samples aged between 2 and 30 days. The droplets stabilized by OCNPs were visualized under a fluorescent microscope to understand the type of emulsions formed. For this purpose, the fluorescently labelled

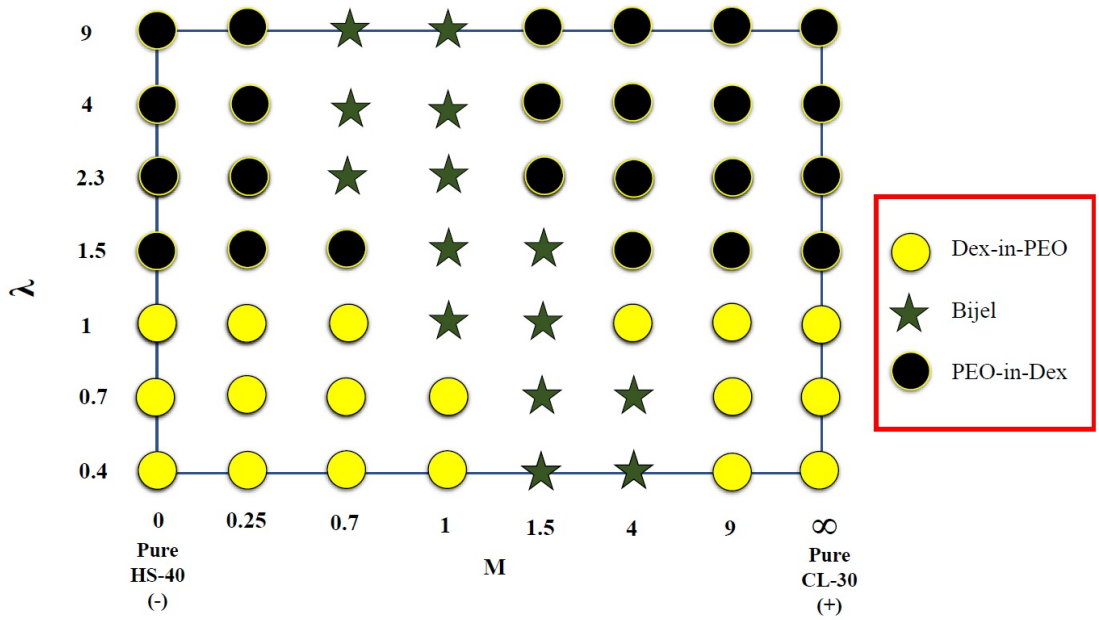


Figure 3.5: Phase diagram depicting the effect of mixing ratio (M) on the structural state of emulsions at different concentration of PEO and dextran. The parameter $\lambda$ on the Y axis represents the ratio of the weight percentage of Dextran to PEO.

dextran polymer was used to trace the dispersed phase. Since only one of the polymers used was labelled with fluorescent, it is expected that the PEO-rich part would appear dark while dextran-rich phases glow distinctly under fluorescent microscopy. As shown by Figure 3.8, the catastrophic phase inversion was observed as the concentration of PEO and dextran correspond to a mixture either increases or decreases. By analyzing Figure 3.5 and Figure 3.8, one can understand that the polymer with lower concentration forms the dispersed phase. In comparison, higher concentration becomes the continuous phase, a trend similar to any alkane-water emulsion system. However, an emulsion mixture containing equal amounts of PEO and dextran favours the dextran-in-PEO emulsion type. It could be attributed to the stabilizer's hydrophilic nature and the higher molecular weight of the medium (PEO), as it provides additional links to the water molecules to confine around the polymer chains.

Further, the transition between droplet and bijel observed through light microscopy is discussed. The morphological evolution from droplets to bi-continuous network structure indicates two-dimensional hierarchical structures such as bijels. This novel structure is known to be formed when the wettability established by the given stabilizer at the water-water interface is equally likely, i.e., $\theta$ is $\approx 90°$. At this equilibrium position, the Gibbs free energy of detachment for bijels is expected to be larger than the droplets, providing enhanced stability, as per the equation described below (Eq. 3.3) for the condition of $\theta$=90°.

$$\Delta G_d = \pi R^2 \gamma_{w/w} \tag{3.3}$$

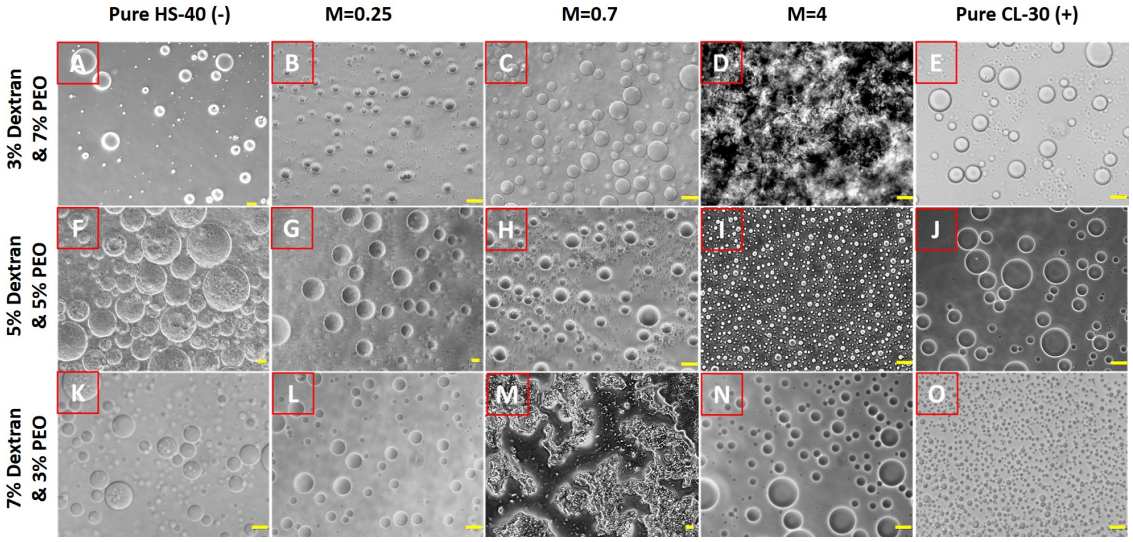


Figure 3.6: Inverted microscopic images showing the evolution of structural state of emulsions stabilized by nanoparticles at different M. A-E) Representative microscopic images correspond to the emulsion mixture containing 3% dextran & 7% PEO at M=0, 0.25, 0.7, 4, $\infty$, respectively. F-J) Representative microscopic images correspond to the emulsion mixture containing 5% dextran & 5% PEO at M=0, 0.25, 0.7, 4, $\infty$, respectively. K-O) Representative microscopic images correspond to the emulsion mixture containing 7% dextran & 3% PEO at M=0, 0.25, 0.7, 4, $\infty$, respectively. Scale bar corresponds to 10 $\mu$m.

In the context of the formation of bijels, various research groups have reported several simulations and experimental studies. Jansen and Harting [35] (2011), demonstrated the structural transition from bijels to emulsion droplets by investigating its dependence on the contact angle, the particle concentration, and ratio of solvents. According to their prediction, for contact angles larger than 90°, between 90-95°, the system always relaxes towards a bijel while the particle concentration has less influence on the final state. In our case, the total particle concentration was maintained at 1% but varied the ratio of weight fraction of individual particle types. Interestingly, the bijels formation was observed for the M value between 0.7 to 4, as shown in the phase diagram, Figure 3.5. Further, as reported by Jansen and Harting [35] (2011), it can be stated that the variation of PEO/dextran concentration affects the state of emulsions formed as one observes a shift in the transition from bijels to droplets at various combinations of polymer mixture starting from 3 wt.% to 9 wt.%.

To prove that the bicontinuous structures produced via a suitable experimental regime are not intermediate, the Z-stack fluorescent imaging has been performed using LAS X software of Leica DMI 6000B equipped with a motorized stage. Figure 3.9 shows the Z-stack images corresponding to 48 hr ageing time (8% dextran & 2% PEO at M=1.0) at different locations in the X-Y plane. The 3D structural features captured by fluorescent microscopy in a liquid state visually confirm the tortuous channels spread across the X-Y-Z plane. The images shown in Figure 3.9 refer to bi-continuous domains filled with

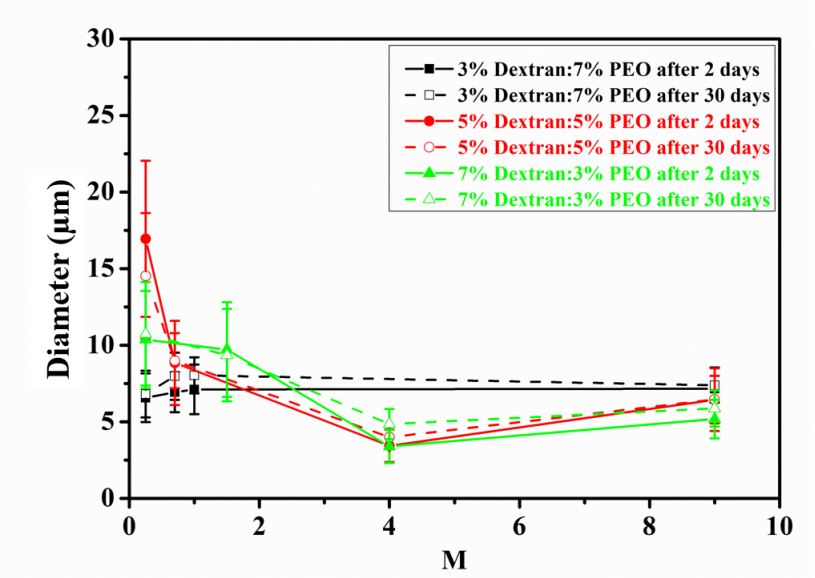


Figure 3.7: Plot of average diameter vs M at different PEO and dextran concentrations to assess the stability of droplets aged between 2 and 30 days.

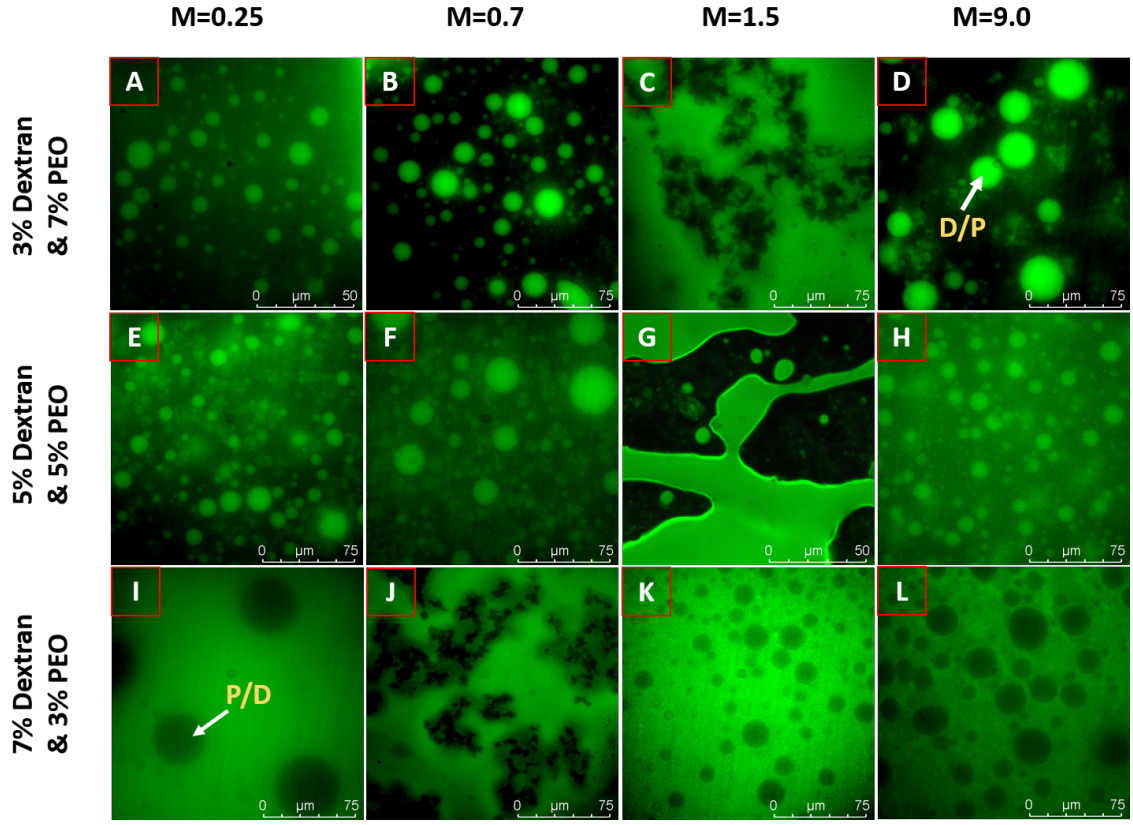


Figure 3.8: Fluorescent microscopic images to visually examine the type of emulsions formed. A-D) Representative images correspond to emulsion mixture containing 3% dextran & 7% PEO at M=0.25, 0.7, 1.5, and 9.0, respectively. E-H) Representative images correspond to emulsion mixture containing 5% dextran & 5% PEO at M=0.25, 0.7, 1.5, and 9.0, respectively. I-L) Representative images correspond to emulsion mixture containing 7% dextran & 3% PEO at M=0.25, 0.7, 1.5, and 9.0, respectively. The bicontinuous network structure of bijels is depicted in Figures C, G, and J.

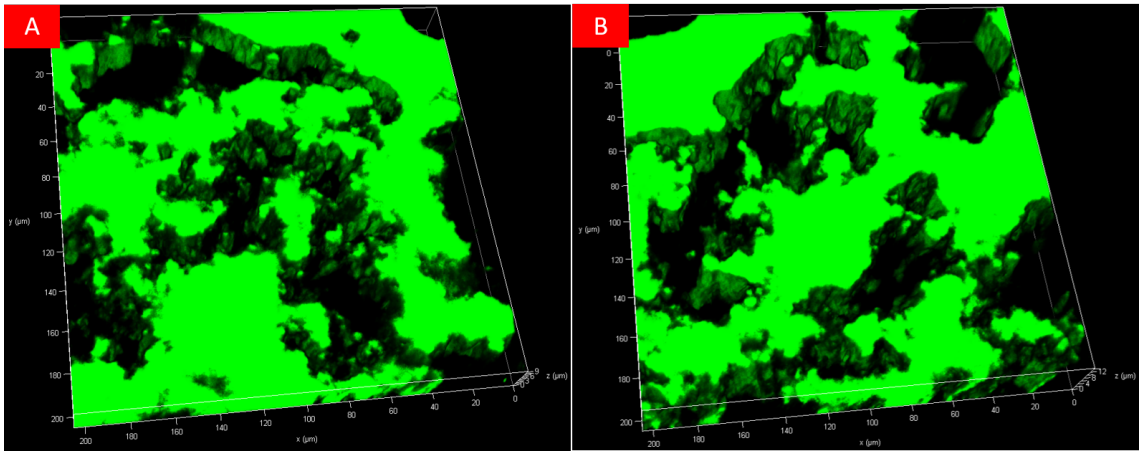


Figure 3.9: Fluorescent Z-stack microscopic images captured after 48 hr at different locations in X-Y plane (A-B) to visually confirm that the bijel formed is not of an intermediate state. Representative images correspond to the emulsion mixture containing 8% dextran & 2% PEO at M=1.0.

fluorescently labelled dextran (glow regions) and PEO (dark regions). It can also be inferred from Figure 3.9 that there are no intermediate or quasi-states emerged during the process of stabilization of bijels as there were no visual signs of the formation of droplets found within any of the PEO-rich or dextran-rich channels, which comes to say that the obtained morphology corresponds to the signature topographies of the bijels. Further, the 2D and 3D microstructures corresponding to bijels show good agreement with numerous studies published in the literature.(Hijnen et al. [105], Kinkead et al. [106], Reeves et al. [96], Firoozmand and Rousseau [39], Cai and Clegg [86], Lee and Mohraz [101], Herzig et al. [93], Frijters et al. [107])

Figure 3.10 depicts the scanning electron microscopic (SEM) images describing the structural change from droplet to bijel. Figure 3.10 A illustrates the samples containing emulsions stabilized by OCNPs at a different ratio, M, and for a fixed concentration of PEO/dextran (8% Dextran and 2% PEO). By taking a close look at the vial images, one can understand that there is a slight increase in the volume of the emulsion part, clearly highlighted by denoting the emulsion phase with the letter 'h' (Please refer to Figure 3.10 A), in the case of stabilized samples correspond to M=0.7. This increase in the gel phase volume is the characteristic nature of the formation of bijels, a structure with an arrangement of bi-continuous domains, utilizing particles' role as stabilizers to the maximum extent possible. The structural state of the behavior of emulsion at different M is experimentally visualized using representative SEM images.

The dried state of bijels (M=0.7) deposited on a silicon wafer is shown in Figure 3.10 B, while the structural state of emulsion droplets corresponding to M at 9, 4, and 1.5 are depicted in Figure 3.10 C, D, and E, respectively. Note: The bijel systems reported by us cannot distinctly show micro or macroporous channels as the evaporation of the solvent leads to the deposition of polymers (PEO and dextran) in the areas confined to the bi-continuous channels. The quantitative measurement of the volume fraction of the

emulsion phase at the different scenarios of M is shown in Figure 3.11. For this, total height, H, measured from the bottom of the vial as a datum point and the height up to which the emulsion phase is spanned (h) are considered. The height of the emulsion phase is defined as h (Please refer to Figure 3.10 A). Thus, the ratio of h/H is defined as the volume fraction of the emulsion phase. Several such measurements are taken for each sample to arrive at a mean value. Figure 3.11 displays the plot showing the effect of change in the composition of OCNPs on the % volume of the emulsion phase. The quantitative measurements make the exact prediction as demonstrated in Figure 3.10 A.

To probe the mechanical strength, the emulsion droplets were subjected to higher centrifugal action by placing a drop of the emulsion samples on a glass substrate and allowing the samples to experience a mechanical disturbance in the form of rotational spinning under centrifugal action. The spin coater (Make: Holmarc, Model. HO-TH-05C) is used to dry these samples at the desired set point. The programmed speed and run time operated by us are 1000 RPM and 2 min, respectively. Figure 3.12A and B reveal the structural state of emulsion droplets imaged using HRSEM at M=4, and M=9, respectively. It has been observed that the droplets and bijels remained stable even after exposing them to higher shear conditions. Although these droplets were not collapsible under shear, they were elongated slightly due to the centrifugal action. Huang and Chou [108] (2003) reported the dependence of final film thickness (H) with spin coating speed as given below in equation 3.4,

$$H = D.\omega^{-b} \tag{3.4}$$

where D, $\omega$, and b are defined as fitting constant, spin coating speed, and exponent, respectively. The equation 3.4 reveals that the increase in speed increases the action of centrifugal force. As a result, it dominates the counteracting viscous and surface tension forces to some extent. Therefore, the droplets start to spread initially in the radial direction as expected.

A few sedimentation experiments were performed to understand the dispersion behavior at different M without the polymers' addition to prove our hypothesis. Figure 3.13 displays the visual appearance of dispersion behaviour of OCNPs corresponding to 48 hr ageing time at various M with total particle concentration kept constant at 1%. Consequently, four different states of dispersions were identified, as shown in Figure 3.13. They include 1) clear dispersion, 2) milky dispersion, 3) sediment with clear supernatant, and 4) sediment with turbid supernatant. Sediment with clear and turbid supernatant indicates that the net charge of aggregate systems could be neutral or weakly charged as the aggregates of these types grow in size and induce sedimentation within a shorter timescale compared to other systems. Hence, the dispersion state of OCNPs at M=0.25 (sediment with turbid supernatant), M=0.7 (sediment with clear supernatant), and M=1.5 (sediment with turbid supernatant) could be linked to the behaviour of aggregates at a different range of M between 0.7 and 4 in the presence of polymer mixture containing PEO and dextran.

This understanding is further strengthened by obtaining the supernatant's turbidity and

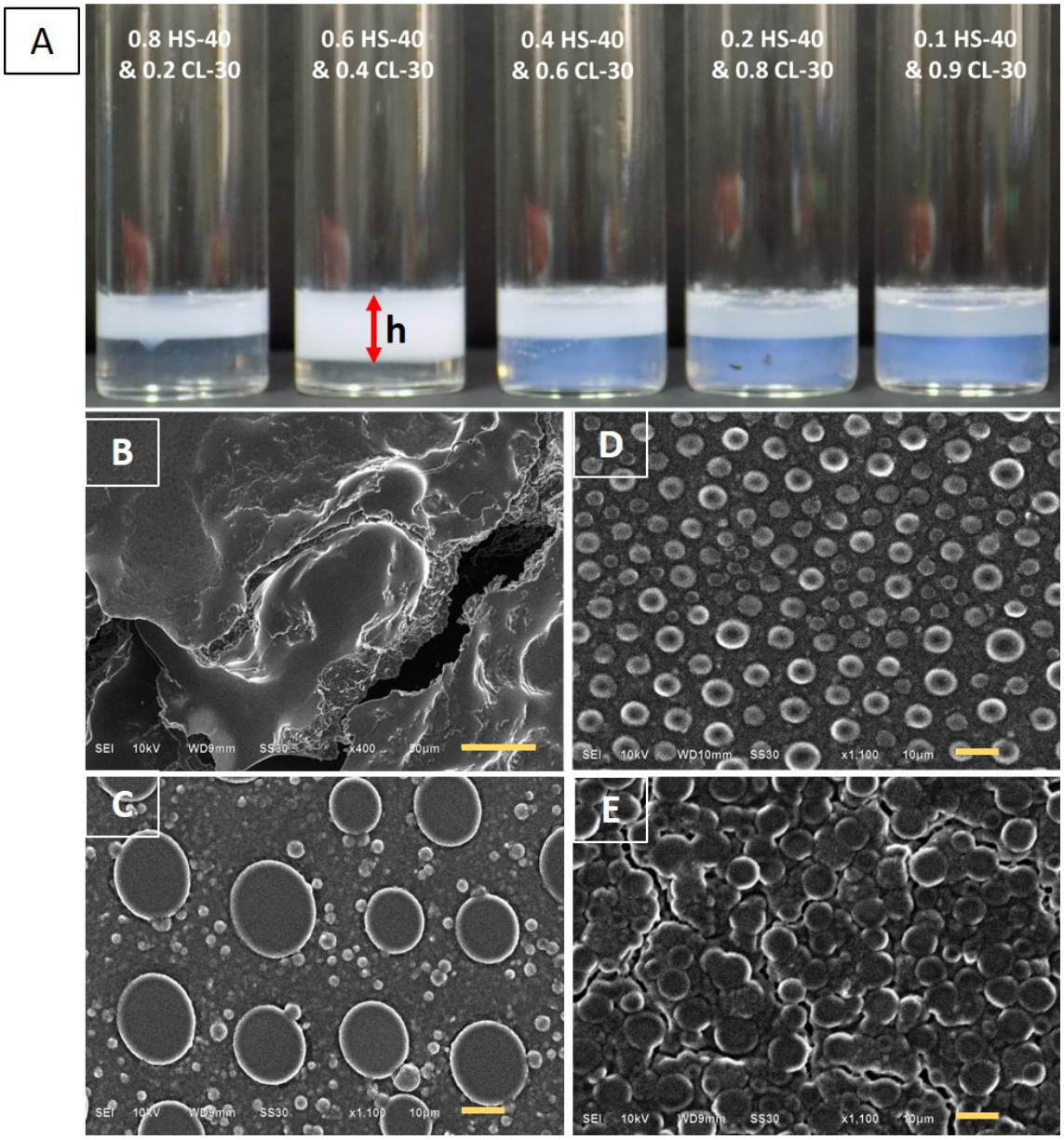


Figure 3.10: Structural transition from droplet to bijels. A) Vials of various emulsion samples prepared at different M values. B) SEM image showing the surface morphology of bijels, M=0.7 in a dried state. C-E) SEM images showing the surface morphology of emulsion droplets prepared at M=9, 4, 1.5, respectively, in a dried state. The scale bar in the images corresponds to 50 $\mu$m (B) and 10 $\mu$m (C-E).

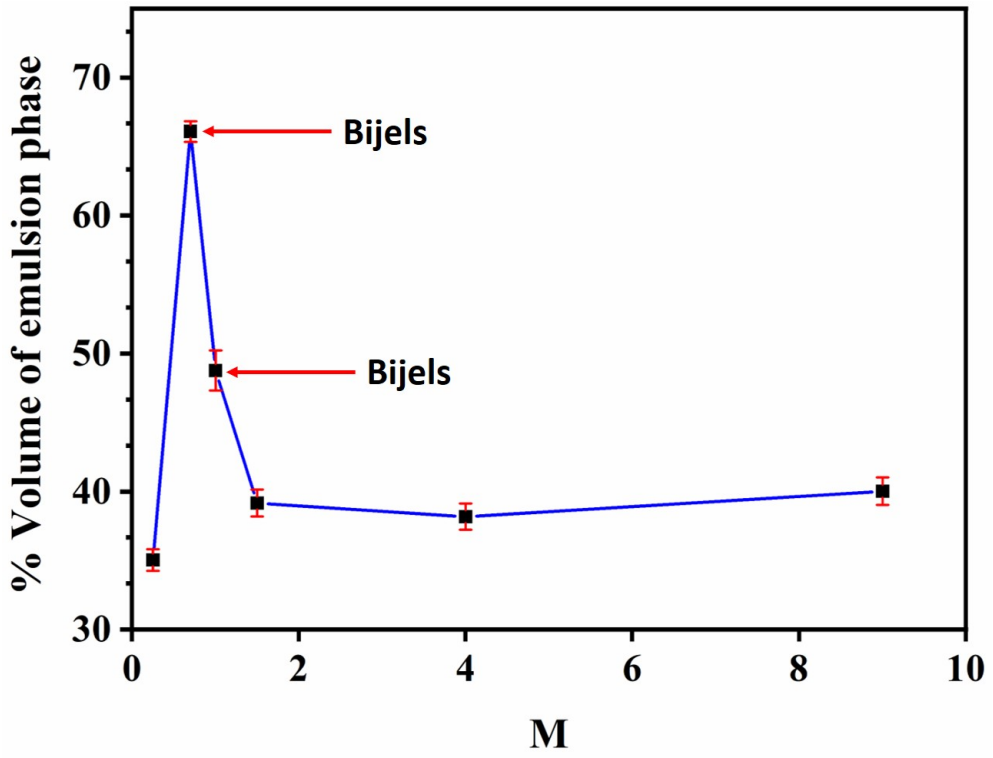


Figure 3.11: Plot showing the % Volume of emulsion phase vs. M. The concentration of polymer solution used for this study was maintained constant at 8% dextran & 2% PEO.

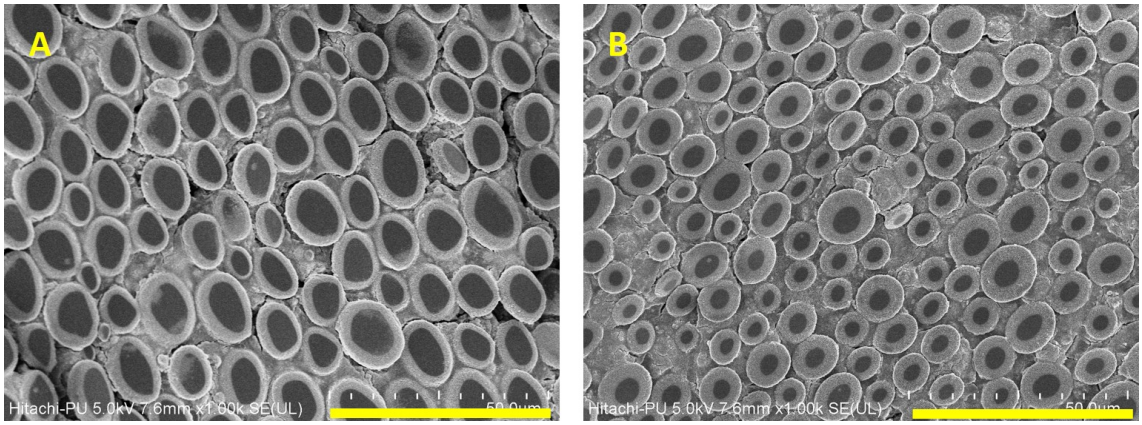


Figure 3.12: Representative HRSEM images showing the structurally stable emulsion droplets in the solid state after mechanical perturbation. A) Emulsion droplets prepared at M=4, B) Emulsion droplets prepared at M=9. The scale bar corresponds to 50 $\mu$m.

zeta potential ($\zeta$) measurement. The $\zeta$ potential of aggregates at various M is shown in Figure 3.14B. It has been found that the $\zeta$ potential values of the samples corresponding to M=0.7 to 1.0 were pretty close to zero, while the measurements with the rest of the samples yielded high positive or negative potentials. These measurements confirm the possibility of clusters with different charge natures at a particular operating regime, favouring the formation of droplets and bijels depending on the nature of charge at a given M. The nephelometric turbidity units (NTU) of aggregates measured using a turbidity meter shown in Figure 3.14B recapitulate the findings of $\zeta$ measurements discussed above.

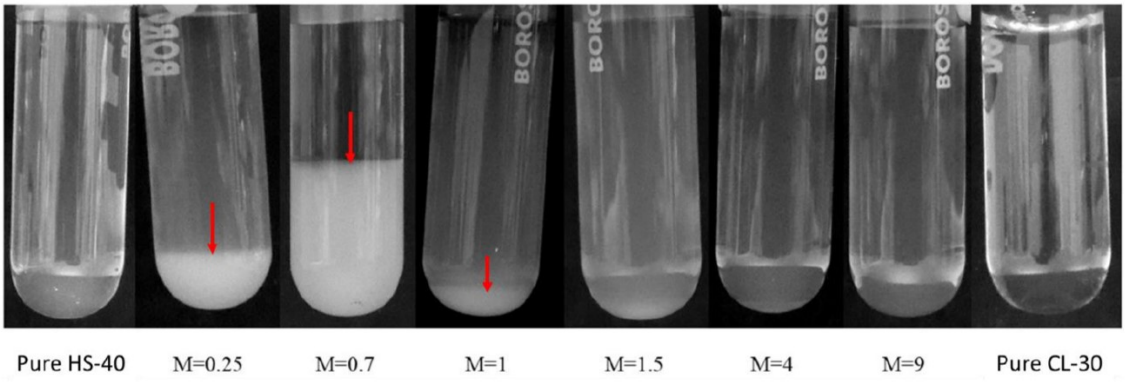


Figure 3.13: The vial images showing the visual appearance of behaviour of binary mixture containing OCNPs at different M.

Since the $\zeta$ and NTU of aggregates measured at M between 0.7-1.0 indicate the values correspond to neutral aggregates, it is asserted that the self-assembly of OCNPs could favour the formation of bijels at a similar range of M corresponding to emulsion systems.

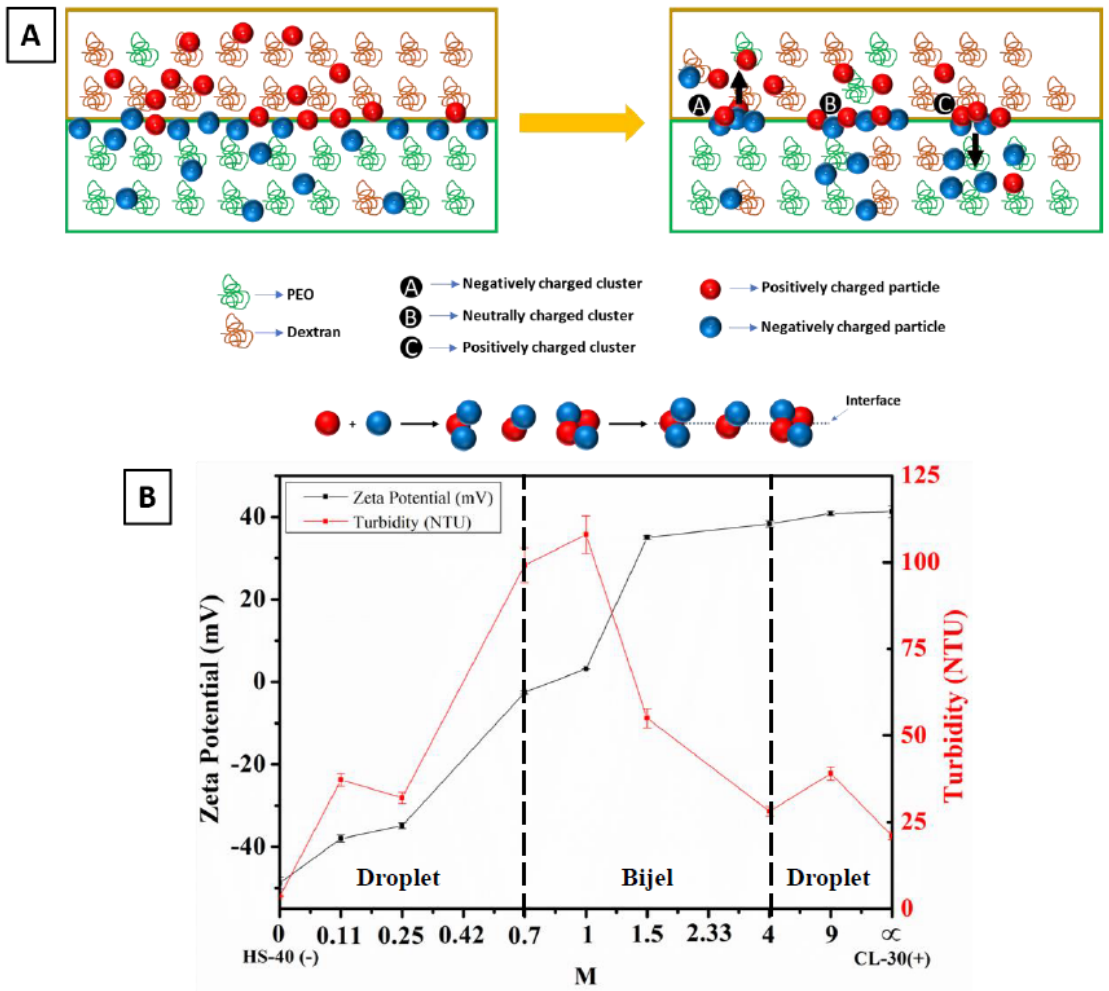


Figure 3.14: A) Schematic description explaining the mechanistic route of the formation of droplets and bijels at different mixing ratios. B) Zeta potential and turbidity measurements of complex aggregates formed at different M.

It can be inferred from Figures 3.5,3.13, and 3.14B that there is a close correspondence between the nature of aggregates' charge and the structural state of emulsions stabilized by nanoparticles. For instance, the droplet-bijel-droplet transition of an emulsion mixture (M=0.7-1.0) prepared at different polymer-polymer concentration ratios of 1% PEO: 9% dextran, 2% PEO: 8% dextran, and 3% PEO: 7% dextran, have a close correspondence with an isoelectric point (IEP) of aggregates. Note: One can understand that there is a rightward shift (Please refer to Figure 3.5) for the rest of the polymer combinations in terms of structural transition ranging from M=0.7-1.0 to M=1.0-4.0, which could be attributed to the effect of change in concentrations of PEO and dextran.

## 3.4 Conclusion

A simple yet straightforward technique to produce stable w/w Pickering emulsions has been demonstrated. While the use of pure commercial grade nanoparticles of type HS-40 (-) and CL-30 (+) did not stabilize the emulsions, combining a binary mixture of nanoparticles at desired M had shown enhanced stability. These droplets have remained stable for up to 30 days and demonstrated good resilience against strong mechanical force. Since the self-assembly route was adopted for the study, it can be envisaged that the combination of OCNPs at desired mass ratio (M) induces a complex assembly of 2D and 3D clusters larger than individual nanoparticles, yielding a significant rise in Gibbs detachment energy. Further, a phase diagram has been developed to identify a droplet-bijel-droplet transition and phase inversion due to changes in polymer and particle concentrations. The structural characterization using bright field, fluorescent, and electron microscopes were carried out to probe the emulsion type (P/D or D/P) and the structural state of bijels or droplets. The bijels are called a new class of bi-continuous soft materials finding suitable applications in multicomponent flows, tissue engineering, electrodes for batteries, and fuel cells.

# Chapter 4

# Probing emulsion-gel transition in aqueous two-phase systems: A simple pathway to fabricate water-in-water emulsion-filled gels

In the preceding Chapter 3, the influence of particle contact angle on the formation of various morphologies in the water-in-water emulsion was illustrated. In this chapter, a method for synthesizing an emulsion-filled gel is presented. This gel formation is achieved by modifying the molecular weight of polyethylene oxide (PEO) in one of the aqueous phases, subsequently influencing the interfacial tension between the other phases. In addition, the utilization of electron and light microscopy in generating a state diagram provides valuable insights into the production of stable emulsion-filled gels and emulsion droplets. The present study aims to elucidate the underlying influence of molecular weight and storage duration through visual examination, brightfield microscopy, and fluorescent microscopy techniques. Subsequently, these studies reveal that the formation of an emulsion-filled gel can be attributed to the arrangement of "active-filler-particles," commonly observed when there is a significant affinity between the droplets stabilized by particles and the polymer. On the other hand, this chapter reports the arrangement of "inactive-filler-particles" for the samples undergoing phase inversion. Eventually, the rheological analysis of shear-induced structures in emulsion-filled gels reveals a clear correlation between their viscoelastic properties and factors such as time, molecular weight, and polymer composition.

## 4.1 Introduction

An emulsion is a mixture of two immiscible liquids in which the droplets of one liquid phase are dispersed into the other. Emulsions are widely available daily in various households, such as agrochemicals, cosmetics, and pharmaceutical products. The conventional water-in-oil (w/o) and oil-in-water (o/w) emulsions have been involved in numerous applications, e.g., cosmetics formulation or healthcare and pharmaceutical industries (Maestro et al. [109]). An extended emulsion system such as an aqueous two-phase system (ATPS) involving polymer-polymer interaction has also been extensively studied

from a unique pathway to make porous materials, bijels, and emulsion gels (Florence and Whitehill [110]). ATPS is an aqueous binary mixture of two thermodynamically incompatible polymer systems (Hatti-Kaul [111]). Water-in-water (w/w) emulsion is a classic example of ATPS, often employed when the oil phase is known to cause harmful effects. For instance, colloidal particles can stabilize w/w emulsions and help address challenges like encapsulating oil-sensitive active ingredients or developing low-fat edible products. These particles, unlike surfactants, can traverse the interfacial boundary, typically a few tens of nanometers thick. However, the water-water interface has unique properties, such as an ultra-low interfacial tension of approximately 1 $\mu$N/m - making the stabilization process even more complex. To overcome these challenges, one has to devise a suitable strategy to achieve stable emulsions by preventing the destabilization of the dispersed phase due to various instabilities such as coalescence, creaming, and sedimentation due to gravity. In previous chapter 3, we reported one such approach to tackle the instabilities earlier using the oppositely charged nanoparticles (OCNPs) by exploiting the interplay between the size and shape of the resulting clusters formed as a result of self-assembly (Shekhar et al. [112]). Alternatively, one can devise an approach in which the droplets are confined within a three-dimensional solid-like aqueous network (hydrogels). In this endeavour, we desired to add another exciting avenue in the domain of ATPS, i.e., emulsion-filled gels or emulgels stabilized by the nanoparticles. The rheological properties of these gels depend on the polymer matrix (Sala et al. [113]). Stabilizing droplets by inducing the formation of three-dimensional polymer networks can provide insight into the roles of polymers and colloids in pharmaceutical, food, and cosmetic formulations. Furthermore, unlike o/w or w/o Pickering emulsions, the particle-stabilized w/w emulsions offer an extended scope to tune the structure of emulsions, shelf-life, and quality of the products via an additional variability, i.e., the molecular weight of dissolved polymers. This property helps us improve droplets' stability by synergistic stabilization and the formation of polymer bridges between the droplets.

An emulsion-filled gel is a soft solid-like composite material (Geremias-Andrade et al. [114], Oliver et al. [115], Lorenzo et al. [116], Sala et al. [117], Oliver et al. [118]). Note: The emulsion-filled gels reported here are different from shake gels which are observed at higher colloidal particle concentration (15-35 wt%), and lower PEO concentration (0.25-0.50 wt%) (Cabane et al. [119], Ramos-Tejada and Luckham [120], Kamibayashi et al. [121], Collini et al. [51]). These emulsion gels can be structurally defined as the emulsion droplets dispersed into the polymeric network-like gel matrix (Geremias-Andrade et al. [114]). One of the significant advantages of these complex emulsion systems is the improved stability as the droplets are stabilized by the particles confined within the three-dimensional network of hydrogels. Such an arrangement of polymer gel provides a simple yet straightforward route to stabilize the w/w emulsion using the nanoparticles. That is, the formation of three-dimensional hydrogels promotes the immobilization of droplets within the gel matrix, thereby preventing the early breakdown of droplets due to coalescence. One of the potential applications of the emulsion-filled gels in food formulations is that

these structures help produce low-fat food products with improved creaminess perception (van Aken et al. [122, 123]). In the context of particle-stabilized gels, there are two idealized models of structured emulsions, 1) emulsion-filled gels and 2) emulsion gels (Esquena [32], Dickinson [124]). In the former case, the droplets are immobilized by the three-dimensional network of polymers, while the enhanced stability in the latter is due to the aggregation of the emulsion droplets. For instance, the work demonstrated by Ben Ayed et al. [56] (2018) represents the model based on emulsion gels. In that work, the authors utilized cellulose nanocrystal (CNC) particles in large amounts, i.e., > 1 g/L, resulting in bridges between the droplets. One can also use an approach that helps immobilize the droplets via the emulsion-filled gels induced by three-dimensional polymer networks. Here, the stabilization of w/w emulsions via the formation of emulsion-filled gels or gel beads in the matrix of the continuous or dispersed phase is demonstrated. This study hypothesizes that the type of emulsion decides the resulting structures. For instance, if the polymer that induces the gelation forms the continuous phase, one would get a structure similar to the interconnected bridges exhibiting the three-dimensional porous channels. On the other hand, the change in the emulsion type puts the gelling polymer on the other side, i.e., the dispersed phase, to yield a structure similar to gel beads (Sagis [125, 126]). Here, the stability becomes enhanced through interlocking the particles at the interface. The improved stability could be attributed to the formation of polymer networks in the dispersed phase and the adsorption of polymer molecules on the surface of particles. The systematic study helped us explore the role of molecular weight, ageing time, and polymer concentrations in stabilizing w/w emulsion droplets. Further, a rheometer was employed to probe the emulsion-to-gel transition at a particular experimental condition and characterize the rheological properties of emulsion-filled gels.

## 4.2 Experimental Section

### 4.2.1 Materials and Methods

We used polyethylene oxide (PEO) and dextran, procured from Sigma-Aldrich Chemicals Pvt. Ltd., India, to prepare an ATPS. A known concentration of PEO and dextran labeled with a particular molecular weight (Mwt) was used to prepare an emulsion mixture. To understand molecular weight's influence on the emulsion products' quality, we used PEO with different Mwt. The average molecular weight of PEO employed for the studies were $1\times10^5$ (1E5), $3\times10^5$ (3E5), $6\times10^5$ (6E5), and $10\times10^5$ (10E5) Da, as per the specification of the manufacturer. The average molecular weight of dextran reported by the manufacturer is $4\times10^4$ Da. All the experiments that involve emulsion were carried out by keeping the Mwt of dextran constant while varying the same for PEO. In a few experiments, we used fluorescently-labeled dextran, procured from Sigma-Aldrich Chemical Pvt. Ltd., India, to probe the type of emulsion formed. To stabilize the emulsion, commercially available negatively charged Ludox grade HS-40 (40 wt.%) colloidal suspension containing silica nanoparticles, procured from Sigma-Aldrich Chemicals Pvt. Ltd., India, was used. The

average diameter of the HS-40 silica nanoparticles found based on the image analysis using a transmission electron microscope (TEM) was 16 ± 2 nm. An electrophoretic study was carried out to determine the particles' potential at the boundary between the shear and diffuse plane, i.e., Zeta potential ($\zeta$). The $\zeta$ of the nanoparticles determined for HS-40 in 1 mM NaCl electrolyte medium was -55 ± 1.8 mV. We used deionized water (18.2 MΩ) obtained from a Milli-Q for all experiments.

### 4.2.2 Prepration of emulsion-filed gel

We first prepared a different set of an aqueous solution of dextran and PEO in the glass vials and kept them undisturbed overnight after stirring the mixture for 2 minutes using a vortex shaker. This procedure is required to generate a homogeneous mixture prior to homogenizer-based emulsification. Subsequently, a known concentration of Ludox grade colloidal solution containing silica particles (HS-40) (1 wt.% of 2.5 g of the total solution) was added to the dextran solution. Please note the mixing was performed without employing any dispersing agent as the nature of the HS-40 nanoparticles is hydrophilic, and the contact angle of water with the same found using the sessile drop study is 14 ± 1°. When added to an aqueous PEO solution, the nanoparticles did not exhibit a preferential orientation effect, since there was no substantial difference in the results. Each vial containing 2.5 g of PEO solution weighing 3, 5, and 7 wt.% was combined with aqueous dextran solutions weighing 7, 5, and 3 wt.%, respectively, in such a way that the total weight of the solution does not exceed 10 wt.%. In every experiment, the nanoparticles concentration in the dextran solution was held constant at 1% by weight. Using a high-pressure homogenizer operating at 10,000 RPM for two minutes, the mixture is emulsified to produce water-in-water emulsion droplets or emulsion-filled gels. Depending on the sample type, these emulsified samples were kept at a constant temperature of 25°C in an incubator for varying amounts of time. Figure 4.1 depicts the schematic explanations of the emulsion-filled gels synthesis procedure. As demonstrated in Figure 4.1, the structure of emulsion products can be modified by varying parameters such as molecular weight, composition, and ageing period.

### 4.2.3 Rheology

The particle-stabilized w/w emulsions and emulsion-filled gels were characterized rheologically using a stress-controlled rheometer with cone-and-plate geometry (d=25mm, angle 2°) equipped with a temperature trap to maintain a constant temperature of 25°C. Using a spatula, the samples were carefully deposited onto the rheometer plate, and then the upper plate was slowly lowered down towards the sample to minimize structural changes in the samples during loading and handling. For the removal of sample history, these samples were initially sheared at a strain rate of 0.01 $s^{-1}$. This method was repeated each time before measurement to get repeatable and geometry-independent data for gel samples, ensuring that our samples lacked wall slip effect and loading history. Each gel sample was subjected to a frequency sweep from $\omega$ = 0.1-100 rad/sec with a continuous

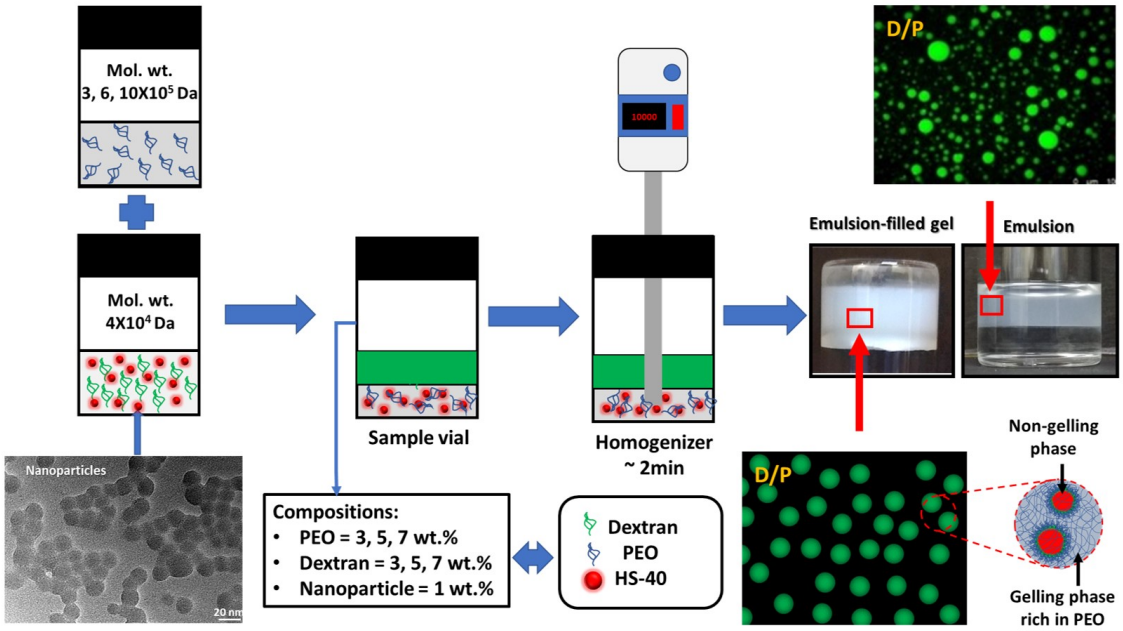


Figure 4.1: Schematic description showing the process of making nanoparticle-stabilized w/w emulsions and emulsion-filled gel.

oscillatory strain of $\gamma = 0.1$ %, followed by an oscillatory strain sweep from $\gamma = 0.01$-100 % at a constant angular frequency $\omega = 10$ rad/sec. During every shear rheological experiment, the storage and loss moduli (G' and G") were measured. The viscosity of the as-synthesized emulsion products was measured at a room temperature of 25°C and a varied shear rate of $0.01 - 100$ $s^{-1}$.

### 4.2.4 Characterization

The electrophoretic study was carried out using the Zeta-sizer (Make: Malvern Panalytical Ltd., Model: Nano ZSP) to measure the $\zeta$ potential of the HS-40 nanoparticles. We used high-resolution transmission electron microscopy (HRTEM), Make: FEI Company, Model: Tecnai G2 20, to deduce the average size of the HS-40 nanoparticles. To visualize the structural state of APTS in the liquid and solid state, we employed inverted light microscopy (Carl Zeiss. AxioVert. A1) and scanning electron microscopy (SEM), JEOL, JSM-6610. To comment on the type of emulsions, whether PEO-in-dextran (P/D) or dextran-in-PEO (D/P), fluorescent microscopy (Leica Microsystem, DMIL) was used in a few sets of experiments. All the rheological experiments were performed on the MCR-702 rheometer, Anton Paar GmbH, Germany, to characterize the emulsion-filled gels and probe the Pickering emulsion-gel transition. The sessile drop experiments were conducted to determine the three-phase contact angle of water with a suitable substrate using an optical tensiometer (Make: Biolin Scientific, Model: Theta Flex).

Note: All experiments were triplicated to ensure the required consistency of the results. The standard deviation for each data point is within the 5-10% tolerance limit. We omitted the error bars from certain rheological graphs and displayed the average data from three

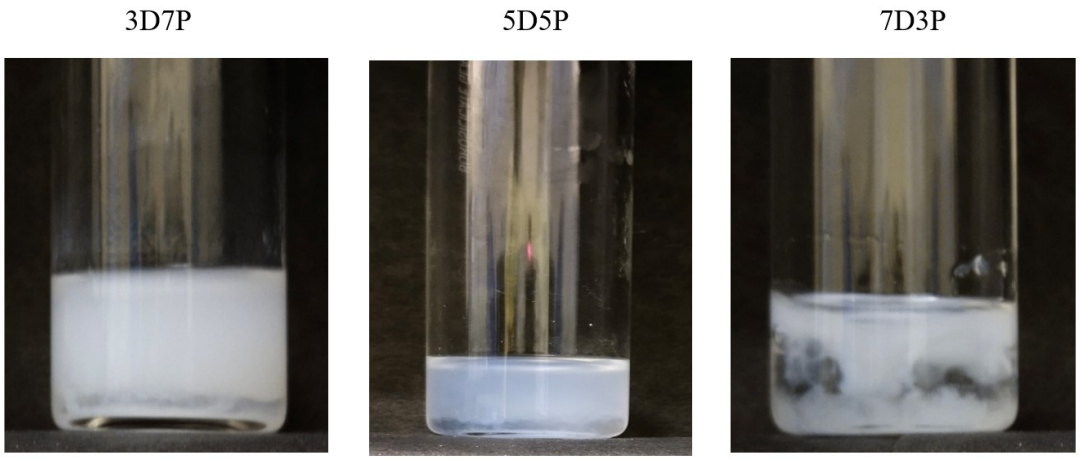


Figure 4.2: Snapshot of vial images depicting the catastrophic destabilization of w/w emulsions stabilized by HS-40 nanoparticles in the presence of low molecular weight PEO ($1\times10^5$ g/mol) and dextran ($4\times10^4$ g/mol).

separate runs. It was done to declutter the information. The creaming index of the as-synthesized emulsion samples was analyzed using Image-J software.

## 4.3 Results and discussion

First, it is demonstrated that adjusting the molecular weight of the polymer constituting the continuous phase influences the stability of the emulsion droplets. It can be inferred from Figure 4.2 that the emulsion droplets stabilized by HS-40 nanoparticles in the presence of PEO labelled with a molecular weight of 1E5 destabilize catastrophically within one week of sample preparation. This finding was consistent with our previous work (Chapter-3) for w/w emulsion droplets stabilized by HS-40 or CL-30 alone using a vortex mixer (Shekhar et al. [112]). Compared to the vortex mixture, the stability of w/w emulsion droplets stabilized by HS-40 alone using homogenizer increased slightly, albeit the entire system remained stable for only up to seven days. Further, it has been investigated to show how the molecular weight of the polymers played a role in producing stable w/w emulsion droplets in addition to the external processing aids like an emulsifying device because, unlike o/w and w/o emulsions, w/w emulsions are primarily concerned with polymer-particle and particle-particle interactions. It is envisaged that a change in molecular weight would impact interactions and viscosity, preventing early droplet disintegration via coalescence.

The systematic experimental observation by adjusting polymers' concentration, molecular weight, and storage time suggests that emulsion-filled gels can be produced without heat treatment, acidification, enzyme treatment, or adding calcium ions to the formulations. The images of vials in Figure 4.3 illustrate the emulsion-gel transition in ATPS. The transition from emulsion to emulsion-filled gels is readily seen in the images of the vials.

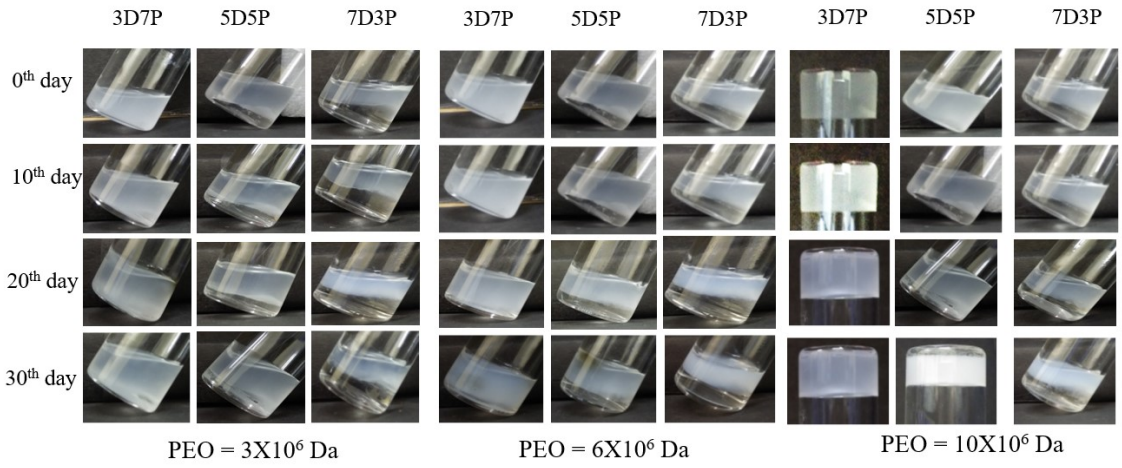


Figure 4.3: Snapshot of vial images showing the state of emulsion phases at different combinations of molecular weight, compositions, and storage time.

On day zero, the sample corresponding to 3D7P (3% dextran and 7% PEO) generated from PEO with an Mwt of $10 \times 10^5$ Da displays emulsion gel formation. Observations made after 48 hours have been used as a reference point, i.e., $0^{th}$ day, for all samples. After 30 days of observation, a similar transition was detected in the 5D5P (5% dextran and 5% PEO) sample of $10 \times 10^5$ Da. Please notice that vials 3D7P (all time points) and 5D5P (30th day), which correspond to the molecular weight $10 \times 10^5$ Da, have been presented inverted. The gel formation was so robust that even after 90 days of observation, it did not flow when held inverted. Figure 4.4 shows that generating emulsion-filled gels requires a combination of high molecular weight PEO, dextran and low-concentration silica nanoparticles. However, high molecular weight PEO and low concentration silica nanoparticles alone did not create permanent gels. Several experiments have shown that when a low molecular weight component (D) is dispersed in a matrix of high molecular weight polymers, such as PEO, the inter-molecular forces between the polymer (D)-polymer (P) and polymer (P)-particles are strong enough to hold their weight. It can be postulated that the silica nanoparticles' strong attraction to the PEO active sites may result in the formation of an intricate three-dimensional network structure.

Figure 4.5 depicts the representative inverted microscopic images of w/w emulsions stabilized by HS-40 nanoparticles. Intriguingly, the droplets produced by the emulsification have stayed stable for 30 days without transforming into a secondary state such as bijels or bi-continuous channels. Note: A transition from droplets to bijels in ATPS stabilized by oppositely charged nanoparticles (OCNPs) is reported in Chapter-1. Therefore, it is asserted that the micro-graphed structure is in a thermodynamic equilibrium condition. Furthermore, fluorescent microscopy has been employed to characterize the samples to probe the type of emulsion formed. For this study, fluorescently-labelled dextran was utilized to visualize the structure of the emulsion

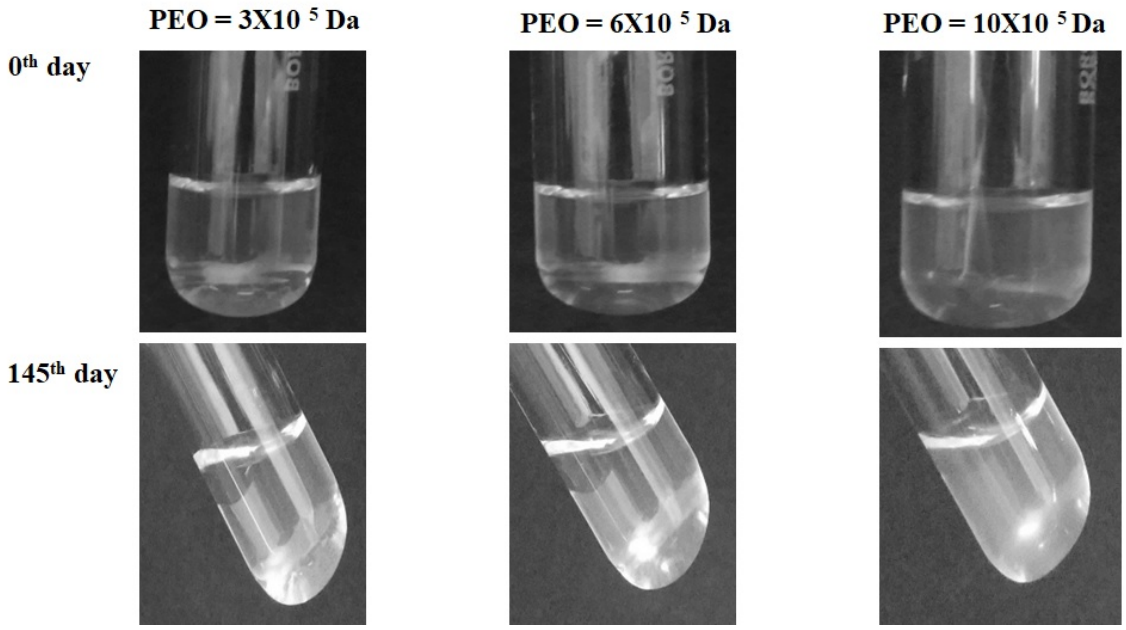


Figure 4.4: Snapshot of vial pictures depicting the state of binary mixtures containing PEO (7 wt.%) and HS-40 (1 wt.%) without the presence of a third component (dextran).

state distinctly. As seen from Figure 4.6, the continuous phase comprises the polymer with the highest concentration. Thus, dextran-in-PEO (D/P) was seen with 3D7P, whereas 7D3P led to the phase inversion of PEO-in-dextran (P/D) independent of the PEO molecular weight employed. This trend agrees with the works of several researchers reported in the literature (Balakrishnan et al. [36], Dumas et al. [127], Gonzalez-Jordan et al. [55], Kulkarni and Mani [61]). The dextran utilized in the emulsification process was fluorescently tagged with FITC. As a result, the droplets in the image become green while the PEO remains black. The investigation based on Figures 4.5 and 4.6 aided in developing the state diagram. Figure 4.7 illustrates the phase inversion and Pickering emulsion-to-emulsion-filled gel transition under specific experimental conditions. Intriguingly, ATPS exhibits three distinct structural states as a function of Mwt, the concentration of PEO and dextran, and ageing time: 1) D/P droplets, 2) P/D droplets, and 3) D/P emulsion-filled gels.

Next, the stability analysis using the "creaming index (CI)" is presented. Note: Since catastrophic breakdown occurs in the sample corresponding to PEO with an Mwt of $1 \times 10^5$ Da, we have excluded them from the CI investigations. It has been chosen to demonstrate the stabilization of w/w emulsion at three different two-phase system compositions, i.e., 3% dextran & 7% PEO (3D7P), 5% dextran & 5% PEO (5D5P), and 7% dextran & 3% PEO (7D3P). These combinations of PEO and dextran represent two-phase systems per the binodal curve, as discussed in Chapter 3. The CI quantifies the volume fraction of emulsion generated in the binary mixture. In the production of emulsion products, a CI of 80-100 % is often considered to be substantial. For the

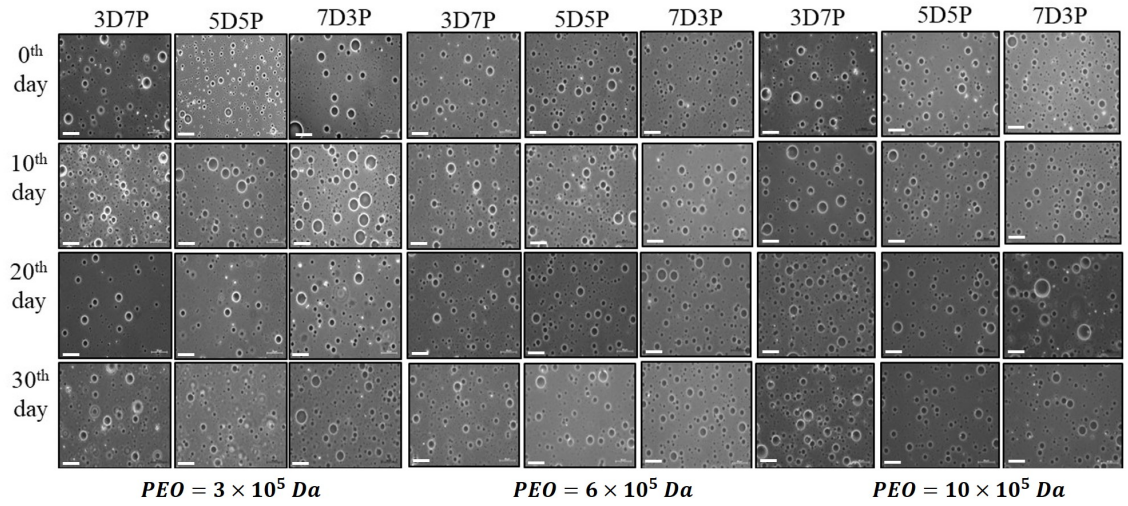


Figure 4.5: Inverted microscopic images showing the structural state of w/w emulsions stabilized by HS-40 at different storage times, molecular weight of PEO, and concentration of PEO/dextran. The scale bar given in the images corresponds to 50 $\mu$m.

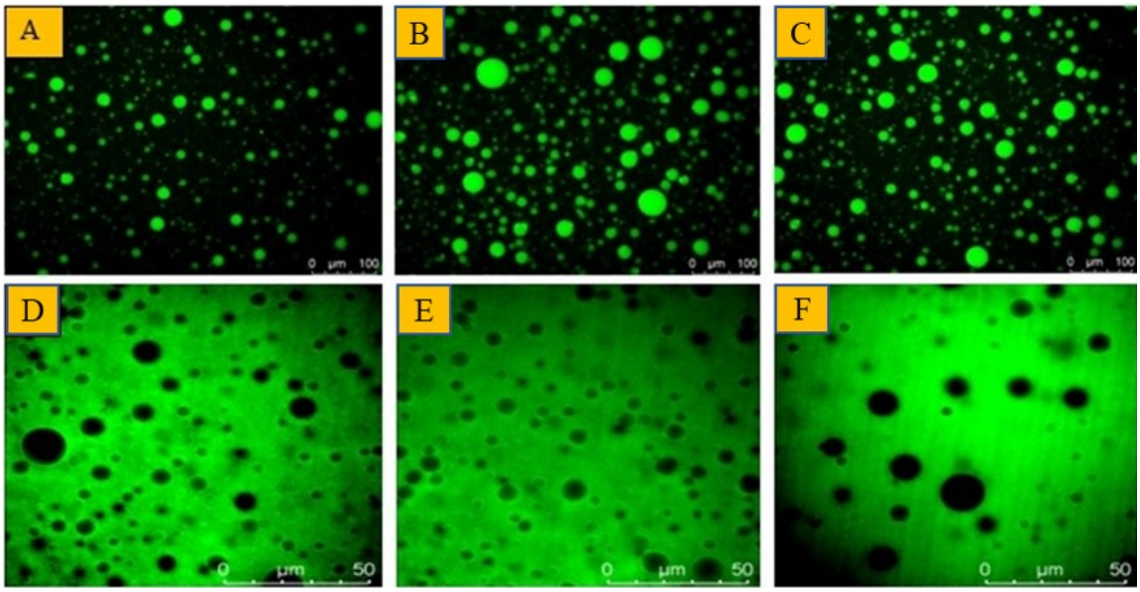


Figure 4.6: Fluorescent microscopic images demonstrating the type of emulsions formed at a different molecular weight of PEO and the concentration of PEO/dextran. A-C) The state of emulsion generated from the aqueous solutions of dextran and PEO with different molecular weights of $3 \times 10^5$, $6 \times 10^5$, and $10 \times 10^5$ Da at 3D7P, respectively. D-F) The state of emulsion generated from the aqueous solutions of dextran and PEO with different molecular weights of $3 \times 10^5$, $6 \times 10^5$, and $10 \times 10^5$ Da at 7D3P, respectively.

calculation of CI, the ratio of h/H is determined based on the image analysis using ImageJ. The average value of h/H is reported by analyzing several images obtained from each vial. Thus, the average CI value multiplied by 100 for each sample is plotted against the number of days to determine any divergence from the reference point (0th day). Figure 4.8 describes the creaming index of the samples corresponding to $3 \times 10^5$, $6 \times 10^5$, and $10 \times 10^5$ Da. Referring to Figure 4.8, it can be observed that the particle-stabilized emulsion or emulsion-filled gels remained intact regardless of the molecular weight of

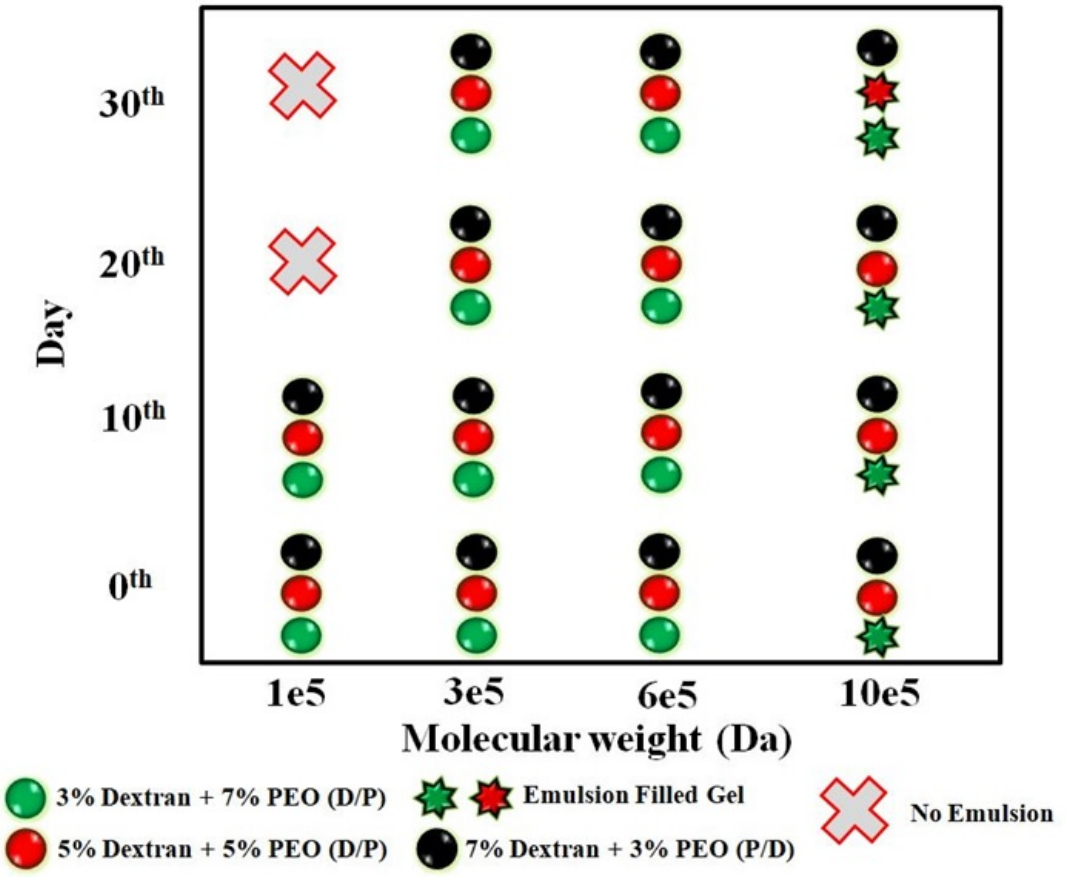


Figure 4.7: State diagram depicting different structural states of ATPS stabilized by HS-40.

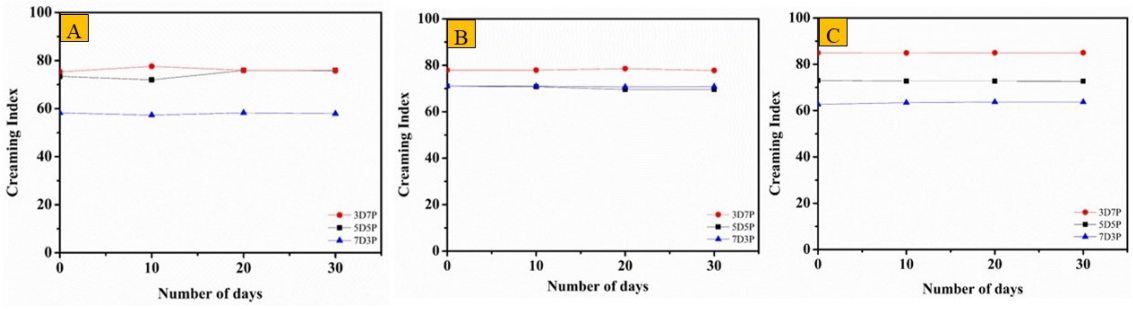


Figure 4.8: Creaming index of ATPS pertaining to different molecular weights. A) 3 × $10^5$ Da, B) 6 × $10^5$ Da, and C) 10 × $10^5$ Da, respectively.

PEO and the compositions of binary systems. This behaviour represents the synergistic ability of a PEO with a larger molecular weight PEO (> 1 × $10^5$) to stabilize ATPS as a stabilizer. As a result of the synergistic action of PEO and nanoparticles, the average value of CI for the sample corresponding to 10 × $10^5$ Da and 3D7P exceed 80%, representing a noteworthy contribution.

Referring to Figure 4.6, it can be asserted that the gels created in our work are not emulsion gels since there is no evidence of fractal network creation or droplet flocculation. The lack of droplet flocculation might be due to steric repulsion generated by polymer

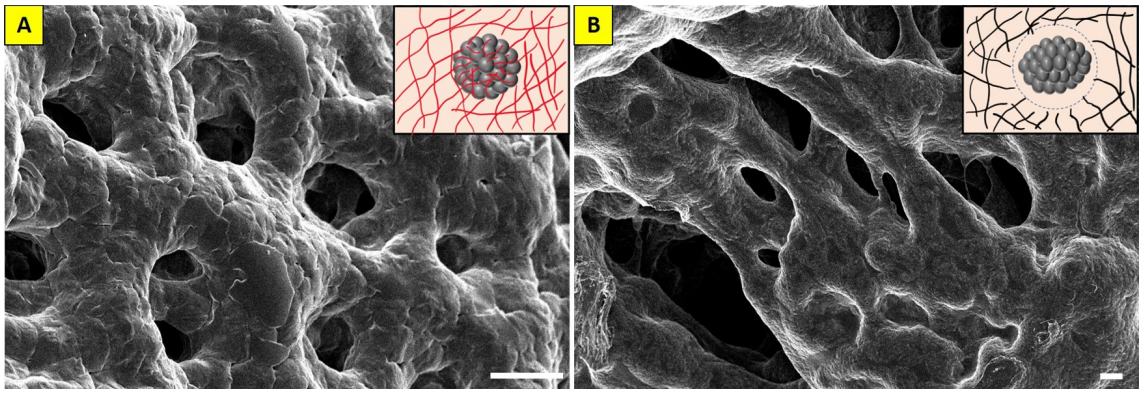


Figure 4.9: The scanning electron microscopy images showing the micro-structure of 10 $\times$ $10^5$ Da samples at different compositions after drying. A) 3D7P B) 7D3P, respectively. The scale bar given in the images corresponds to 50 $\mu$m.

molecules grafted to the surface of silica nanoparticles. However, the transition from emulsion to emulsion-filled gels observed in the samples corresponding to 10 $\times$ $10^5$ Da as shown in Figure 4.3 intrigued us to probe the micro-morphology of the obtained structures. It can be visualized that the dried form of the textural features of the sample by scanning electron microscopy (SEM). The sample's microstructure corresponding to Figure 4.9A depicts the gelling nature of PEO and droplets (active filler) due to the adsorption of PEO on the silica nanoparticles. In contrast, the morphology shown in Figure 4.9B is analogous to the inactive filler particle arrangement, as reported by several researchers in the literature (Oliver et al. [118], Dickinson [124], Chen and Dickinson [128]). The weak interaction between PEO-dextran and dextran-particles and the strong interaction between PEO-particles can be attributed to the structural arrangement of "inactive and active filler particles". The weak interaction between particle-stabilized droplets and dextran causes discontinuity at the junction, and therefore, the gel formed at dextran-rich compositions (7D3P) did not yield emulsion-filled gels even when PEO with a higher molecular weight (10E5) was employed. Consequently, the classification of the diverse ATPS samples revealed two main types of gels: 1) permanent gel and 2) weak gel. According to the state diagram in Figure 4.7, these permanent and weaker gels are described as particle-stabilized emulsion-filled gels and P/D or D/P emulsions. It is essential to resort to suitable structural probing as the light microscopic analysis did not aid in visualizing the emulsion-filled gel distinctly. Several ATPS samples have been tested using a rheometer to qualitatively and quantitatively characterize the transition.

We performed oscillatory shear tests by subjecting samples to strain and frequency sweeps. First, strain sweep tests were performed for all the samples generated with various molecular weights of the polymer at strain $\gamma$ = 0.01% - 100% (see Figure 4.10) at constant angular frequency $\omega$ = 10 rad/sec and constant temperature 25$^o$ C. In Figure 4.10, we plotted the ratio of loss to storage modulus ($\tan(\delta) = G''/G'$) v/s $\gamma$ for different times. The constant value of $\tan(\delta)$ indicates that the linear viscoelastic zone occurred until 10% strain and that all molecular weight systems exhibited liquid-like behaviour.

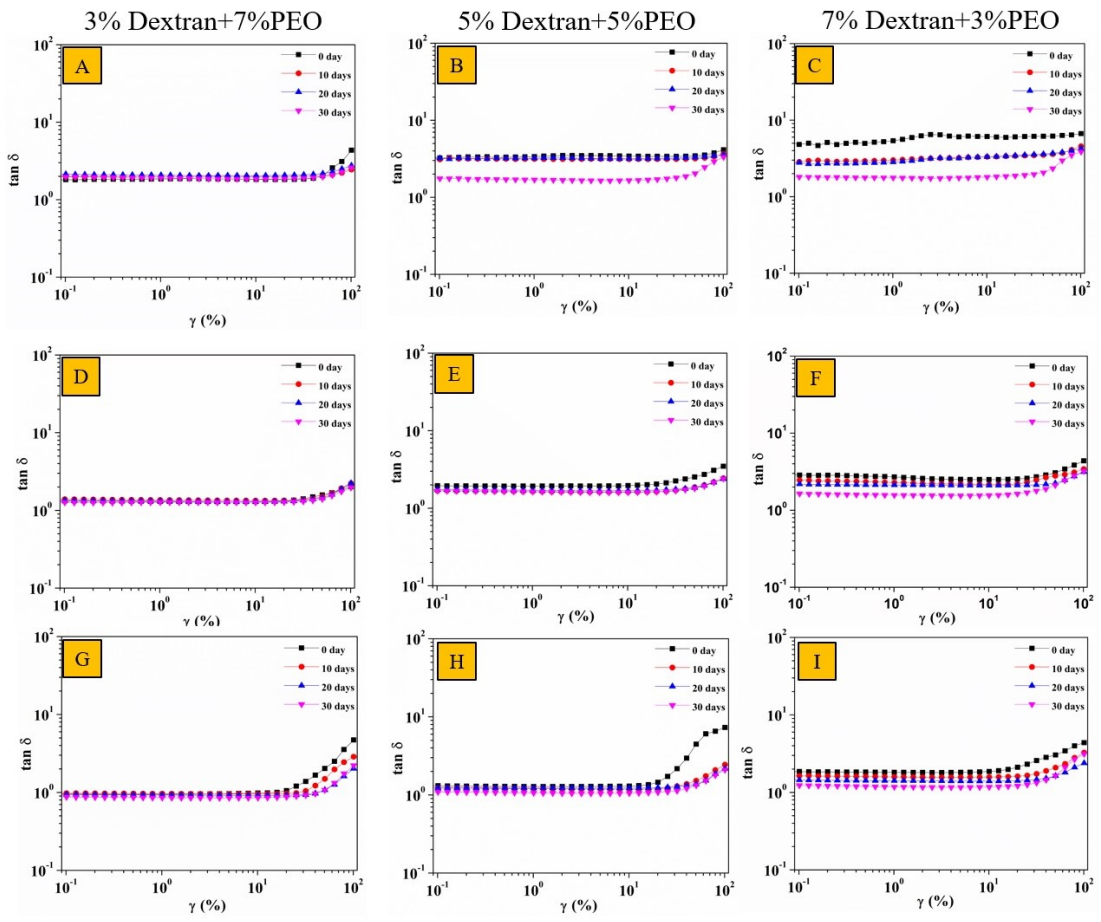


Figure 4.10: Strain sweep of the formed emulsion gel. A-C) PEO with the molecular weight of $3 \times 10^5$ Da, D-F) PEO with the molecular weight of $6 \times 10^5$ Da, G-I) PEO with the molecular weight of $10 \times 10^5$ Da.

Further rise in shear strain $\gamma$ results in a rapid increase in $\tan(\delta)$, indicating that the produced gel is deforming or droplets are elongated in the direction of the applied shear. As can be inferred from Figures 4.10 A, D, and G, there is no change in the $\tan(\delta)$ with time, which represents the usual rheological properties of emulsion systems and can be deformed when high shear is applied. On the other hand, as the concentration of non-gelling phase polymer went up, we observed a slight or significant change in $\tan(\delta)$ over time, regardless of the molecular weight (Please refer to Figures 4.10 B, C, E, F, H, and I). Changes in $\tan(\delta)$ over time suggest that gels are forming and emulsion phases are changing because the composition of the systems is changing from 7D3P to 3D7P. We did not observe a crossover between $G'$ and $G''$ in the strain sweep, which suggests that the gel is like a liquid or is soft.

All emulsions act as liquids at lower frequencies, confirming the frequency-dependent behaviour of the system. Experiments on frequency sweeps were conducted at a constant $\gamma = 0.1\%$ (under linear viscoelastic region (LVE)) from $\omega = 100 - 0.1$ rad/sec at $25^oC$ (Figure 4.11). The produced emulsion/gel exhibits frequency-dependent molecular weight

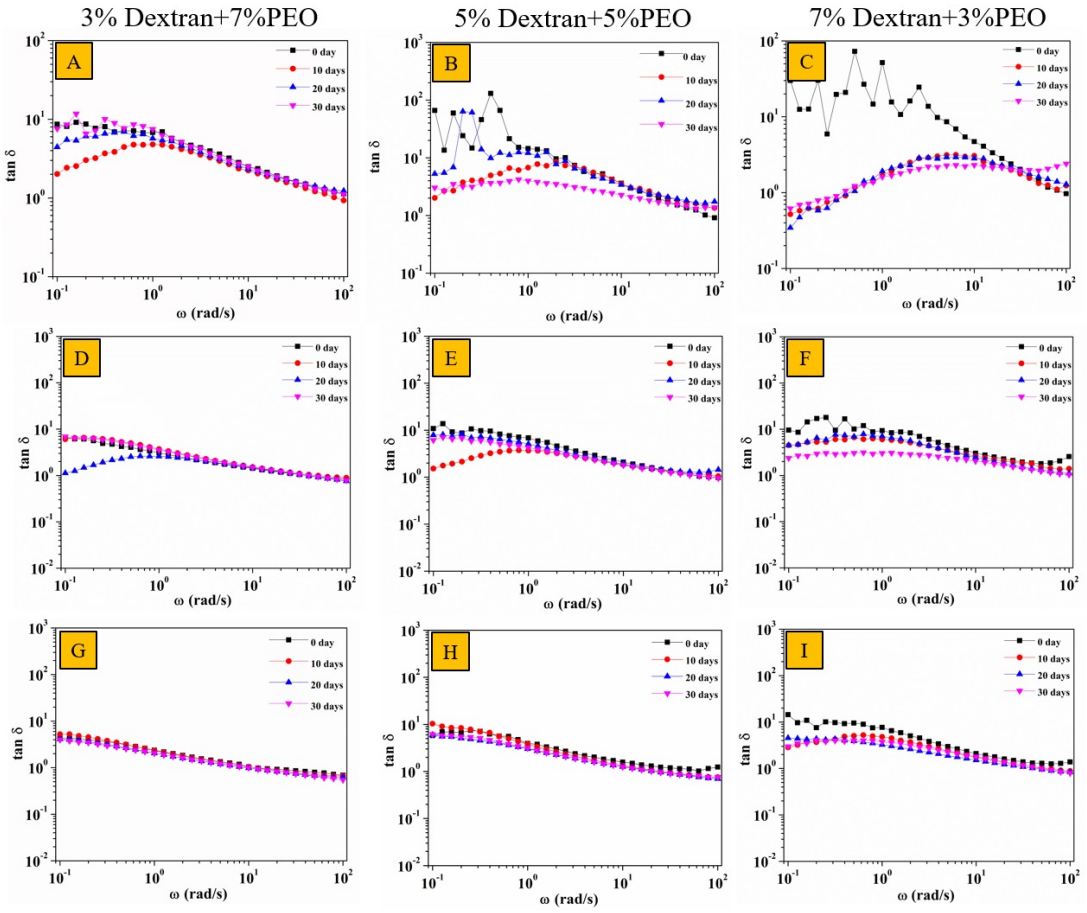


Figure 4.11: Frequency sweep of the generated emulsion systems. A-C) PEO with the molecular weight of $3 \times 10^5$ Da, D-F) PEO with the molecular weight of $6 \times 10^5$ Da, G-I) PEO with the molecular weight of $10 \times 10^5$ Da.

and polymer concentration behaviour. At a low molecular weight of PEO (Please refer to Figures 4.11A-C) and at a higher frequency, there is no crossover of $G'$ & $G''$ and tan($\delta$) is almost equal to 1 for all polymer concentrations except for 7D3P at lower frequencies. In addition, the rise in tan($\delta$) with decreasing frequency indicates no gel formation in the system, as it acts as a liquid. The tan($\delta$) shows maxima for all concentrations. This maximum shifts towards the higher frequency as we increase the concentration of non-gelling polymer, i.e. dextran (Figure 4.11A-C). We ascribe the small reduction in tan($\delta$) for the 7D3P system below 1 to the solid-like behaviour of droplets at lower frequencies.

Further increasing the molecular weight from $3 \times 10^5$ to $6 \times 10^5$ Da of PEO, no gel formation has been seen until the 30th day (Please refer to Figures 4.11 D-F). However, a further increase in the molecular weight of the PEO from $6 \times 10^5$ to $10 \times 10^5$ Da leads to the gel formation, and hence the crossover at a frequency of $\omega \approx 30$ rad/s is observed. For the maximum concentration of gelling polymer (3D7P), the ratio of loss to storage modulus is less than 1 (tan($\delta$) $< 1$), indicating the solid-like behaviour as early as the 0th day. On day 30, gel formation is detected at a frequency of $\omega = 80$ rad/sec when the

concentration of dextran is raised to 5D5P. This trend demonstrates that gel formation is a time-dependent phenomenon, implying that the adsorption of free polymer in the continuous phase is sluggish at equal polymer concentrations. We hypothesize that the change in the continuous phase composition at the end of 30 days would have caused the transition from emulsion to a gel state. In other words, the diffusion of PEO molecules from the interior of droplets to the exterior (bulk) would have helped attain the required concentration of PEO to induce gelling.

Next, the emulsions' viscosity for all PEO compositions and molecular weights is demonstrated. As shown in Figure 4.12, the viscosity of the emulsion was measured as a function of shear rate ($\dot{\gamma}$ = 0.01 - 100 $s^{-1}$). Due to changes in the structure and arrangement of the droplets, the viscosity of all emulsion compositions exhibits shear-thinning behaviour at high shear rates. The viscosity drops gradually in all cases, followed by a sudden reduction at a high shear rate. At first, confined droplets resist the shear force. Further increment in the shear rate forces the droplets to lengthen in the direction of the applied shear, resulting in a minor reduction in viscosity. After a critical shear rate, the elongated droplets fragment into smaller droplets, and the viscosity stabilizes after a rapid decrease. Tea et al. [59] (2020) demonstrated similar phenomena of droplet deformation under shear in w/w emulsion. Increasing the molecular weight of the polymers leads to an increase in the emulsion's viscosity (Please refer to Figure 4.12). As shown in Figures 4.12 A-C, for the emulsion with low molecular weight PEO ($3 \times 10^5$ Da) at a high concentration of PEO (3D7P), viscosity is high, and the droplets are stable concerning the time, while at low concentration (7D3P) the emulsion shows the low viscosity and increment with time because the trapped droplets tend to form weak network structures in non-gelling phase. This increase in viscosity with time is consistent with the gel formation findings as a function of time stated before. The emulsion with an equal concentration of both polymers (5D5P) shows the intermediate results in all the molecular weight systems. Further increasing the molecular weight (from 6 to $10 \times 10^5$ Da) (Please refer to Figures 4.12D-F and G-I) leads to an increase in the viscosity of the system, which is in agreement with the typical characteristics of a polymer solution, i.e., higher molecular weight corresponds to a high number of polymer chains and thus the higher viscosity. By referring to Figure 4.12, we infer that the droplets tend to rupture under shear, resulting in the shifting of a dramatic reduction in viscosity. This behaviour is often encountered in emulsions that undergo a phase transition. The increase in viscosity with time demonstrates the increased adsorption of the polymer on the particle-stabilized droplets.

The change in storage and loss moduli at $\gamma$ = 0.1% and $\omega$ = 10 rad/sec is observed within the LV region and viscosity at $\dot{\gamma} = 0.1$ $s^{-1}$, concerning time, as shown in Figure 4.13, to understand the influence of time on the emulsion and the gel. At low molecular weight ($3 \times 10^5$ Da), we observed that the loss modulus is more than the storage modulus

till 30 days in all compositions, which shows that there are no gel formations at the low molecular weight shown in Figure 4.13A. The slight increase in $G'$ & $G''$ is due to the droplet arrangement under the shear as shown in Figure 4.14. The viscosity of all emulsions increases till the 10th day in all the compositions, while in 3D7P and 5D5P is constant after the 10th day as shown in Figure 4.13D. Further increasing the molecular weight of the gelling phase polymer ($6 \times 10^5$ Da) shown in Figure 4.13B, increases the adsorption of the polymer chain on the particles showing a significant rise in $G'$ as compared to lower molecular weight. However, no gel formation is happening till 30 days, irrespective of the compositions. The plot of viscosity vs time for the sample corresponding to $6 \times 10^5$ Da capitulates the similar behaviour described in Figure 4.13E.

The gel formation has been observed for the 3D7P sample with the maximum molecular weight ($10 \times 10^5 Da$) of PEO represented in Figure 4.13C) from day zero, resulting in $G' = G''$. This trend shows the gel-like property up to the $30^{th}$day, indicating the maximal polymer coverage on the droplets. In the case of 5D5P, although $G'$ & $G''$ are slightly different, they are constant after $10^{th}$day. Intriguingly, both $G'$ & $G''$ exhibit a falling trend after 20 days, which may be attributable to the change in PEO concentration from

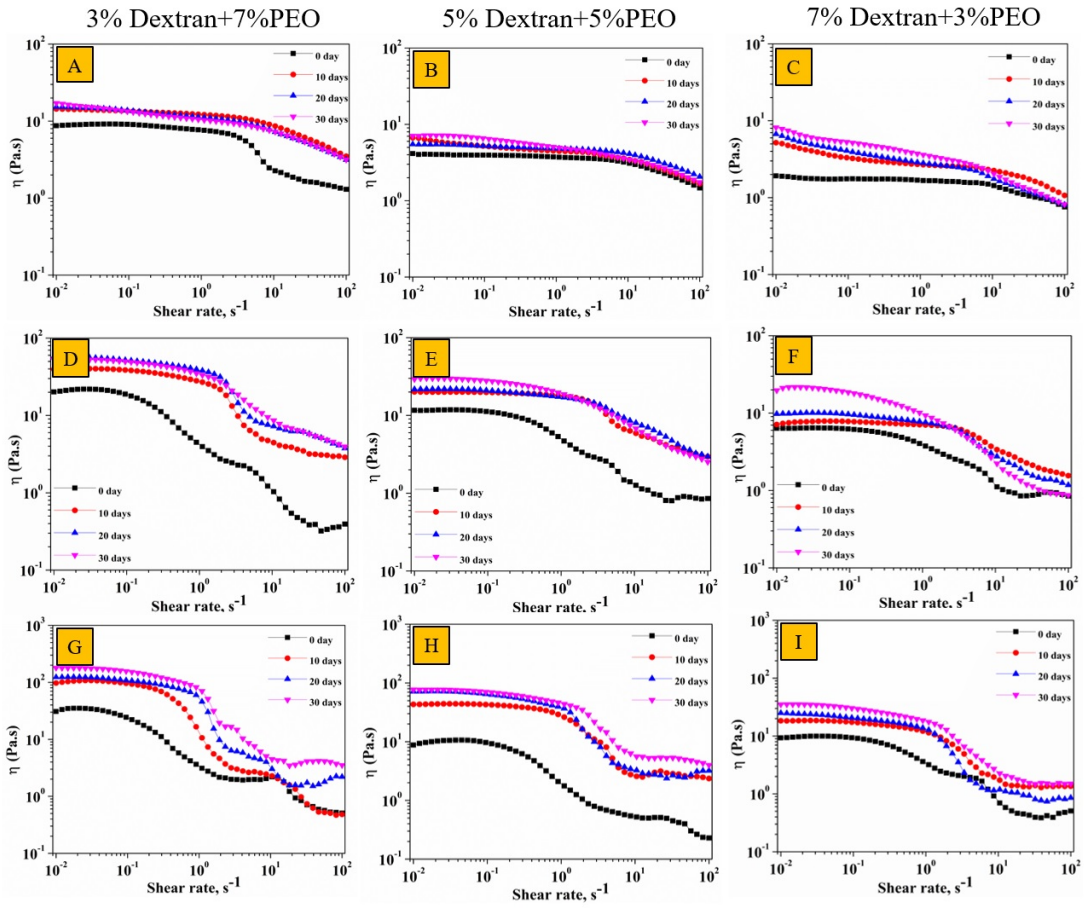


Figure 4.12: Viscosity of the formed emulsion. A-C) PEO with the molecular weight of $3 \times 10^5$ Da, D-F) PEO with the molecular weight of $6 \times 10^5$ Da, G-I) PEO with the molecular weight of $10 \times 10^5$ Da.

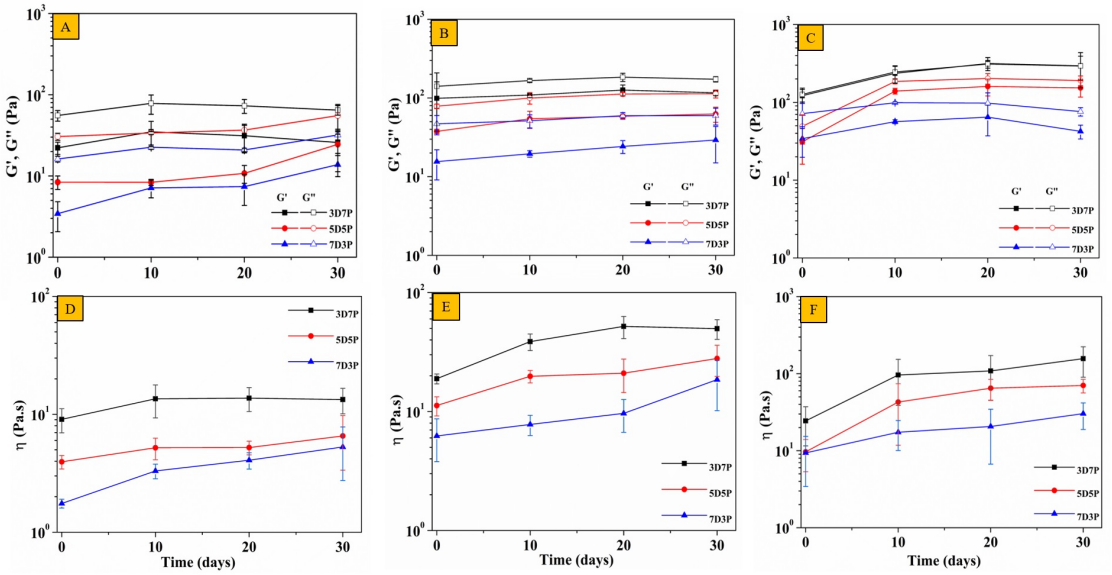


Figure 4.13: Effect of storage time. A-C) Change in storage and loss moduli of the emulsion samples prepared at a different molecular weight of PEO such as $3 \times 10^5$, $6 \times 10^5$, and $10 \times 10^5$ Da, respectively. D-F) Viscosity of the emulsion samples prepared at a different molecular weight of PEO, such as $3 \times 10^5$, $6 \times 10^5$, and $10 \times 10^5$ Da, respectively.

5% to 3%. Nevertheless, the magnitude of $G'$ is $\approx 5$ times more than the case of $6 \times 10^5$ Da at 7D3P. On the other hand, the viscosity of the gel after the $10^{th}$day is constant but shows a slight increase on the $30^{th}$ day. It is speculated that this constancy in viscosity is due to the adsorbed polymers and the arrangement of the droplets under the shear, as shown in Figure 4.14. The phase transition occurs in emulsion with composition 7D3P for all molecular weights of PEO. As shown in Figure 4.13F, the viscosity of 7D3P emulsions shows a continuous increase from $0^{th}$ day to $30^{th}$ day which can be attributed to the gel droplets dispersed in the non-gelling polymer. These observations reiterate that the emulsion is stable up to $30^{th}$ day. On a lighter side, we established the emulsions' stability using the CI investigations shown in Figure 4.8).

An attempt has been made to compare the flow behaviour of emulsion and emulsion-filled gel to well-known constitutive models that typically describe the non-Newtonian behaviour of the suspensions. Krieger [129] (1963) presented a dimensional approach to colloidal rheology. This approach is devised to apply dimensional analysis to compare the rheological behaviour of colloidal systems. The system chosen in our study is analogues to the suspension of the rigid spheres in a continuous medium. The viscosity of the model suspension proposed by I.M. Krieger depends on several factors, such as the viscosity of the medium ($\eta_0$), the radius of the spheres (a), the number density of the particles (n), density of the particles ($\rho_p$), density of the medium ($\rho_0$), shear rate ($\dot{\gamma}$), time (t), and thermal energy ($k_B$T). Krieger arranged these nine variables in different combinations to form six independent dimensionless groups, expressible in three dimensions, to get some

physical insight. Among these, the internal Reynolds number ($R_i$) and colloid number (C) best signify the motion of the colloidal spheres when exposed under different shear rates. With this insight into dimensionless groups, the rheological equation for the rigid sphere can be written as shown in Eq. 4.1.

$$\eta_r = f(v, C, t_r, \rho_r, R_i) \tag{4.1}$$

The parameters $v$, C, $t_r$, $\rho_r$, and $R_i$ refer to volume fraction, colloid number, reduced time, density ratio, and internal Reynolds number, respectively.

The colloid number is described as below Eq. 4.2 (Krieger [129])

$$C = \eta_0 a^3 \dot{\gamma} / k_B T \tag{4.2}$$

The parameters $\eta_0$, $a^3$, $\dot{\gamma}$, $k_B$T refer to the viscosity of the medium, radius of droplets, rate of shear, and thermal energy, respectively.

The reduced viscosity ($\eta_r$) is defined as follows,

$$\eta_r = \frac{\eta}{\eta_0} \tag{4.3}$$

Where $\eta$ and $\eta_0$ refer to the viscosity of the sample measured at a particular rate of shear and viscosity of the medium, respectively.

The purpose of using the Krieger constitutive relation discussed above is to compare the motion of the colloids in the emulsion as well as the gel state. The Krieger model will hold for the emulsion system as it can be treated as rigid spheres but not for the gel system, which is more complicated than a simple sphere. So, it is anticipated that the samples that showed emulsion characteristics would fit the Krieger model very well.

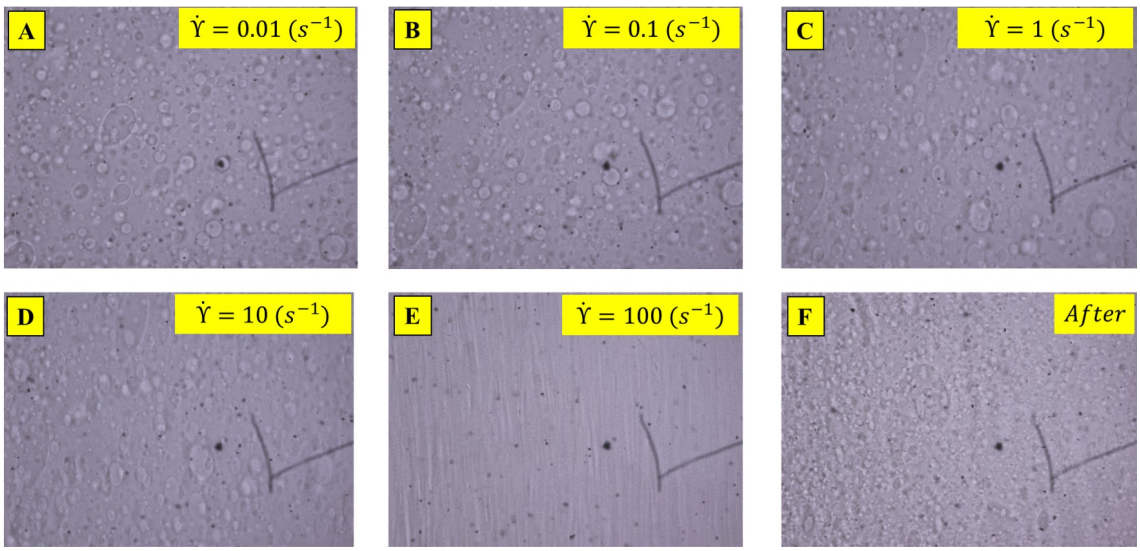


Figure 4.14: Effect of shear on the emulsion droplets. A) $\dot{\gamma}$ = 0.01 $s^{-1}$, B) $\dot{\gamma}$ = 0.1 $s^{-1}$, C) $\dot{\gamma}$ = 1 $s^{-1}$, D) $\dot{\gamma}$ = 10 $s^{-1}$, E) $\dot{\gamma}$ = 100 $s^{-1}$, and F) After releasing the shear.

Consequently, the structural transition from emulsion to gel was distinctly seen when the molecular weight of PEO was tuned from $3 \times 10^5$ to $10 \times 10^5$ Da. This method helped us understand the difference between the formation of emulsion-filled gels and other structures. For brevity, the studies have been restricted to higher shear rates at which the droplets would invalidate the assumptions of rigid spheres. Therefore, the shear rheology has been performed with a maximum shear rate of 100 $s^{-1}$ as the droplets exposed within this range did not elongate throughout our tests. Figure 4.15 shows the model fitting on the experimental data corresponding to formed emulsion and emulsion-filled gel. The fitting of the Krieger model to the experimental data proves that the emulsion behaves like a suspension of soft polymer particles, and droplets behave like soft particles under the applied shear. Figure 4.15 A and B display the characteristics behaviour of emulsion systems at $0^{th}$day and $30^{th}$day under different strain rates. It can be inferred that there is no significant change in the rheological behaviour of the samples when compared at different storage times. Furthermore, the line drawn using the constitute relation proposed by Krieger passes through the experimental data points with no or little deviation. This trend confirms that the droplets behave like rigid particles and tend to develop robust resilience against coalescence and creaming for at least 30 days, as there was no deviation between model and experimental points on the samples corresponding to $30^{th}$day. Similar arguments can be presented for the case of $6 \times 10^5$ Da. It is intriguing to note that the behaviour of the samples made up of $10 \times 10^5$ Da PEO agrees with the findings of other rheological studies such as frequency sweep, amplitude sweep, and a flow curve. As shown in Figure 4.15 E and F, the deviation between the model and experimental data is seen. Since the sample represents the emulsion-filled gels at $0^{th}$day, the rheological behaviour corresponding to data points shown in the case of 3D7P lags behind the Krieger model to a significant level. Further, the three-dimensional network-like structure is evident from the nature of the trend that shows substantial deviation from the ideal at both $0^{th}$ and $30^{th}$day for 3D7P and 5D5P, which strengthens our understanding of the occurrence of emulsion-gel transition at a particular experimental regime.

Here, the probable mechanism of structural evolution to form a three-dimensional network-like permanent gel is presented. As discussed through the control studies, the combination of high molecular weight PEO, low molecular weight dextran, and a low concentration of silica nanoparticles is required to trigger the gel formation. The stability and gel formation could be attributed to the depletion flocculation induced by the PEO adsorption on the particles' surface. Numerous studies have discussed the nature of PEO-silica interactions, leading to the steric (entropic) stabilization of PEO with particles in the aqueous suspensions (Napper [130], Liu et al. [131], Saito et al. [132]). To cite a few, the work of Napper [130] (1977) and Liu et al. [131] (1994) present the fact about the adsorption of the poly (ethylene oxide) on silica particles due to the steric stabilization of the polymer. The rheological features of silica suspensions flocculated by a high molecular weight polyacrylamide in a given mixture were described by Saito et al. [132]

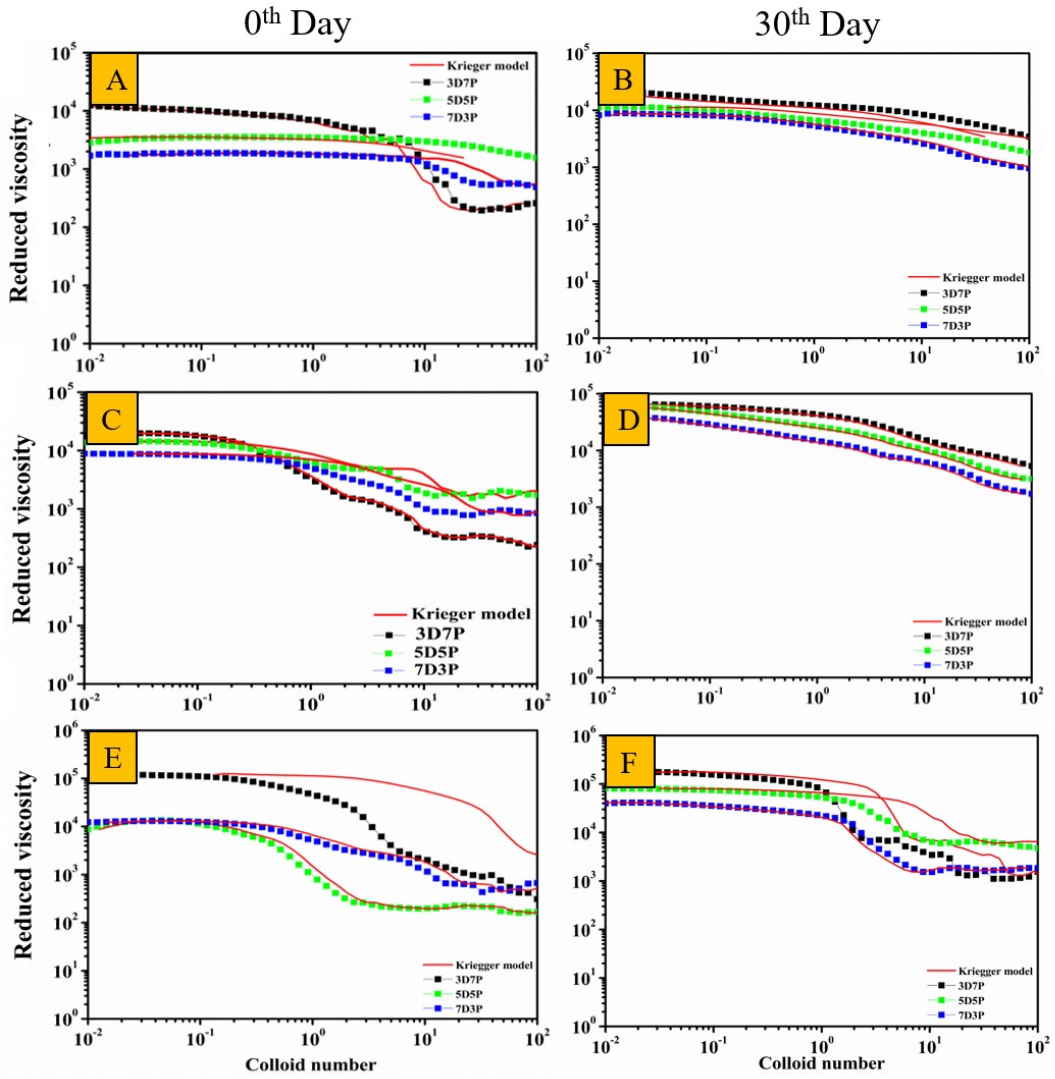


Figure 4.15: Dimensional approach using Krieger model. A, B) non-Newtonian flow curve corresponding to the PEO molecular weight of $3 \times 10^5$ Da at $0^{th}$ and $30^{th}$day, respectively. C, D) non-Newtonian flow curve corresponding to the PEO molecular weight of $6 \times 10^5$ Da at $0^{th}$ and $30^{th}$day, respectively. E, F) non-Newtonian flow curve corresponding to the PEO molecular weight of $10 \times 10^5$ Da at $0^{th}$ and $30^{th}$day, respectively.

(2011). This study revealed that an infinite network and irreversible polymer bridging of the particles could spontaneously form. Liu and Xiao [133] (2008) studied the adsorption of PEO with different molecular weights on the surface of silica nanoparticles. In that study, they reported that PEO molecules adsorb on the surface of silica nanoparticles via strong hydrogen bonding between OH groups of silica and ether oxygen groups of PEO. These authors have selected PEO with various molecular weights, including 10,00,000 g/mol (10E5) and 10 nm silica nanoparticles with a specific surface area of 250 $m^2/g$. The molecular weight and the specific surface area of interest to our study are 10E5 and 150 $m^2/g$ (calculated), respectively. We understand from the study of Liu and Xiao [133] (2008) that the zeta potential ($\zeta$) decreases with an increase in molecular weight at the same concentration of PEO due to the configuration change of the PEO segments

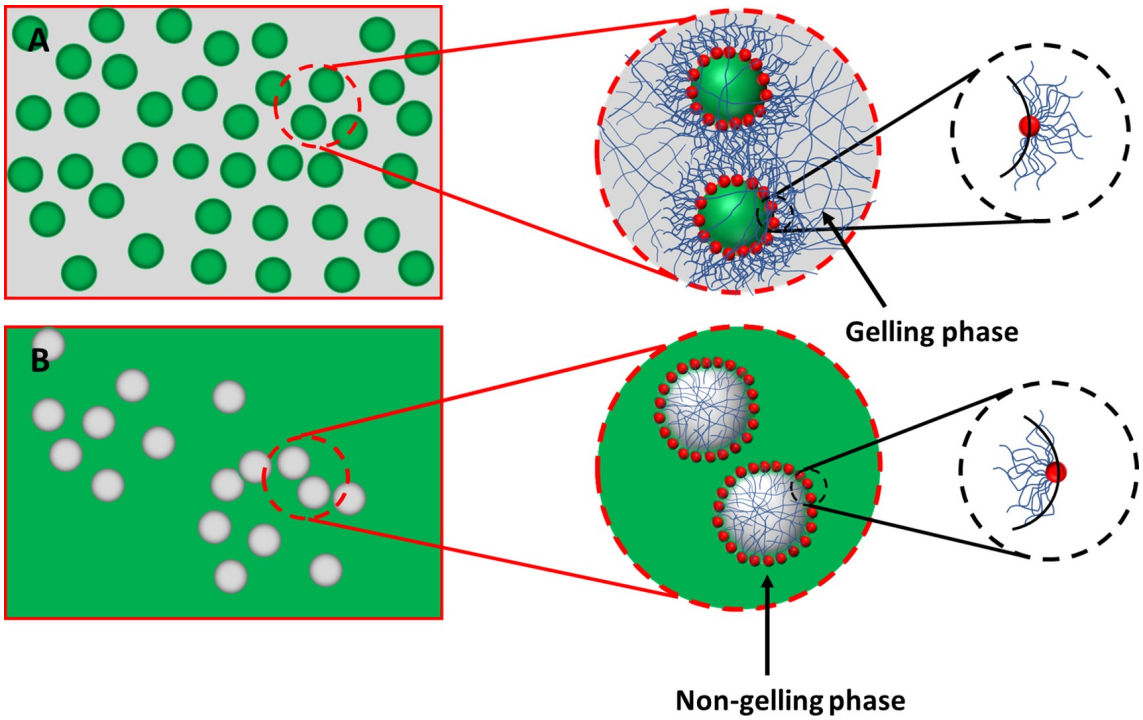


Figure 4.16: Schematic illustration describing the mechanism of generating different emulsion structures depending on the type of emulsions involved, i.e., P/D or D/P. A) Emulsion-filled gel and B) Particle-stabilized emulsion.

to loops. The decrease in $\zeta$ values contributes significantly to the net electrostatic attraction between the particles and polymers. The combined effect of net electrostatic attraction and flocculation (due to depletion effect) give rise to three-dimensional polymer network-like structures at a particular experimental regime, i.e., 3D7P and 5D5P at 10E5 molecular weight. Figure 4.16 displays the probable mechanism of forming an emulsion-filled gel under certain conditions. As shown in Figure 4.16, when the high molecular weight PEO-rich phase becomes a continuous phase, and the polymer molecules are induced to adsorb on the surface of the particles exposed to the PEO side (continuous phase), it results in the formation of particle-stabilized emulsion-filled gels instead of just w/w emulsion (Please refer to Figure 4.16A). However, the opposite is true when the samples corresponding to 7D3P in ATPS undergo phase inversion, i.e., the continuous phase becomes dispersed. In this scenario, the generated droplets will behave like soft particles due to the polymer's adsorption from the droplets' interior on the surface of the nanoparticles exposed to the dispersed phase (Please refer to Figure 4.16B). In short, the interactions between PEO and silica and adequate surface area drive the spontaneous formation of three-dimensional network-like emulsion-filled gels at a particular experimental regime. For instance, in the case of samples corresponding to 3D7P, the particles would maximize their contact area towards PEO being a continuous phase, as shown in Figure 4.16 A. In this case, the maximum surface exposure ensured the fast adsorption of PEO molecules on the silica particles.

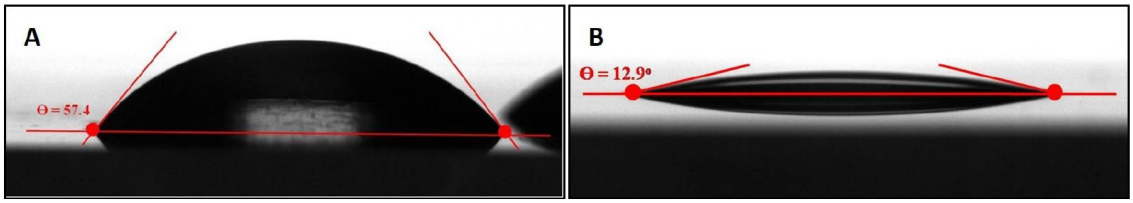


Figure 4.17: Determination of three-phase contact angle using sessile drop experiments. A) droplet containing 7% PEO and B) droplet containing 3% dextran.

Further, several sessile drop experiments have been conducted to assert the hypothesis above. As shown in Figure 4.17, the contact angle of water droplets containing PEO or dextran at a known concentration is determined using an optical tensiometer (Make: Biolin Scientific, Model: Theta Flex) by spreading the droplet on the modified-glass substrate. Figure 4.17 A shows the contact angle of an aqueous droplet containing 7% PEO established with a glass substrate modified with HS-40 nanoparticles. The glass modification is achieved by depositing a multilayer of HS-40 nanoparticles through dip coating using the procedures outlined by Sabapathy et al. [134, 135, 136] (2015, 2015, 2022). The contact angle of an aqueous droplet containing 3% dextran is shown in Figure 4.17 B. It can be inferred from Figure 4.17 B that the contact angle established by the aqueous dextran droplet on the HS-40-modified glass surface is 13 ± 1° (rounded off). However, since the droplet rich in PEO (7 wt.%) favours the spontaneous adsorption of PEO molecules on the silica, the surface becomes modified instantly so that the system experiences pinning at the contour line. Therefore, the contact angle of the PEO droplet remained intact at 57 ± 1° (rounded off) for a prolonged time. This pinning behaviour is attributed to the fast adsorption of PEO molecules on the surface of HS-40 nanoparticles Liu and Xiao [133] (2008). A similar observation of droplet pinning with rapid adsorption of oppositely charged polyelectrolytes was reported by Damak et al. [137] (2016).

## 4.4 Conclusion

This chapter reported a simple pathway to fabricate w/w emulsion-filled gels. These gels are permanent and remain stable against gravity for a long time. The transition from emulsion-to-emulsion-filled gels has been probed using characterization techniques such as inverted light microscopy, fluorescent microscopy, and rheometer. For the first time, it is shown that increasing the molecular weight of the polymer that makes up the continuous phase makes the emulsion droplets more stable. This trend is because the change in molecular weight affects interactions and viscosity, which stops droplets from coming together and breaking down too quickly. The systematic experimental findings proved that the emulsion-filled gels could be produced by adjusting the combinations of concentration, molecular weight, and storage time of the ternary systems without heat

treatment, acidification, enzyme treatment or addition of calcium ions to the formulations. The rheometer has been employed to characterize the particle-stabilized emulsions and emulsion-filled gels quantitatively, obtaining frequency sweep, amplitude sweep and flow curve data for the samples with different molecular weights of PEO. All rheological findings strengthen gel formation for 3D7P and 5D5P samples with the highest molecular weight ($10\times10^5$ Da) of PEO. Experimental data on frequency sweep exhibited a crossover at a frequency of $\omega = 30$ rad/s for the system with the highest concentration of PEO (3D7P), and the same has been shifted towards the right, i.e., $\omega = 80$ rad/s, as the concentration of PEO that constitutes the continuous phase decreases (5D5P). We employed the constitutive model proposed by I.M. Krieger to describe the behaviour of emulsion and emulsion-filled gels. The model fitting on the experimental data showed good agreement with the Krieger model for all cases except for the samples corresponding to $10\times10^5$ Da PEO (3D7P and 5D5P compositions) at a higher shear rate. This trend captures a significant deviation from the ideal and confirms the emulsion-filled gel's state at a particular experimental regime. These gels are increasingly used in pharmaceutics, cosmetics and food industries. Therefore, we believe the proposed study will shed some light on the characteristics of the generated emulsion-based gels and their correlation with the quality of the products.

# Chapter 5

# Single-step generation of double emulsions in aqueous two-phase systems

Chapters 3 and 4 demonstrated the methodology of synthesizing bijels and emulsion-filled gels. While Chapter 3 discusses the effect of M without changing the molecular weight of the polymer that constitutes the continuous phase, Chapter 4 mainly covers the effect of the molecular weight of PEO on the resulting structures and emulsion products by utilizing pure nanoparticles (M=0) of type HS-40. However, this chapter discusses the simultaneous effect of the M and molecular weight on the quality and state of the w/w emulsions formed. Thus, this chapter proposes a simple yet straightforward technique for preparing water-in-water-in-water (w/w/w) particle-stabilized double emulsions, also known as Pickering double emulsions. The approach exploits oppositely charged nanoparticles (OCNPs) in two distinct fluid phases, promoting self-assembly and the formation of aggregates with varying sizes and compositions. Enhancing the interfacial area through the adsorption of aggregates at the interface increases the Gibbs detachment energy of particles between the two aqueous phases, forming stable double emulsions. Furthermore, the impact of the molecular weight of the polyethylene oxide and dextran in the respective fluid phases and the mass ratio (M) of the OCNPs on double emulsion formation was investigated. It can be shown later in this chapter that polymer-particle and particle-particle complex interaction is a critical parameter to influence the microstructures and generate the double emulsions. Consequently, the double emulsions are formed when equal molecular weight polymer mixtures are employed at an appropriate M, with the dispersed phase placed in the highly viscous continuous phase. The proposed method offers easy preparation and exhibits excellent stability with a shelf life of at least 30 days after preparation. This study is the first reported approach for single-step synthesis of double/multiple emulsions in ATPS stabilized by charged nanoparticles.

## 5.1 Introduction

An emulsion is a heterogeneous mixture of two immiscible liquids, where one liquid is dispersed throughout the other in the form of droplets. The recent advances in emulsion droplet generation have led to the development of multiple emulsions, which have found diverse applications in various fields, including food industries, drug delivery, oil

extraction, cosmetics, emulsion explosives and reaction media. These multiple emulsions are complex systems that consist of droplets of one liquid dispersed within another liquid, which in turn is dispersed in a third liquid, resulting in a water-in-oil-in-water (w/o/w) or oil-in-water-in-oil (o/w/o) multiple emulsion. Figure 5.1 provides various possible configurations of double emulsions reported in the literature for different types of water-alkane systems. These emulsions show improved stability, making them highly attractive for various applications, such as the controlled release of active ingredients.

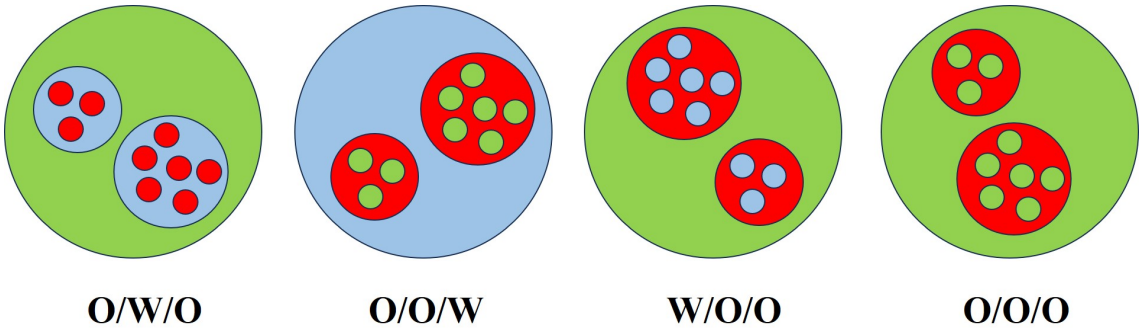


Figure 5.1: Schematic representation of the different types of double emulsions generated in various alkane-water systems.

Recently, Akram et al. [138] (2019) demonstrated the formation of double emulsions in an oil-in-water system, creating micro and nano double emulsions using a double emulsion approach. They employed silica particles as stabilizers for the inner droplets and surfactants for the outer droplets. However, long-term stability remained a challenge. Khadem et al. [139] (2020) investigated the release and swelling phenomena during preparation and storage. In that work, they reported various parameters affecting the preparation of double emulsions and the stability of double emulsions during storage. Furthermore, they examined the evolution of the outer droplet size and release rate in double emulsions, highlighting the impact of overswelling-breakdown on the quality of these emulsions. Consequently, there has been significant interest in developing new and innovative methods for synthesizing and characterizing multiple emulsions (Stone et al. [140], Squires and Quake [141], Basaran [142], Günther and Jensen [143], Muschiolik [144], Dickinson [145], Matos et al. [146]). This type of system is characterized by two interfaces, one between the inner droplets and the surrounding droplets and another between the outer droplets and the external environment. Multiple emulsions can be further classified based on the number and size of the dispersed droplets. The most common type of double emulsions is the droplets dispersed within another droplet, and triple emulsions in which two sets of droplets are dispersed within the same continuous phase (Dickinson [145], Wang et al. [147], Basaran [142], Song and Shum [77]). Multiple and double emulsions in oil-water systems, such as water-in-oil-in-water (w/o/w), water-in-water-in-oil (w/w/o), and oil-in-water-in-oil (O/W/O) emulsions, exhibit excellent stability and are used for a wide range of applications in biomedical

and biological screening assays. They are also utilized in fabricating liposomes and colloidosomes capsules for drug delivery. These emulsions have unique structural and physical properties, such as high surface area and controlled release characteristics, that make them attractive for these applications. In addition, they can be easily modified by incorporating various functional additives, such as drugs or biomolecules, to tailor their properties for specific applications (Yang et al. [148], Kumar et al. [149], Chen et al. [150]). The formation of double emulsions is a complex process, often requiring two steps, which can pose challenges for large-scale production. Available techniques for generating double emulsions include microfluidics, double-step mixing, and phase inversion. Microfluidic methods involve using microchannels to generate emulsions, but they require sophisticated equipment and are often not scalable to larger production volumes. Double-step mixing methods involve the formation of primary emulsions followed by a second mixing step to generate the double emulsion, which can be time-consuming and may result in low yields. Phase inversion methods rely on manipulating the interfacial tension between the two immiscible phases to form the double emulsion, but the resulting emulsions may be unstable and difficult to control. As such, there is a need to develop more efficient and scalable methods for forming double emulsions for use in various applications (Utada et al. [151], Liu et al. [152], Kim et al. [153]). The current literature has grown significantly with numerous examples of the various morphologies observed in oil/water multiple emulsion systems, including o/w/o, w/o/w, and other. However, despite their inherent stability and effective stabilisation, there has been a dearth of research on water-in-water-in-water emulsions, which may offer new opportunities in various fields such as drug delivery, food science, and materials engineering (Song et al. [154], Song and Shum [77], Sauret and Cheung Shum [76]).

An aqueous two-phase system (ATPS) is a thermodynamically equilibrated system combining two incompatible hydrophilic polymers in two phases. In a classical ATPS, a water-in-water emulsion is formed by dispersing one aqueous phase as droplets within the other, which serves as the continuous phase. The interfacial tension between the two aqueous phases in this emulsion type is extremely low, typically between 1-10 $\mu$N/m. This low interfacial tension results from the similar chemical nature of the two aqueous phases, which results in weak intermolecular forces and minimal thermodynamic barriers at the interface between the two phases. The unique properties of ATPS, such as their biocompatibility, tunable selectivity, and mild processing conditions, have led to their use in various applications, including bioseparation, biocatalysis, and drug delivery (Shekhar et al. [112], Dickinson [155], Nicolai and Murray [156]). To date, there have been relatively few studies on the formation of water-water-water (W/W/W) emulsions, and most of the reported methods involve either microfluidic techniques or two-step processes. The pioneering work in applying microfluidics with flow focusing for generating mono-dispersed droplets, particles, and bubbles was carried out by Gañán-Calvo [157] (1998) (Gañán-Calvo [157], Ganán-Calvo and Gordillo

[158], Gañán-Calvo [159], Martín-Banderas et al. [160]). While microfluidic methods are highly efficient and enable precise control over droplet size and morphology, they may not be scalable for larger production volumes. Two-step methods involve generating a primary water-in-water emulsion, which is then subjected to a second emulsification step to generate the W/W/W emulsion. Although these methods are relatively simple and do not require specialized equipment, they may result in low yields and are often time-consuming.

Norton and Frith [161] (2001) have demonstrated the formation of multiple water-in-water-in-water (w/w/w) emulsions at or near 50/50 volume fraction using the phase transition technique in a biopolymer system comprising gelatin and methyl dextran. This method involves exploiting the thermodynamic properties of the polymer system to induce a phase transition that results in the formation of emulsions. The multiple W/W/W emulsions were observed to have stable morphologies and were found to be tunable by varying the polymer concentration and emulsion volume fraction. Nonomura et al. [162] (2011) have proposed an excellent method for forming multiple emulsions using micro bowls. They have reported that anisotropic particles can stabilize multiple emulsions in a single step, and they have demonstrated the formation of oil-in-water-in-oil (o/w/o) emulsions using this approach. They observed that the particle shape and surface chemistry played a critical role in stabilizing the emulsions. Anisotropic particles are particles with a non-spherical shape, exhibiting unique surface properties that enable them to act as effective stabilizers for emulsions. Several researchers have also reported using microfluidic techniques to prepare W/W/W emulsions, which provide excellent control over the structure and morphology of the formed droplets (Song and Shum [77], Jeyhani et al. [81]).

Jeyhani et al. [81] (2020) studied the stabilization of double and triple emulsions in an aqueous two-phase system (ATPS) consisting of polyethylene glycol (PEG) and dextran. They utilized a microfluidics device to generate the emulsions and employed lysozyme as a stabilizer for the formed emulsions. However, the stability of the emulsions remained a subject of uncertainty or lack of understanding. However, there has been little exploration of the single-step process for forming these double emulsions as it involves the simultaneous formation of multiple emulsion droplets in a mixture. Therefore, research is needed to optimize the process parameters and understand the mechanisms underlying the formation and stabilization of these emulsions.

The proposed approach involved using polyethylene oxide and dextran bio-polymer with varying molecular weights, as well as oppositely charged silica nanoparticles, to induce in-situ hetero-aggregate formation in an aqueous phase. This chapter mainly focuses on synthesizing double emulsions in aqueous two-phase systems (ATPS) consisting of two immiscible aqueous phases in thermodynamic equilibrium. The results of our study demonstrate the potential of our single-step approach for the scalable and efficient

production of W/W/W double emulsions with controlled morphology and stability.

## 5.2 Experimental Section

### 5.2.1 Materials and Methods

To generate double emulsions, the polyethylene oxide (PEO) and dextran biopolymer mixtures with varying molecular weights, including $1X10^5$ ($1e5$), $2X10^5$ ($2e5$), $3X10^5$ ($3e5$), $6X10^5$ ($6e5$) Da and $6X10^3$ ($6e3$), $4X10^4$ ($4e4$), $1X10^5$ ($1e5$), $2X10^5$ ($2e5$) Da, respectively, were used. The study employed Ludox HS-40 (40 wt%) and CL-30 (30 wt%) silica nanoparticles, which had a diameter of 16 ± 2 nm and 16 ± 2 nm as determined by transmission electron microscopy (see Figure 3.3), and zeta potential of -55 ± 1.8 mV and 51 ± 2.1 mV, obtained through electrophoretic light scattering, respectively. Figure 5.2 depicts a schematic representation of the emulsion preparation process. Each aqueous phase was formulated separately, and an equivalent quantity of both polymers (5 wt%) was included along with the deionized water. The mixture was allowed to soak overnight and then subjected to 2 minutes of mixing using a vortex shaker to achieve a homogeneous solution. Following this, a single type of particle (CL-30 in PEO or HS-40 in dextran solution) was added to one of the phases while ensuring that the total concentration of the nanoparticles did not exceed 1 wt% of the entire solution. Notably, all experiments were performed in triplicate to ensure the reproducibility and reliability of the results. The two solutions were combined using a homogenizer (Make: IKA, Model: Ultra Turrax T25) operating at 10000 rpm for 2 min and then incubated at a constant temperature of 25°C for 48 hr. To discern the type of emulsion created, we fluorescently labelled the dextran with FITC (Fluorescein-5-isothiocyanate). Deionized water (18.2 MΩ), obtained from the Barnstead$^{TM}$ Smart2Pure$^{TM}$ water purification system (Make: Thermo Fisher Scientific), was used for all experiments. The viscosity of the polymers was measured using a twin-drive rheometer (Make: Anton Paar, Model: MCR-702) at a steady temperature (25°C). Notably, all samples were examined after 48 hours, which serves as a reference point for comparison, i.e., t = 0 days.

### 5.2.2 Characterization

The zeta potential of the pure nanoparticles of type HS-40 (−) and CL-30 (+) was measured based on the electrophoretic light scattering (ELS) technique using Zetasizer procured from Malvern Instruments, Zetasizer Nano ZSP. The size of HS-40 (−) and CL-30 (+) nanoparticles were determined using a high-resolution transmission electron microscope (HRTEM), FEI Company, Tecnai G2 20. The inverted light microscope (Zeiss, AxioVert.A1) was used to carry out the structural characterization of single and double emulsions. The fluorescent microscope (Leica Microsystems, DMI 6000B) was used to visualize the type of emulsions, whether single or multiple.

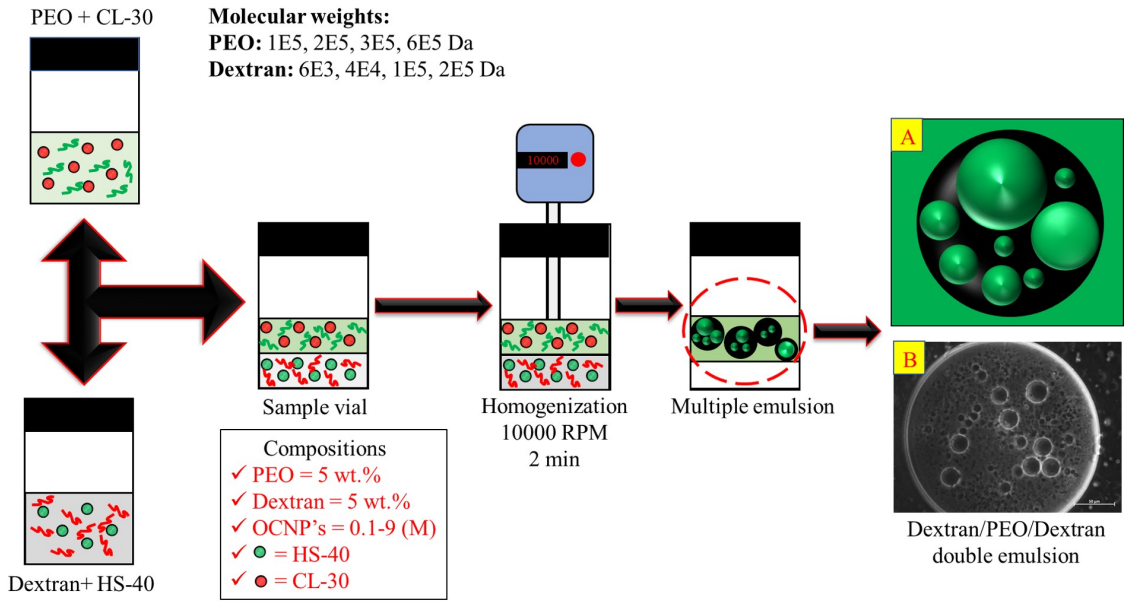


Figure 5.2: Schematic description of the double emulsion formation A) schematic of D/P/D emulsion B) Microscopic image of D/P/D emulsion (Note: scale bar corresponds to 50 $\mu$m)

## 5.3 Results and Discussion

Here, a simple approach for synthesizing multiple water-in-water emulsions was proposed. By preparing an aqueous phase with polymers of equal molecular weight, and choosing a particular weight ratio of positively charged nanoparticles to negatively charged nanoparticles (referred to as M), the w/w/w Pickering emulsion template was created to gain a deeper understanding of the double emulsion formation. Previous research by Norton and Frith [161] (2001) has shown that multiple/bicontinuous emulsions can be formed at the phase volume line concentration on the binodal curve of the polymer system. Beyond this concentration, phase inversion occurs. The research work presented here has found that high-speed mixing of the two polymers leads to the initial separation of the polymers within the droplets rather than by diffusion to already-formed droplets due to the differences in solution viscosity. Once the primary droplets have formed, they behave as if they were isolated phases, and a second separation occurs within these microenvironments, resulting in the formation of included droplets. These findings contribute to a deeper understanding of double emulsion formation's physical mechanisms and practical implications for developing water-in-water emulsions. The stability of the emulsion products is a concern, as the low surface tension between the phases in ATPS can lead to instability. The polymer concentrations based on the PEO and dextran binodal curve were utilized to address this. The phase line was observed at a 50:50 phase volume ratio of PEO and dextran biopolymer. Additionally, Nonomura et al. [162] (2011) have reported that anisotropic particles can synthesize double emulsions in a single step in the O/W emulsion system. To investigate the effect of anisotropic particles on the structural state and stability of the emulsion, we used hetero-aggregates

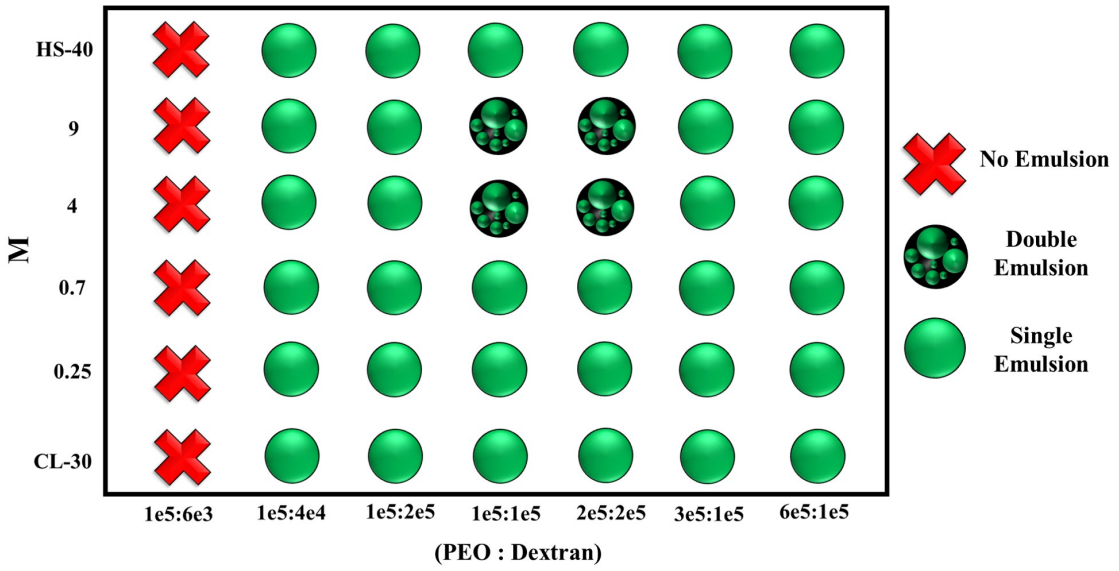


Figure 5.3: State diagram demonstrating the double emulsion formation concerning the molecular weight ratios of the biopolymers and M.

formed using oppositely charged nanoparticles (OCNPs). Through a systematic study, we varied the molecular weight of the polymer and M (the ratio of charged particles) and observed changes in the structure of the synthesized emulsion. The proposed strategy could produce double emulsions in a single step without a microfluidic approach. Based on the experimental observation, we constructed a state diagram demonstrating the structural formation and transition from a single to double emulsion by varying the molecular weight and composition of OCNPs of a two-phase mixture stabilized by the homogenizer at a programmed speed of 10000 rpm. This state diagram is illustrated in Figure5.3.

In this study, an exciting observation was made that double emulsion formation occurred at M values of 4 and 9, corresponding to positively charged hetero-aggregates of nanoparticles (Shekhar et al. [112]) when the equal molecular weight of the polymers was employed. We attribute this phenomenon to the wettability of the aggregate particles in the Pickering emulsion, which is responsible for emulsion formation. Furthermore, we envisage that the formation of multiple emulsions could be linked to the contact angle distribution of the anisotropic particles. This trend suggests that the anisotropy of the particles is a crucial factor in the formation of double emulsions, as it influences the contact angle and, thus, the stability of the emulsion (Nonomura et al. [162]). On the other hand, it can be envisaged that the steric stabilization of polymer on silica particles would result in a modification of the wettability characteristics of the particles (Binks and Rodrigues [163]). However, the spatial distribution and positioning of the particles across various interfaces in multiple emulsions still need to be fully elucidated (Tiwari et al. [164]). The stabilization study revealed that dextran, with a molecular weight of 6E3 Da, did not exhibit emulsion formation as the viscosity of the polymer solution was similar to that of water, as shown in Figure 5.4.

In contrast, other molecular weights of dextran showed single emulsion formation in all

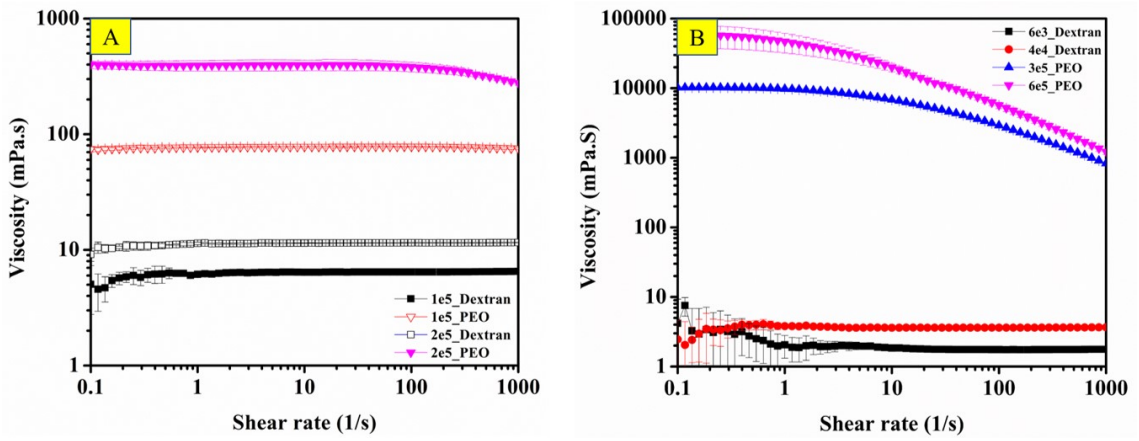


Figure 5.4: Viscosity measurement of the polymers: A) for the equal molecular weight of PEO and dextran polymers B) for the different molecular weight of PEO and dextran polymers

mass ratios (M) of the particles, except for equal molecular weight (1E5:1E5, 2E5:2E5 Da) of polymers at M = 4 and 9 due to changes in the viscosity of the phases and arrangements of particles at the interface of the system. The formation of the emulsion structure was confirmed using microscopic images Figure 5.5, 5.6, and the type of emulsion formed was determined using a FITC-labeled dextran (Figure 5.7). The Microscopic images of the emulsion droplets were utilized to assess the stability of formed emulsions. The rectangular box highlighted in red indicates the stable morphology of double emulsion formation observed for up to 30 days. Conversely, in the case of the 1e5:6e3 (PEO: Dextran) polymer ratio, no emulsion droplets were observed, suggesting the formation of a complete solution or the absence of a two-phase system. The stability of emulsions comprising of 1e5:4e4 (PEO: Dextran) Da polymers and either CL-30 or HS-40 single-type charged particles was found to be stable for up to 7 days; however, after 30 days, no droplets were discernible under microscopy, indicating short-lived stability. The study also established that the stability of the emulsions formed was positively correlated with an increase in the molecular weight of the polymers in the two-phase system. This trend was confirmed through microscopic images and emulsion index measurements of the formed emulsion. Specifically, the experimental results consistently demonstrate that the formulation comprising higher molecular weight polymers exhibits superior stability characteristics. Figures 5.5, 5.6 illustrate the morphological characteristics of the formed emulsion in the molecular weight system at t=0 day and 30 days. These images were obtained using an inverted microscope (Model: Axio Vert A1; Make: Carl Zeiss, India) with brightfield mode at 40X magnification to cover the large surface area of the sample, providing a visual representation of the stability of the emulsions over time. The samples were carefully prepared on the cleaned glass slide and covered with a coverslip to enhance the viewing and minimize the evaporation rate of the emulsion sample. Specifically, the images allow for assessing changes in the emulsion morphology, such as the droplets' size, shape, and distribution. Such information is valuable in determining the stability of the

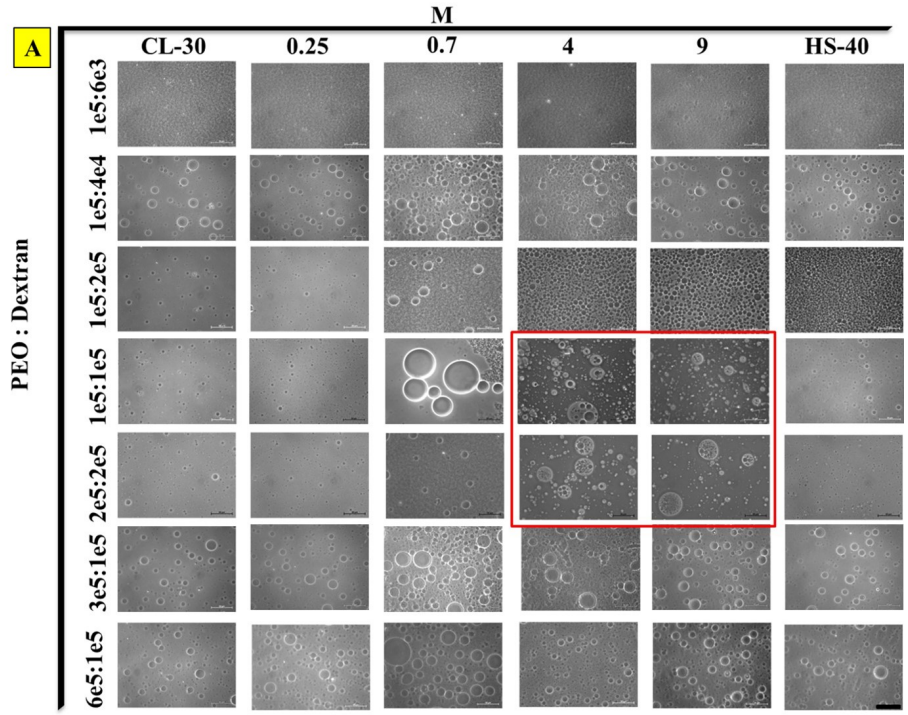


Figure 5.5: Representative microscopic images of the formed emulsions at $0^{th}$ day. The scale bars given in the images correspond to 50µm.

emulsions and evaluating the effectiveness of the stabilizing agents used in the system. The formed emulsion was identified as Dextran/PEO/Dextran (D/P/D) emulsion, as shown in Figure 5.7.

To investigate the influence of mixing on the formation of double emulsion, the emulsions with varying mixing speeds at a 50:50 volume ratio of polymer with 1e5 Da molecular weight, where both polymers have equal molecular weight, at M=4, were prepared, as indicated in the state diagram shown in Figure5.3. The results depicted in Figure 5.8 demonstrate that double emulsion formation occurred at all mixing speeds, indicating that the process depends on the viscosity of both phases. Specifically, the polymers with equal molecular weights exhibited a one-order magnitude difference in the viscosity of the phases, as shown in Figure 5.4. This finding suggests that once primary droplets are formed, they behave like an isolated phase in the highly viscous medium and exhibit the emulsion's double structure morphology. A recent study conducted by Sabri et al. [165] (2020) demonstrated that multiple emulsions could be generated in a single step by a phase inversion mechanism using silica particles in a highly viscous oil-in-water emulsion system.

The scalability of the proposed technique for double emulsion formation was also investigated to understand the dependency of batch sizes. For the study, a separate set of experiments was conducted at different batch sizes, measured in 5, 10, and 15 g of the total solutions, using polymers with an equal molecular weight of 1e5 Da and 1 wt% of the OCNPs at all mass ratios (M). To ensure meaningful comparisons, we focused on the experiments at one favourable set of double emulsion formation conditions, namely

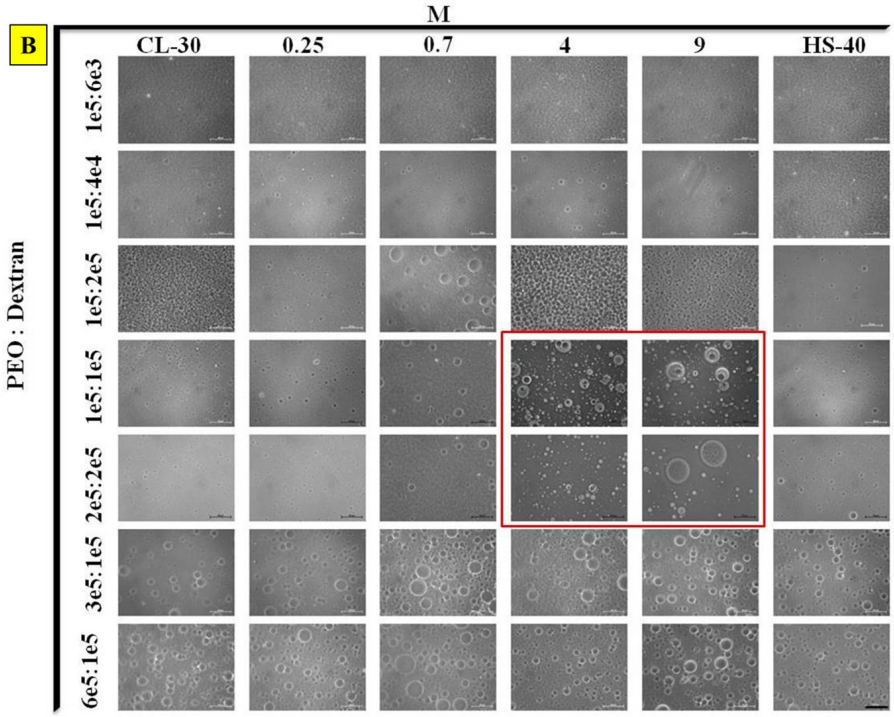


Figure 5.6: Representative microscopic images of the formed emulsions: After $30^{th}$ day. The scale bars given in the images correspond to 50µm.

equal molecular weight at 1e5 Da. Intriguingly, double emulsion formation consistently occurred across all batch sizes, as depicted in Figure 5.9. However, except for M=4 and 9, the experiments conducted under other conditions resulted in the formation of single emulsions.

The above findings indicate that the formation of double emulsions is independent of the size (volume) of the experiment. However, it was anticipated that the nanoparticles' stabilization capacity may affect the emulsions' quality. Several samples with different particle concentrations were prepared at a suitable mass ratio (M) to gain deeper insight into the effect of the nanoparticles. The results revealed a dependency on the concentration of OCNPs to form double emulsions. It comes to say that the concentrations exceeding 1 wt% led to the formation of single emulsions. These findings are consistent with the work of He et al. [166] (2013). The stability of the formed emulsion was assessed for 30 days. The emulsion stability was quantified by calculating the emulsion index (%), which was determined based on the following equation (please refer to eq. 5.1),(Shahaliyan et al. [167]) as shown in Figure 5.12, for various mass ratios (M) of nanoparticles using vial images displayed in Figures 5.10, 5.11 corresponding to $0^{th}$ day and $30^{th}$ day respectively.

$$EI = \frac{h}{H} \times 100 \tag{5.1}$$

wherein h and H refer to the height of the emulsion phase and total sample height, respectively. To calculate this index, the percentage ratio of the height of the emulsion

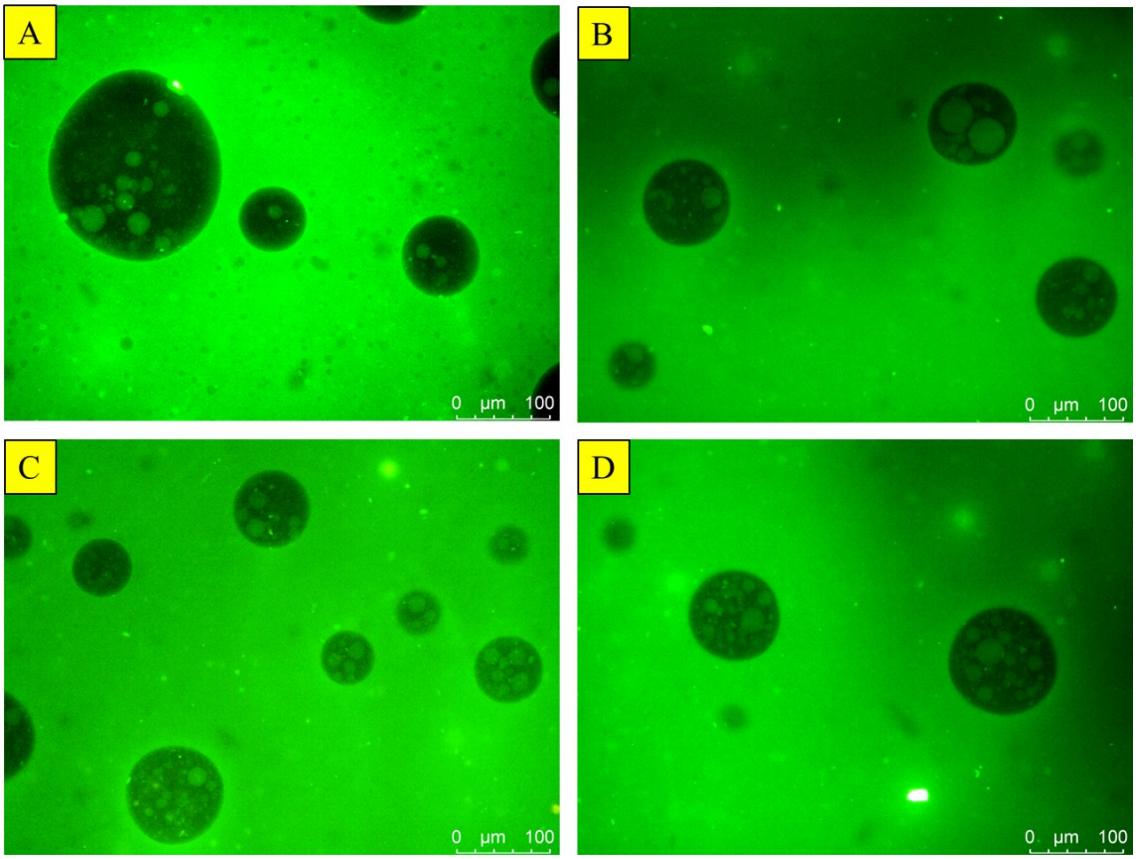


Figure 5.7: Representative fluorescent images of formed double emulsion A and B) corresponds to the 1E5:1E5 Da C and D) corresponds to 2E5:2E5 Da molecular weight ratios of the polymer at M = 4 and 9, respectively. The scale bar corresponds to the 100$\mu$m. In the image, green corresponds to the fluorescently labelled Dextran phase, while black corresponds to the non-fluorescent PEO phase.

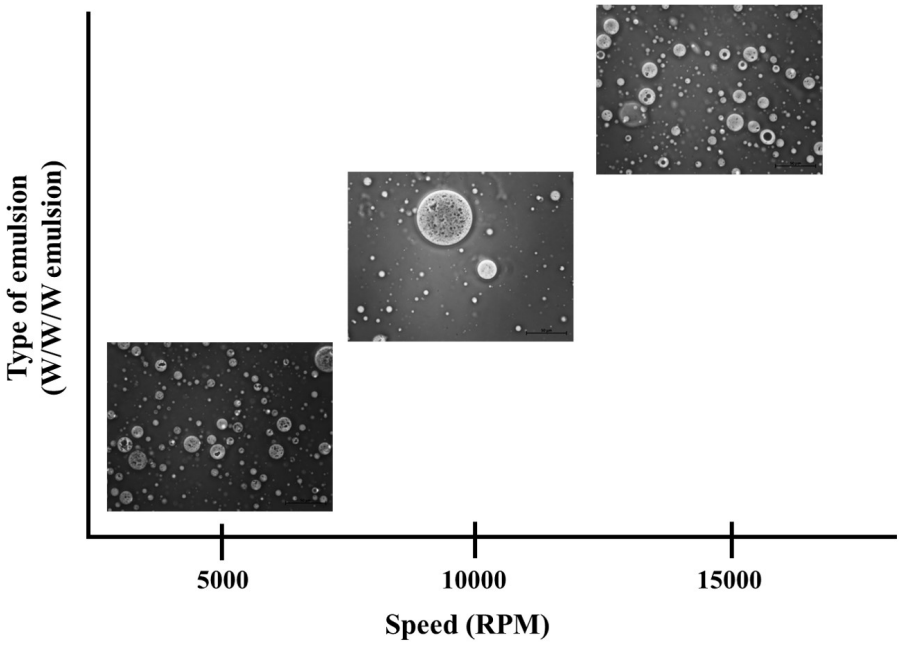


Figure 5.8: Mixing effect on the emulsion formation for 1E5 (PEO):1E5 (Dextran) Da, at M=4. The scale bar corresponds to the 50$\mu$m.

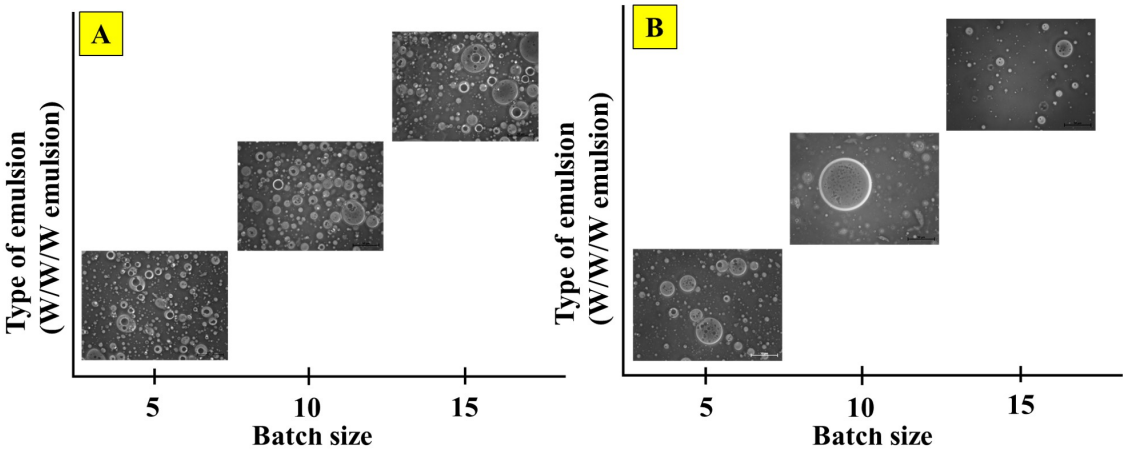


Figure 5.9: Plot showing the effect of scaling by batch size on the formation of double emulsion, A) for M =4, B) for M=9 for 1e5 (PEO):1e5 (Dextran) Da in an equal amount of polymers (5 wt%).

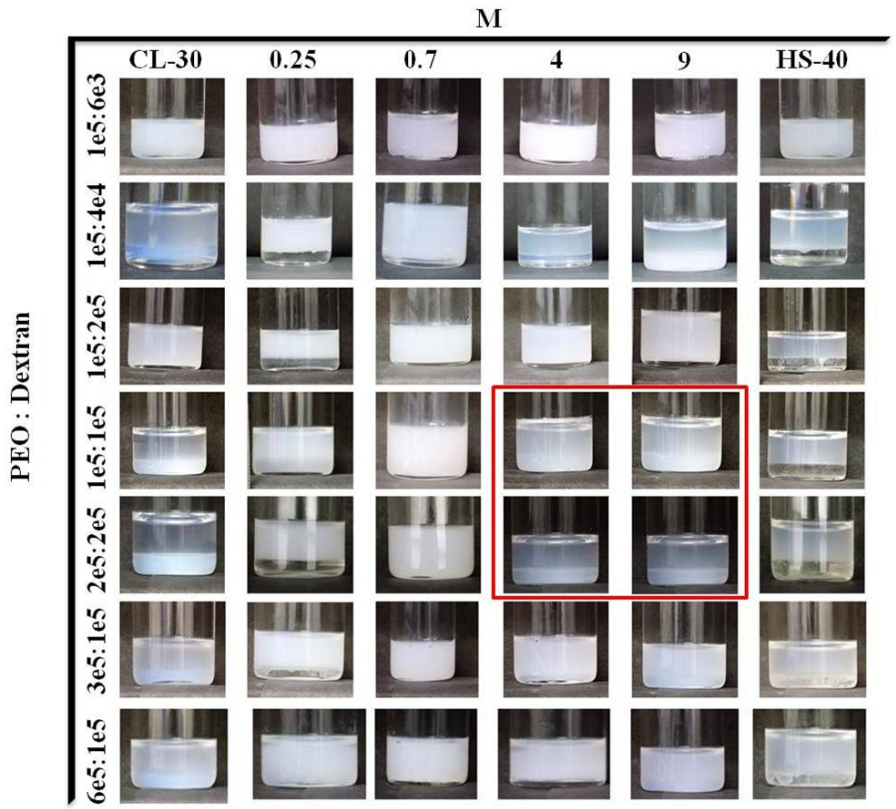


Figure 5.10: Vial images of the formed emulsion at t = 0-day.

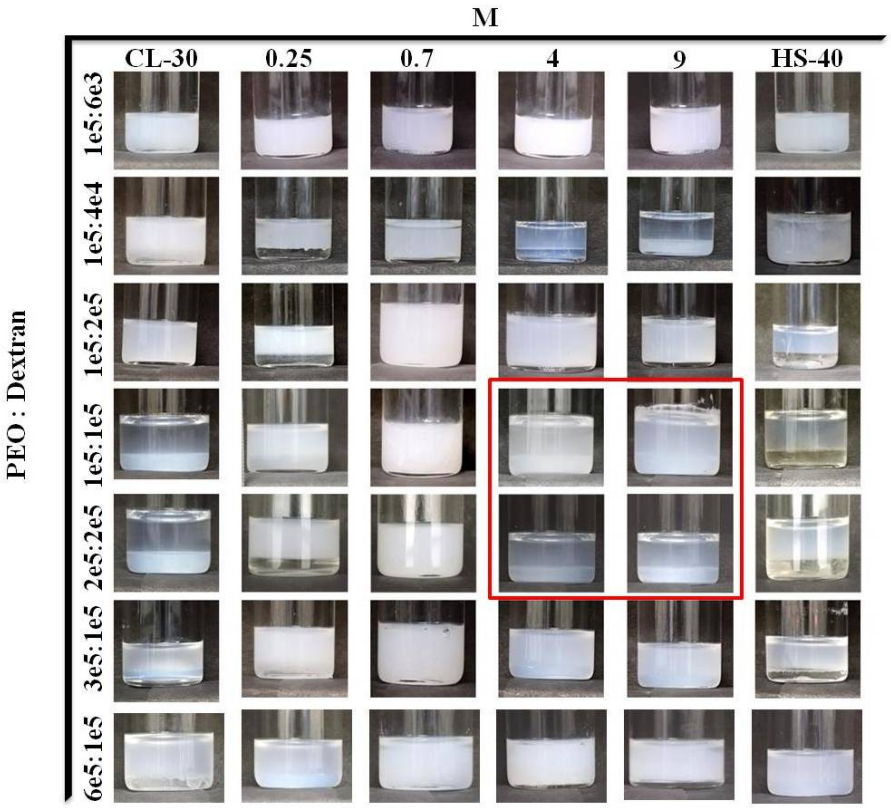


Figure 5.11: Vial images of the formed emulsion at t = 30 days.

(height up to which the emulsion spanned) to the total height corresponding to the mixture after emulsification was measured using Image-J software (an open-source software tool).

The results indicated that emulsions formed with single particles, such as HS-40 and CL-30, in low molecular weight PEO (4e4 Da) were destabilized after 48 hours. A quick overview of the state of formed emulsions at different M can be obtained by referring to the vial images in Figure 5.10 and 5.11 for $0^{th}$ day and $30^{th}$ day respectively. The stability of the formed emulsion starts to increase with the increase in the molecular weight of the continuous phase (PEO), in the case of pure HS-40 or CL-30, due to the strong adsorption of the PEO in the continuous phase on silica nanoparticles. According to the work of Liu and Xiao [133] (2008), the zeta potential decreases with an increase in molecular weight at the same concentration of PEO due to the configuration change of the PEO segments to loops which eventually contributes significantly to the net electrostatic attraction between the particles and polymers. The stability of the emulsion was confirmed through microscopic analysis using an inverted microscope, as evidenced by the presence of stable droplets observed for up to 30 days after emulsion formation. The high viscosity of the polymers, in conjunction with particulate barriers at the interfaces within the aqueous phase, contributed to the stabilization of the water sub-inclusions and prevented their transfer into the continuous aqueous phase during processing. This mechanism is similar to the formation of sub-inclusions in highly viscous melt-processed polymer blends, wherein phase inversion during processing results in the kinetic trapping of sub-inclusions within

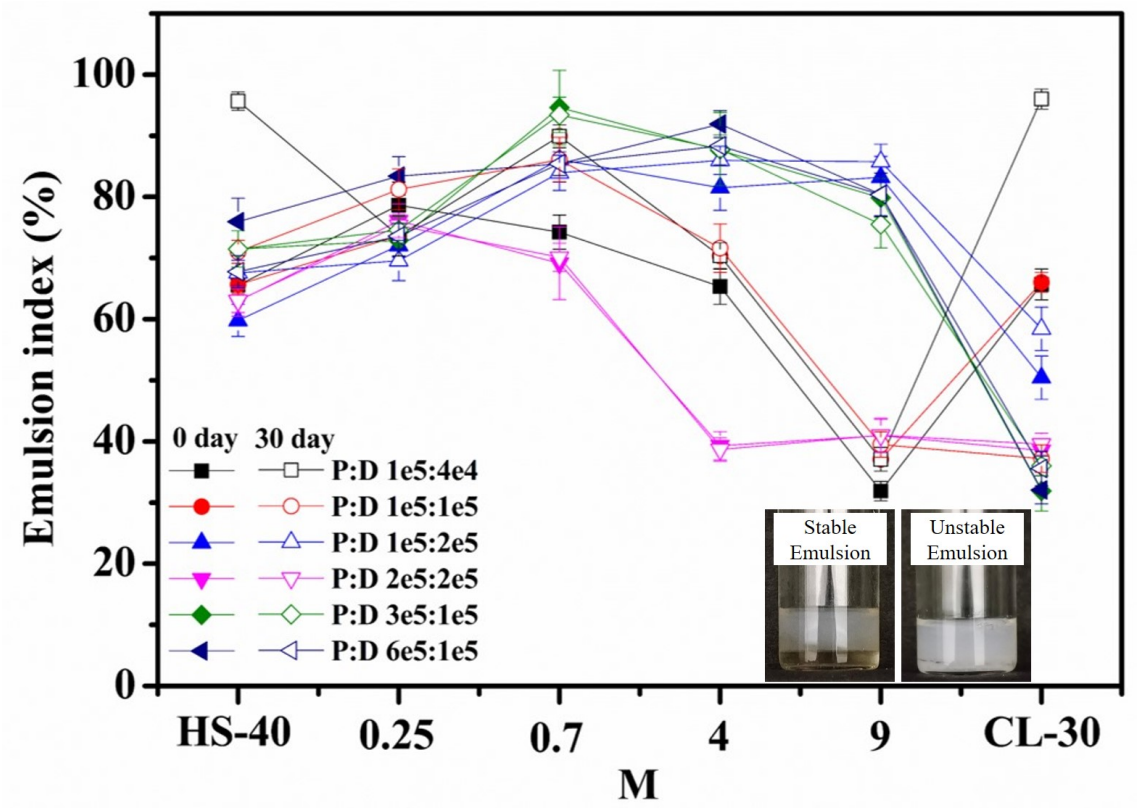


Figure 5.12: Plot showing the stability of the formed emulsion filled symbol for 0th day and open symbol represent for 30th day respectively

the dispersed phase, leading to the formation of multiple emulsions.

## 5.4 Conclusion

This chapter reports a single-step approach that enables the generation of double emulsions at a suitable experimental regime. The results demonstrate that the molecular weight of the polymers used to form the aqueous phase is a critical factor in the structural formation of the emulsion, resulting in the formation of double emulsions. The proposed strategy is easy to implement and can offer excellent throughput over the fabrication of double emulsions with precise control of the structural qualities. Since the proposed technique involves stabilizing the droplets using the aggregate particles formed due to the self-assembly of oppositely charged nanoparticles, the required increment in Gibbs detachment energy is naturally gained without adding any unconventional stabilizers. This study is the first report to demonstrate the formation of a W/W/W emulsion using a Pickering emulsion template in an ATPS system through a single-step process.

# Chapter 6

# Conclusions and Future work

## 6.1 Conclusions

This thesis shows several significant findings and advancements in w/w emulsion science, demonstrating a simple yet straightforward technique approaches to produce stable w/w Pickering emulsions by utilizing a combination of a binary mixture of nanoparticles. These emulsions exhibit enhanced stability, remaining intact for up to 90 days. By adopting a self-assembly route, it has been observed that the combination of nanoparticles at desired mass ratios induces the formation of complex 2 and 3D clusters, leading to a substantial increase in Gibbs detachment energy.

**Chapter 3** described the successful demonstration of a straightforward technique for producing stable w/w Pickering emulsions. It is observed that the emulsions were not sufficiently stable when pure commercial-grade nanoparticles of type HS-40 (-) or CL-30 (+) nanoparticles were used. However, enhanced stability is achieved by employing a binary mixture of nanoparticles at desired mass ratios (M). These emulsion droplets remained stable for up to 30 days and exhibited excellent resistance to strong mechanical forces. Further, to understand the behaviour of the emulsions, a phase diagram was developed that allowed us to identify the transitions between droplets and bijels, which occurred due to changes in polymer and particle concentrations. The structural characterization was performed using bright field, fluorescent, and electron microscopes to determine the emulsion type (P/D or D/P) and the state, whether bijels or droplets. These results provided sufficient insights into the self-assembly behaviour of oppositely charged nanoparticles and their effects on forming varying structural states of bijels and droplets. The formation of bijels, a new class of bi-continuous soft materials, holds great potential for various applications. They can be used in multicomponent flows, tissue engineering, and as batteries and fuel cell electrodes. The findings from this study contribute to the advancement of soft materials and open up possibilities for their applications in diverse fields without any surface modifications of the particles.

**Chapter 4** demonstrated a simple pathway for fabricating w/w emulsion-filled gels that exhibit long-term stability against gravity. Several characterization techniques, such as inverted light microscopy, fluorescent microscopy, and rheometry, were employed to investigate the transition from emulsion to emulsion-filled gels. Increasing the molecular weight of the polymer in the continuous phase increases the stability of the emulsion

droplets, which is the principal finding of the proposed work. This trend is due to the effect of molecular weight on interactions and viscosity, which inhibits droplets from rapidly coalescing and disintegrating. Furthermore, the systematic study of the production of emulsion-filled gels by adjusting the combinations of concentration, molecular weight, and storage time of the ternary systems was conducted. Notably, the gel formed without needing heat treatment, acidification, enzyme treatment, or the addition of calcium ions to the formulations. A rheometer was used to characterize the particle-stabilized emulsions and emulsion-filled gels. Several data for samples with different molecular weights of PEO were obtained through frequency sweep, amplitude sweep, and flow curve measurements. The rheological analysis consistently supported the formation of gels, particularly for the 3D7P and 5D5P samples with the highest molecular weight ($10^5$ Da) of PEO. The frequency sweep experiments revealed a crossover at a frequency of $\omega = 30$ rad/s for the system with the highest concentration of PEO (3D7P). As the concentration of PEO in the continuous phase decreased (5D5P), the crossover frequency shifted to $\omega = 80$ rad/s. These observations provide valuable insights into the gel formation process and the rheological behaviour of the emulsion-filled gels. Additionally, the constitutive model proposed by I.M. Krieger was also employed to describe the behaviour of the emulsion and emulsion-filled gels. The model fitting agreed well with the experimental data, except for the samples corresponding to $10^5$ Da PEO (3D7P and 5D5P compositions) at higher shear rates. This deviation from the ideal behaviour confirms the state of the emulsion-filled gel under specific experimental conditions. These emulsion-filled gels find various applications in industries such as pharmaceutics, cosmetics, and food. In short, this chapter summarizes a simple pathway to fabricate emulsion-filled gels, which exhibit long-term stability against gravity, was proposed. Furthermore, **Chapter 4** uncovered that increasing the molecular weight of the polymer in the continuous phase enhances the stability of the emulsion droplets within the gel structure - highlighting the influence of molecular weight on interactions and viscosity, preventing droplet coalescence and breakdown.

**Chapter 5** presents a novel single-step approach for generating double emulsions within a specific experimental range. This chapter demonstrates that the molecular weight of the polymers used to create the aqueous phase plays a crucial role in determining the structural formation of the emulsion, leading to the formation of double emulsions. The proposed strategy is characterized by its ease of implementation and ability to facilitate the efficient production of double emulsions. Additionally, it offers precise control over the structural properties of these emulsions. One of the main advantages of the proposed technique lies in its utilization of the self-assembly process of oppositely charged nanoparticles, forming finite-sized clusters or aggregates. This self-assembly effectively stabilizes the droplets, eliminating the need for unconventional stabilizer requirements. The adsorption of aggregates resulting from the self-assembly process naturally increases the Gibbs detachment energy required for stabilization, which is one of the main

advantages of the proposed technique. As a result, the proposed approach provides a simple and effective means to achieve stable W/W/W emulsions using a Pickering emulsion template in an aqueous two-phase system (ATPS) through a single-step process. By introducing this innovative approach, the technique offers significant advancements in the field of double emulsions. The strategy's simplicity and efficiency render it highly appealing for diverse applications that depend on double emulsions, including materials science, pharmaceuticals, and cosmetics. In summary, **Chapter 5** introduces a single-step approach for generating double emulsions, emphasizing the importance of polymer molecular weight in the structural formation of emulsions. This approach enables precise control over the fabrication of double emulsions and offers excellent throughput.

Overall, the thesis work contributes to a deeper understanding of w/w emulsion science and presents practical implications in various fields, such as multicomponent flows, tissue engineering, batteries, fuel cells, pharmaceutics, cosmetics, and food industries. The findings from this research shed light on the characteristics and quality correlations of the generated emulsion-based materials, paving the way for further advancements and applications in the future.

## 6.2 Future work:

### 6.2.1 Synthesis and characterization of sub-micron-sized spherical capsules and evaluate the release kinetics based on model drug systems for drug delivery application:

Nowadays, submicron carriers are required for effective/targeted drug delivery at a specific location and time-dependent manner via active (self-propulsion) or passive targeting. The submicron-sized capsules range from 0.01 - 1 $\mu$m. Submicron carriers in drug delivery can be synthesized by various materials such as polysaccharides, proteins, inorganic metallic salts and synthetic polymers with different techniques, such as microfluidics and high-pressure mixing (Two-step). Further, a hybrid method for submicron droplet formation using high-pressure mixing devices (Homogenizer, Sonication) in ATPS using a Pickering emulsion template with OCNP's can be developed. As part of the preliminary study, a hybrid method has been developed by optimizing the homogenizer's mixing speed and amplitude of the mixing for the sonicator. Here, Figure 6.1 shows the synthesized submicron droplet in PEO and dextran system using OCNPs in the hybrid method by utilizing an equal amount of both phases (5% dextran + 5% PEO) with M=4 ratio of the OCNP's using different mixing devices; using a homogenizer at 10000 RPM speed and 70% amplitude using a sonicator, the minimum size of the formed droplets is 850±150 nm at M=4. Furthermore, optimizing the particle concentration at optimized speed and amplitude can lead to submicron droplet formation.

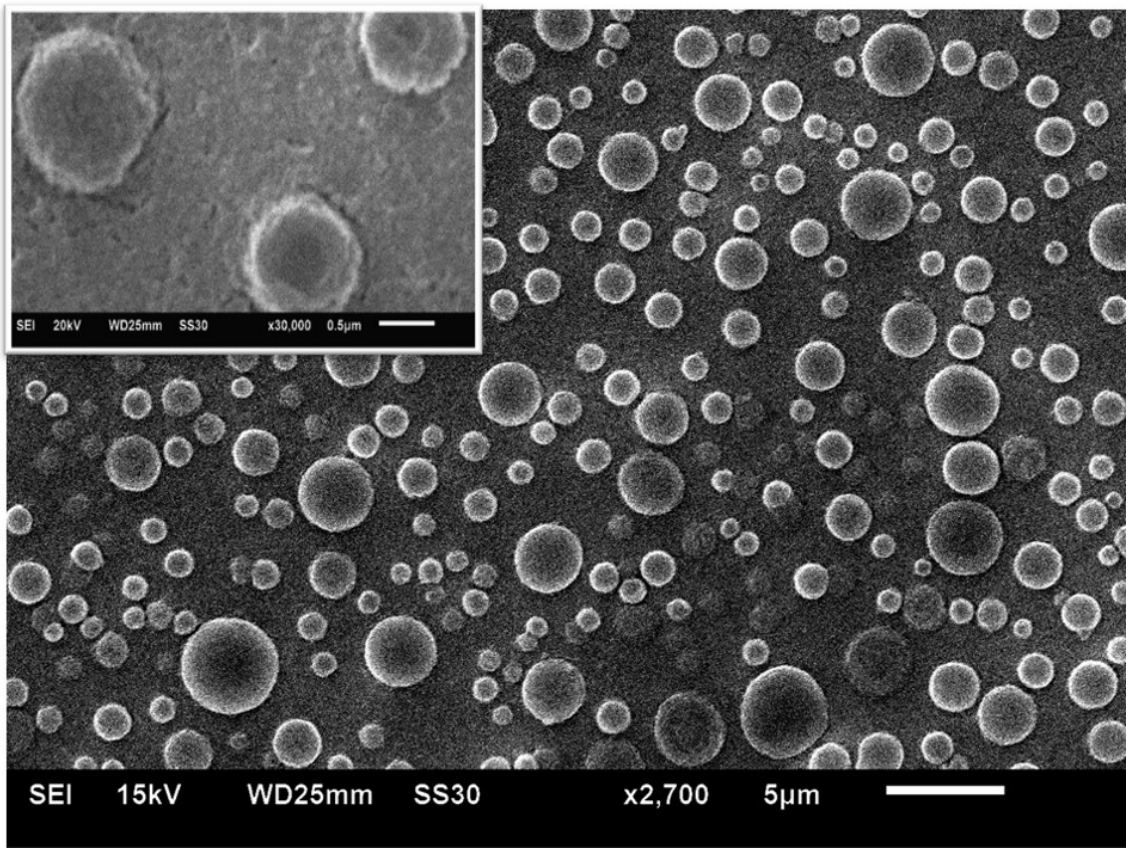


Figure 6.1: SEM image of showing sub-micron sized capsules; Inset, is zoomed view of the dried capsules

### 6.2.2 Exploration of new techniques to fabricate non-spherical colloidal capsules for biomedical applications:

The formation of non-spherical droplets in water-in-water (w/w) emulsions remains challenging due to the low interfacial tension between the two aqueous phases. Typically, non-spherical droplets are formed using microscopic devices such as narrow tubes or microfluidic devices, which have been reported in the literature for various oil-water systems. However, a simple method for synthesizing non-spherical droplets in w/w emulsions is desired without relying on microfluidic devices. This work uses centrifugal force to convert spherical capsules in w/w emulsions into non-spherical shapes. First, we stabilized the spherical droplets using oppositely charged nanoparticles, as described in previous chapters. Subsequently, we subjected these spherical capsules to centrifugal force, a common technique used in the spinning drop method to measure the interfacial tension of systems with low interfacial tension. The spinning drop method, initially proposed by Bernard Vonnegut in 1942, is based on the principle of mechanical equilibrium, interfacial tension, and centrifugal force. According to Vonnegut's theory, the droplet's length (L) is assumed to be much greater than its radius (R). As the angular velocity ($\omega$) increases, the droplet's radius decreases while maintaining a fixed $LR^2$ value to conserve volume. The ratio of length to diameter (L/D) greater than 2 confirms the non-spherical shape of the

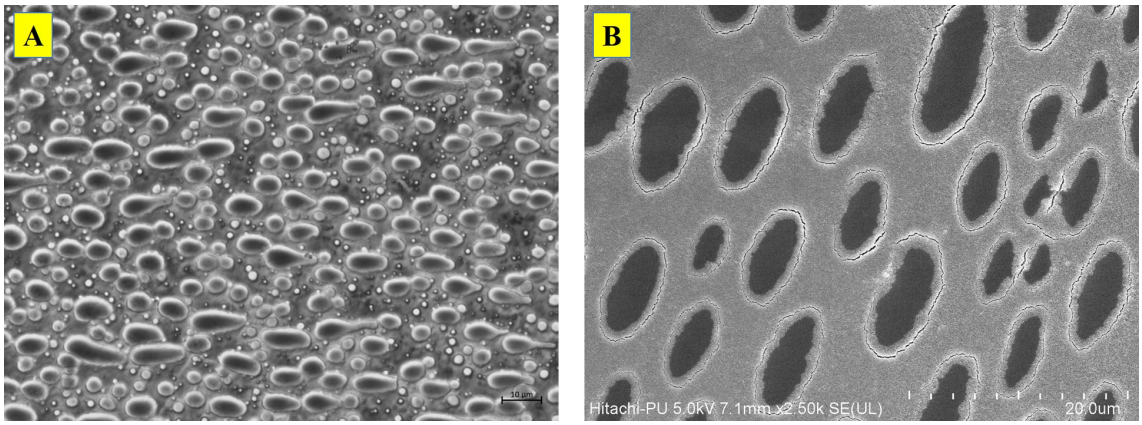


Figure 6.2: A) Microscopic; B) SEM imges showing non-spherical droplet

capsules. Several preliminary experiments were conducted using a spin coater at speeds exceeding 10,000 rpm with a solution composed of 5% dextran and 5% PEO at a desired mass ratio (M) of 4 to induce non-spherical capsule formation. Figure 6.2 A shows that the resulting capsules exhibited non-spherical shapes. Additionally, the effect of polymer concentration using a solution of 8% dextran and 2% PEO at M=4 was investigated. These results confirmed non-spherical capsule formation with L/D ratios greater than 2 $\mu$m, as shown in Figure 6.2 B. The particle concentration was maintained at 1% of the total solution throughout the experiments.

These findings demonstrate that a simple and effective approach for synthesizing non-spherical droplets could be synthesized in w/w emulsions without relying on microfluidic devices. The ability to control the shape of the capsules opens up new possibilities for their application in various fields, such as targeted drug delivery carriers and cosmetics.

### 6.2.3 Exploration for the self-propelled capsules as a catalyst for biomedical applications:

Apart from synthesizing spherical and non-spherical capsules, there has been significant interest in developing self-propelled capsules, also known as active capsules. The capsules demonstrated in Chapters 3 and 4 can be self-propelled using patchy and Janus particles. This property can be achieved by incorporating platinum-coated patchy and Janus particles, which generate bubbles for propulsion, or by using light-responsive particles as stabilizers. While there is a strong focus on sub-micron-sized and non-spherical droplets, the development of self-propelled droplets holds excellent potential for targeted drug delivery and has garnered considerable attention.

### 6.2.4 Study of the effect of pH and temperature on the stability of droplets, bijels, and emulsion-filled gels:

Examining the effects of pH and temperature on the resultant emulsion has yet to be undertaken. It will be intriguing to get insight into the change in the structures caused by changes in the pH and temperature of the medium. The results could be handy in predicting the stability of the formulation against changes in various environmental conditions like pH and temperature change.

# References


[1] Mujahid Iqbal, Yanfei Tao, Shuyu Xie, Yufei Zhu, Dongmei Chen, Xu Wang, Lingli Huang, Dapeng Peng, Adeel Sattar, Muhammad Abu Bakr Shabbir, et al. Aqueous two-phase system (atps): an overview and advances in its applications. *Biological procedures online*, 18(1):1–18, 2016.

[2] Rajni Hatti-Kaul. *Aqueous two-phase systems: methods and protocols*, volume 11. Springer Science & Business Media, 2008.

[3] Malcolm SY Tang, TJ Whitcher, KH Yeoh, CL Chua, KL Woon, PL Show, YK Lin, and TC Ling. The removal of metallic single-walled carbon nanotubes using an aqueous two-phase system. *Journal of Nanoscience and Nanotechnology*, 14(5): 3398–3402, 2014.

[4] PAJ Rosa, IF Ferreira, AM Azevedo, and MR Aires-Barros. Aqueous two-phase systems: a viable platform in the manufacturing of biopharmaceuticals. *Journal of Chromatography A*, 1217(16):2296–2305, 2010.

[5] Per-Åke Albertsson. Partition of proteins in liquid polymer–polymer two-phase systems. *Nature*, 182:709–711, 1958.

[6] Yee Koon Yau, Chien Wei Ooi, Eng-Poh Ng, John Chi-Wei Lan, Tau Chuan Ling, and Pau Loke Show. Current applications of different type of aqueous two-phase systems. *Bioresources and Bioprocessing*, 2(1):1–13, 2015.

[7] Åke Gustafsson, Håkan Wennerström, and Folke Tjerneld. The nature of phase separation in aqueous two-polymer systems. *Polymer*, 27(11):1768–1770, 1986.

[8] Youchuang Chao and Ho Cheung Shum. Emerging aqueous two-phase systems: from fundamentals of interfaces to biomedical applications. *Chemical Society Reviews*, 49 (1):114–142, 2020.

[9] Mohammed Taghi Zafarani-Moattar, Sholeh Hamzehzadeh, and Saeed Nasiri. A new aqueous biphasic system containing polypropylene glycol and a water-miscible ionic liquid. *Biotechnology Progress*, 28(1):146–156. doi: https://doi.org/10.1002/btpr.718.

[10] Juan A Asenjo and Barbara A Andrews. Aqueous two-phase systems for protein separation: phase separation and applications. *Journal of Chromatography A*, 1238: 1–10, 2012.

[11] MH Salamanca, JC Merchuk, BA Andrews, and JA Asenjo. On the kinetics of phase separation in aqueous two-phase systems. *Journal of Chromatography B: Biomedical Sciences and Applications*, 711(1-2):319–329, 1998.

[12] Jacob Israelachvili. The science and applications of emulsions—an overview. *Colloids and surfaces A: physicochemical and engineering aspects*, 91:1–8, 1994.

[13] Jérôme Bibette, F Leal Calderon, and P Poulin. Emulsions: basic principles. *Reports on Progress in Physics*, 62(6):969, 1999.

[14] Tharwat Tadros, Paqui Izquierdo, Jordi Esquena, and Conxita Solans. Formation and stability of nano-emulsions. *Advances in colloid and interface science*, 108: 303–318, 2004.

[15] W Ramsden. Separation of solids in the surface-layers of solutions and 'suspensions'(observations on surface-membranes, bubbles, emulsions, and mechanical coagulation).—preliminary account. *Proceedings of the royal Society of London*, 72(477-486):156–164, 1904.

[16] Spencer Umfreville Pickering. Cxcvi.—emulsions. *Journal of the Chemical Society, Transactions*, 91:2001–2021, 1907.

[17] Robert Aveyard, Bernard P Binks, and John H Clint. Emulsions stabilised solely by colloidal particles. *Advances in Colloid and Interface Science*, 100:503–546, 2003.

[18] Bernard P Binks and Tommy S Horozov. *Colloidal particles at liquid interfaces*. Cambridge University Press, 2006.

[19] Yves Chevalier and Marie-Alexandrine Bolzinger. Emulsions stabilized with solid nanoparticles: Pickering emulsions. *Colloids and Surfaces A: Physicochemical and Engineering Aspects*, 439:23–34, 2013.

[20] Eric Dickinson. Exploring the frontiers of colloidal behaviour where polymers and particles meet. *Food Hydrocolloids*, 52:497–509, 2016.

[21] Claire Albert, Mohamed Beladjine, Nicolas Tsapis, Elias Fattal, Florence Agnely, and Nicolas Huang. Pickering emulsions: Preparation processes, key parameters governing their properties and potential for pharmaceutical applications. *Journal of Controlled Release*, 309:302–332, 2019.

[22] Sonia Melle, Mauricio Lask, and Gerald G Fuller. Pickering emulsions with controllable stability. *Langmuir*, 21(6):2158–2162, 2005.

[23] William J Frith. Mixed biopolymer aqueous solutions–phase behaviour and rheology. *Advances in Colloid and Interface Science*, 161(1-2):48–60, 2010.

[24] Albert T Poortinga. Microcapsules from self-assembled colloidal particles using aqueous phase-separated polymer solutions. *Langmuir*, 24(5):1644–1647, 2008.

[25] Hassan Firoozmand, Brent S Murray, and Eric Dickinson. Interfacial structuring in a phase-separating mixed biopolymer solution containing colloidal particles. *Langmuir*, 25(3):1300–1305, 2009.

[26] Shizhang Yan, Joe M Regenstein, Shuang Zhang, Yuyang Huang, Baokun Qi, and Yang Li. Edible particle-stabilized water-in-water emulsions: Stabilization mechanisms, particle types, interfacial design, and practical applications. *Food Hydrocolloids*, page 108665, 2023.

[27] Jordi Esquena. Recent advances on water-in-water emulsions in segregative systems of two water-soluble polymers. *Current Opinion in Food Science*, 51:101010, 2023.

[28] Jie Wu and Guang-Hui Ma. Recent studies of pickering emulsions: particles make the difference. *Small*, 12(34):4633–4648, 2016.

[29] MW Beijerinck. Uber eine eigentumlichkeit der loslichen starke, centr-bl. *Bakteriol. Parasitenkd. Infekt. krankh*, 2:697, 1896.

[30] Otto Bütschli. *Untersuchungen über Strukturen insbesondere über Strukturen nichtzelliger Erzeugnisse des Organismus und über ihre Beziehungen zu Strukturen, welche ausserhalb des Organismus entstehen*, volume 1. W. Engelmann, 1898.

[31] MW Beijerinck. Ueber emulsionsbildung bei der vermischung wässeriger lösungen gewisser gelatinierender kolloide. *Zeitschrift für Chemie und Industrie der Kolloide*, 7:16–20, 1910.

[32] Jordi Esquena. Water-in-water (w/w) emulsions. *Current Opinion in Colloid & Interface Science*, 25:109–119, 2016.

[33] Hassan Firoozmand, Brent S Murray, and Eric Dickinson. Microstructure and rheology of phase-separated gels of gelatin+ oxidized starch. *Food Hydrocolloids*, 23(4):1081–1088, 2009.

[34] Ladislava Van den Berg, Yael Rosenberg, Martinus AJS Van Boekel, Moshe Rosenberg, and Fred Van de Velde. Microstructural features of composite whey protein/polysaccharide gels characterized at different length scales. *Food Hydrocolloids*, 23(5):1288–1298, 2009.

[35] Fabian Jansen and Jens Harting. From bijels to pickering emulsions: A lattice boltzmann study. *Physical Review E*, 83(4):046707, 2011.

[36] Gireeshkumar Balakrishnan, Taco Nicolai, Lazhar Benyahia, and Dominique Durand. Particles trapped at the droplet interface in water-in-water emulsions. *Langmuir*, 28(14):5921–5926, 2012.

[37] D Martin A Buzza, Paul DI Fletcher, Theoni K Georgiou, and Negar Ghasdian. Water-in-water emulsions based on incompatible polymers and stabilized by triblock copolymers–templated polymersomes. *Langmuir*, 29(48):14804–14814, 2013.

[38] Bach T Nguyen, Taco Nicolai, and Lazhar Benyahia. Stabilization of water-in-water emulsions by addition of protein particles. *Langmuir*, 29(34):10658–10664, 2013.

[39] Hassan Firoozmand and Dérick Rousseau. Tailoring the morphology and rheology of phase-separated biopolymer gels using microbial cells as structure modifiers. *Food Hydrocolloids*, 42:204–214, 2014.

[40] Daniel C Dewey, Christopher A Strulson, David N Cacace, Philip C Bevilacqua, and Christine D Keating. Bioreactor droplets from liposome-stabilized all-aqueous emulsions. *Nature communications*, 5(1):4670, 2014.

[41] Brent S Murray and Nataricha Phisarnchananan. The effect of nanoparticles on the phase separation of waxy corn starch+ locust bean gum or guar gum. *Food Hydrocolloids*, 42:92–99, 2014.

[42] Mark Vis, Joeri Opdam, Ingo SJ Van't Oor, Giuseppe Soligno, René Van Roij, R Hans Tromp, and Ben H Erné. Water-in-water emulsions stabilized by nanoplates. *ACS Macro Letters*, 4(9):965–968, 2015.

[43] Bach T Nguyen, Wenkai Wang, Brian R Saunders, Lazhar Benyahia, and Taco Nicolai. ph-responsive water-in-water pickering emulsions. *Langmuir*, 31(12): 3605–3611, 2015.

[44] David N Cacace, Andrew T Rowland, Joshua J Stapleton, Daniel C Dewey, and Christine D Keating. Aqueous emulsion droplets stabilized by lipid vesicles as microcompartments for biomimetic mineralization. *Langmuir*, 31(41):11329–11338, 2015.

[45] Rilton A de Freitas, Taco Nicolai, Christophe Chassenieux, and Lazhar Benyahia. Stabilization of water-in-water emulsions by polysaccharide-coated protein particles. *Langmuir*, 32(5):1227–1232, 2016.

[46] Karthik R Peddireddy, Taco Nicolai, Lazhar Benyahia, and Isabelle Capron. Stabilization of water-in-water emulsions by nanorods. *ACS Macro Letters*, 5(3): 283–286, 2016.

[47] Alberto Gonzalez Jordan, Taco Nicolai, and Lazhar Benyahia. Influence of the protein particle morphology and partitioning on the behavior of particle-stabilized water-in-water emulsions. *Langmuir*, 32(28):7189–7197, 2016.

[48] Sahar Soltani and Ashkan Madadlou. Two-step sequential cross-linking of sugar beet pectin for transforming zein nanoparticle-based pickering emulsions to emulgels. *Carbohydrate Polymers*, 136:738–743, 2016.

[49] PM Welch, MN Lee, ANG Parra-Vasquez, and CF Welch. Jammed limit of bijel structure formation. *Langmuir*, 33(45):13133–13138, 2017.

[50] Alberto Gonzalez-Jordan, Lazhar Benyahia, and Taco Nicolai. Cold gelation of water in water emulsions stabilized by protein particles. *Colloids and Surfaces A: Physicochemical and Engineering Aspects*, 532:332–341, 2017.

[51] Harry Collini, Markus Mohr, Paul Luckham, Jiawen Shan, and Andrew Russell. The effects of polymer concentration, shear rate and temperature on the gelation time of aqueous silica-poly (ethylene-oxide)"shake-gels". *Journal of colloid and interface science*, 517:1–8, 2018.

[52] Poonam Singh, Bruno Medronho, Maria G Miguel, and Jordi Esquena. On the encapsulation and viability of probiotic bacteria in edible carboxymethyl cellulose-gelatin water-in-water emulsions. *Food Hydrocolloids*, 75:41–50, 2018.

[53] Hai-Tao Liu, Hui Wang, Wen-Bo Wei, Hui Liu, Lei Jiang, and Jian-Hua Qin. A microfluidic strategy for controllable generation of water-in-water droplets as biocompatible microcarriers. *Small*, 14(36):1801095, 2018.

[54] Jianrui Zhang, Jongkook Hwang, Markus Antonietti, and Bernhard VKJ Schmidt. Water-in-water pickering emulsion stabilized by polydopamine particles and cross-linking. *Biomacromolecules*, 20(1):204–211, 2018.

[55] Alberto Gonzalez-Jordan, Taco Nicolai, and Lazhar Benyahia. Enhancement of the particle stabilization of water-in-water emulsions by modulating the phase preference of the particles. *Journal of colloid and interface science*, 530:505–510, 2018.

[56] Emna Ben Ayed, Remy Cochereau, Cyrille Dechancé, Isabelle Capron, Taco Nicolai, and Lazhar Benyahia. Water-in-water emulsion gels stabilized by cellulose nanocrystals. *Langmuir*, 34(23):6887–6893, 2018.

[57] Bernard P Binks and Hui Shi. Phase inversion of silica particle-stabilized water-in-water emulsions. *Langmuir*, 35(11):4046–4057, 2019.

[58] Marko Pavlovic, Alexander Plucinski, Lukas Zeininger, and Bernhard VKJ Schmidt. Temperature sensitive water-in-water emulsions. *Chemical Communications*, 56(50): 6814–6817, 2020.

[59] Lingsam Tea, Taco Nicolai, Lazhar Benyahia, and Frederic Renou. Viscosity and morphology of water-in-water emulsions: The effect of different biopolymer stabilizers. *Macromolecules*, 53(10):3914–3922, 2020.

[60] Hui Wang, Haitao Liu, Xu Zhang, Yaqing Wang, Mengqian Zhao, Wenwen Chen, and Jianhua Qin. One-step generation of aqueous-droplet-filled hydrogel fibers as organoid carriers using an all-in-water microfluidic system. *ACS Applied Materials & Interfaces*, 13(2):3199–3208, 2021.

[61] Neha Kulkarni and Ethayaraja Mani. Stabilization of water-in-water pickering emulsions by charged particles. *Journal of Dispersion Science and Technology*, pages 1–7, 2021.

[62] Jinglin Zhang, Lei Mei, Peihua Ma, Yuan Li, Yang Yuan, Qing-Zhu Zeng, and Qin Wang. Microgel-stabilized hydroxypropyl methylcellulose and dextran

water-in-water emulsion: Influence of ph, ionic strength, and temperature. *Langmuir*, 37(18):5617–5626, 2021.

[63] Yitong Wang, Jin Yuan, Yunpeng Zhao, Ling Wang, Luxuan Guo, Lei Feng, Jiwei Cui, Shuli Dong, Shanhong Wan, Weimin Liu, et al. Water-in-water emulsions, ultralow interfacial tension, and biolubrication. *CCS Chemistry*, 4(6):2102–2114, 2022.

[64] Yitong Wang, Jin Yuan, Shuli Dong, and Jingcheng Hao. Multilayer-stabilized water-in-water emulsions. *Langmuir*, 38(15):4713–4721, 2022.

[65] Noëmie Coudon, Laurence Navailles, Frédéric Nallet, Isabelle Ly, Ahmed Bentaleb, Jean-Paul Chapel, Laure Beven, Jean-Paul Douliez, and Nicolas Martin. Stabilization of all-aqueous droplets by interfacial self-assembly of fatty acids bilayers. *Journal of Colloid and Interface Science*, 617:257–266, 2022.

[66] João PE Machado, Isabelle Capron, Rilton A de Freitas, Lazhar Benyahia, and Taco Nicolai. Stabilization of amylopectin-pullulan water in water emulsions by interacting protein particles. *Food Hydrocolloids*, 124:107320, 2022.

[67] Théo Merland, Léa Waldmann, Oksana Guignard, Marie-Charlotte Tatry, Anne-Laure Wirotius, Véronique Lapeyre, Patrick Garrigue, Taco Nicolai, Lazhar Benyahia, and Valérie Ravaine. Thermo-induced inversion of water-in-water emulsion stability by bis-hydrophilic microgels. *Journal of Colloid and Interface Science*, 608:1191–1201, 2022.

[68] Alexander Plucinski and Bernhard VKJ Schmidt. ph sensitive water-in-water emulsions based on the pullulan and poly (n, n-dimethylacrylamide) aqueous two-phase system. *Polymer Chemistry*, 13(28):4170–4177, 2022.

[69] Xiaoli Qian, Guangni Peng, Lingling Ge, and Defeng Wu. Water-in-water pickering emulsions stabilized by the starch nanocrystals with various surface modifications. *Journal of Colloid and Interface Science*, 607:1613–1624, 2022.

[70] Chan Lei, Yunxiao Xie, Yilan Wu, Yan Li, Bin Li, Ying Pei, and Shilin Liu. Properties and stability of water-in-water emulsions stabilized by microfibrillated bacterial cellulose. *Food Hydrocolloids*, 130:107698, 2022.

[71] Wanying Cui, Chunmiao Xia, Sheng Xu, Xinke Ye, Yihao Wu, Shukai Cheng, Rongli Zhang, Cuige Zhang, and Zongcheng Miao. Water-in-water emulsions stabilized by self-assembled chitosan colloidal particles. *Carbohydrate Polymers*, 303:120466, 2023.

[72] Chaoyi Zhou, Yunxiao Xie, Yan Li, Bin Li, Yangyang Zhang, and Shilin Liu. Water-in-water emulsion stabilized by cellulose nanocrystals and their high enrichment effect on probiotic bacteria. *Journal of Colloid and Interface Science*, 633:254–264, 2023.

[73] Kwan-Mo You, Brent S Murray, and Anwesha Sarkar. Tribology and rheology of water-in-water emulsions stabilized by whey protein microgels. *Food Hydrocolloids*, 134:108009, 2023.

[74] Maria Moutkane, Lazhar Benyahia, and Taco Nicolai. Stable protein microcapsules by crosslinking protein particles in water in water emulsions. *Colloids and Surfaces A: Physicochemical and Engineering Aspects*, 656:130353, 2023.

[75] Iwona Ziemecka, Volkert Van Steijn, Ger JM Koper, Michiel T Kreutzer, and Jan H Van Esch. All-aqueous core-shell droplets produced in a microfluidic device. *Soft Matter*, 7(21):9878–9880, 2011.

[76] Alban Sauret and Ho Cheung Shum. Forced generation of simple and double emulsions in all-aqueous systems. *Applied Physics Letters*, 100(15):154106, 2012.

[77] Yang Song and Ho Cheung Shum. Monodisperse w/w/w double emulsion induced by phase separation. *Langmuir*, 28(33):12054–12059, 2012.

[78] Serhii Mytnyk, Iwona Ziemecka, Alexandre GL Olive, J Wim M van der Meer, Kartik A Totlani, Sander Oldenhof, Michiel T Kreutzer, Volkert van Steijn, and Jan H van Esch. Microcapsules with a permeable hydrogel shell and an aqueous core continuously produced in a 3d microdevice by all-aqueous microfluidics. *RSC advances*, 7(19):11331–11337, 2017.

[79] Sarah D Hann, Kathleen J Stebe, and Daeyeon Lee. Awe-somes: All water emulsion bodies with permeable shells and selective compartments. *ACS applied materials & interfaces*, 9(29):25023–25028, 2017.

[80] Chen Cui, Changfeng Zeng, Chongqing Wang, and Lixiong Zhang. Complex emulsions by extracting water from homogeneous solutions comprised of aqueous three-phase systems. *Langmuir*, 33(44):12670–12680, 2017.

[81] Morteza Jeyhani, Risavarshni Thevakumaran, Niki Abbasi, Dae Kun Hwang, and Scott SH Tsai. Microfluidic generation of all-aqueous double and triple emulsions. *Small*, 16(7):1906565, 2020.

[82] W. Ramsden. Separation of solids in the surface-layers of solutions and suspensions. *Proc. R. Soc. London*, 72:156–164, 1903.

[83] Spencer Umfreville Pickering. Emulsions. *J. Chem. Soc. Trans.*, 91:2001–2021, 1907.

[84] AD Dinsmore, Ming F Hsu, MG Nikolaides, Manuel Marquez, AR Bausch, and DA Weitz. Colloidosomes: selectively permeable capsules composed of colloidal particles. *Science*, 298(5595):1006–1009, 2002.

[85] Kevin Stratford, Ronojoy Adhikari, Ignacio Pagonabarraga, J-C Desplat, and Michael E Cates. Colloidal jamming at interfaces: A route to fluid-bicontinuous gels. *Science*, 309(5744):2198–2201, 2005.

[86] Dongyu Cai and Paul S Clegg. Stabilizing bijels using a mixture of fumed silica nanoparticles. *Chemical Communications*, 51(95):16984–16987, 2015.

[87] Dongyu Cai, Paul S Clegg, Tao Li, Katherine A Rumble, and Joe W Tavacoli. Bijels formed by direct mixing. *Soft matter*, 13(28):4824–4829, 2017.

[88] Martin F Haase, Kathleen J Stebe, and Daeyeon Lee. Continuous fabrication of hierarchical and asymmetric bijel microparticles, fibers, and membranes by solvent transfer-induced phase separation (strips). *Advanced Materials*, 27(44):7065–7071, 2015.

[89] Anju Toor, Tao Feng, and Thomas P Russell. Self-assembly of nanomaterials at fluid interfaces. *The European Physical Journal E*, 39(5):57, 2016.

[90] Joe Forth and Paul S Clegg. Using a molecular stopwatch to study particle uptake in pickering emulsions. *Langmuir*, 32(25):6387–6397, 2016.

[91] Caili Huang, Joe Forth, Weiyu Wang, Kunlun Hong, Gregory S Smith, Brett A Helms, and Thomas P Russell. Bicontinuous structured liquids with sub-micrometre domains using nanoparticle surfactants. *Nature nanotechnology*, 12(11):1060–1063, 2017.

[92] Mengmeng Cui, Todd Emrick, and Thomas P Russell. Stabilizing liquid drops in nonequilibrium shapes by the interfacial jamming of nanoparticles. *Science*, 342 (6157):460–463, 2013.

[93] Eva M Herzig, Kathryn A White, Andrew B Schofield, Wilson CK Poon, and Paul S Clegg. Bicontinuous emulsions stabilized solely by colloidal particles. *Nature materials*, 6(12):966–971, 2007.

[94] Eunhye Kim, Kevin Stratford, and Michael E Cates. Bijels containing magnetic particles: A simulation study. *Langmuir*, 26(11):7928–7936, 2010.

[95] Katherine A Macmillan, John R Royer, Alexander Morozov, Yogesh M Joshi, Michel Cloitre, and Paul S Clegg. Rheological behavior and in situ confocal imaging of bijels made by mixing. *Langmuir*, 35(33):10927–10936, 2019.

[96] Matthew Reeves, Kevin Stratford, and Job HJ Thijssen. Quantitative morphological characterization of bicontinuous pickering emulsions via interfacial curvatures. *Soft Matter*, 12(18):4082–4092, 2016.

[97] Alan Gabelman and Sun-Tak Hwang. Hollow fiber membrane contactors. *Journal of Membrane Science*, 159(1-2):61–106, 1999.

[98] Michael E Cates and Paul S Clegg. Bijels: a new class of soft materials. *Soft Matter*, 4(11):2132–2138, 2008.

[99] Junzhi Li, Haoran Sun, and Min Wang. Phase inversion-based technique for fabricating bijels and bijels-derived structures with tunable microstructures. *Langmuir*, 36(48):14644–14655, 2020.

[100] Matthew N Lee, Job HJ Thijssen, Jessica A Witt, Paul S Clegg, and Ali Mohraz. Making a robust interfacial scaffold: bijel rheology and its link to processability. *Advanced Functional Materials*, 23(4):417–423, 2013.

[101] Matthew N Lee and Ali Mohraz. Bicontinuous macroporous materials from bijel templates. *Advanced Materials*, 22(43):4836–4841, 2010.

[102] JA Witt, DR Mumm, and A Mohraz. Microstructural tunability of co-continuous bijel-derived electrodes to provide high energy and power densities. *Journal of Materials Chemistry A*, 4(3):1000–1007, 2016.

[103] M Koroleva, D Bidanov, and E Yurtov. Emulsions stabilized with mixed sio2 and fe3o4 nanoparticles: mechanisms of stabilization and long-term stability. *Physical Chemistry Chemical Physics*, 21(3):1536–1545, 2019.

[104] Trivikram Nallamilli, Srikanth Ragothaman, and Madivala G Basavaraj. Self assembly of oppositely charged latex particles at oil-water interface. *Journal of colloid and interface science*, 486:325–336, 2017.

[105] Niek Hijnen, Dongyu Cai, and Paul S Clegg. Bijels stabilized using rod-like particles. *Soft Matter*, 11(22):4351–4355, 2015.

[106] Brandy Kinkead, Rachel Malone, Geena Smith, Aseem Pandey, and Milana Trifkovic. Bicontinuous intraphase jammed emulsion gels: A new soft material enabling direct isolation of co-continuous hierarchial porous materials. *Chemistry of Materials*, 31(18):7601–7607, 2019.

[107] Stefan Frijters, Florian Günther, and Jens Harting. Domain and droplet sizes in emulsions stabilized by colloidal particles. *Physical Review E*, 90(4):042307, 2014.

[108] Ya-Yu Huang and Kan-Sen Chou. Studies on the spin coating process of silica films. *Ceramics international*, 29(5):485–493, 2003.

[109] Alicia Maestro, José M Gutiérrez, Esther Santamaría, and Carmen González. Rheology of water-in-water emulsions: Caseinate-pectin and caseinate-alginate systems. *Carbohydrate Polymers*, 249:116799, 2020.

[110] AT Florence and D Whitehill. Some features of breakdown in water-in-oil-in-water multiple emulsions. *Journal of Colloid and Interface Science*, 79(1):243–256, 1981.

[111] Rajni Hatti-Kaul. Aqueous two-phase systems. *Molecular biotechnology*, 19(3): 269–277, 2001.

[112] Chandra Shekhar, Abhimanyu Kiran, Vishwajeet Mehandia, Venkateshwar Rao Dugyala, and Manigandan Sabapathy. Droplet–bijel–droplet transition in aqueous two-phase systems stabilized by oppositely charged nanoparticles: A simple pathway to fabricate bijels. *Langmuir*, 37(23):7055–7066, 2021.

[113] Guido Sala, George A Van Aken, Martien A Cohen Stuart, and Fred Van De Velde. Effect of droplet–matrix interactions on large deformation properties of emulsion-filled gels. *Journal of Texture Studies*, 38(4):511–535, 2007.

[114] Ivana M Geremias-Andrade, Nayla PBG Souki, Izabel CF Moraes, and Samantha C Pinho. Rheology of emulsion-filled gels applied to the development of food materials. *Gels*, 2(3):22, 2016.

[115] Laura Oliver, Elke Scholten, and George A van Aken. Effect of fat hardness on large deformation rheology of emulsion-filled gels. *Food Hydrocolloids*, 43:299–310, 2015.

[116] Gabriel Lorenzo, Noemí Zaritzky, and Alicia Califano. Rheological analysis of emulsion-filled gels based on high acyl gellan gum. *Food Hydrocolloids*, 30(2): 672–680, 2013.

[117] Guido Sala, Fred van de Velde, Martien A Cohen Stuart, and George A van Aken. Oil droplet release from emulsion-filled gels in relation to sensory perception. *Food hydrocolloids*, 21(5-6):977–985, 2007.

[118] Laura Oliver, Lieke Berndsen, George A van Aken, and Elke Scholten. Influence of droplet clustering on the rheological properties of emulsion-filled gels. *Food Hydrocolloids*, 50:74–83, 2015.

[119] B Cabane, K Wong, P Lindner, and F Lafuma. Shear induced gelation of colloidal dispersions. *Journal of Rheology*, 41(3):531–547, 1997.

[120] M Mar Ramos-Tejada and Paul F Luckham. Shaken but not stirred: The formation of reversible particle–polymer gels under shear. *Colloids and Surfaces A: Physicochemical and Engineering Aspects*, 471:164–169, 2015.

[121] Masashi Kamibayashi, Hironao Ogura, and Yasufumi Otsubo. Shear-thickening flow of nanoparticle suspensions flocculated by polymer bridging. *Journal of colloid and interface science*, 321(2):294–301, 2008.

[122] George A. van Aken, Monique H. Vingerhoeds, and René A. de Wijk. Textural perception of liquid emulsions: Role of oil content, oil viscosity and emulsion viscosity. *Food Hydrocolloids*, 25(4):789–796, 2011. ISSN 0268-005X. doi: https://doi.org/10.1016/j.foodhyd.2010.09.015.

[123] George A. van Aken, Laura Oliver, and Elke Scholten. Rheological effect of particle clustering in gelled dispersions. *Food Hydrocolloids*, 48:102–109, 2015. ISSN 0268-005X. doi: https://doi.org/10.1016/j.foodhyd.2015.02.001.

[124] Eric Dickinson. Emulsion gels: The structuring of soft solids with protein-stabilized oil droplets. *Food hydrocolloids*, 28(1):224–241, 2012.

[125] Leonard MC Sagis. Dynamics of encapsulation and controlled release systems based on water-in-water emulsions: negligible surface rheology. *The Journal of Physical Chemistry B*, 112(43):13503–13508, 2008.

[126] Leonard MC Sagis. Dynamics of controlled release systems based on water-in-water emulsions: a general theory. *Journal of controlled release*, 131(1):5–13, 2008.

[127] Florence Dumas, Jean-Pierre Benoit, Patrick Saulnier, and Emilie Roger. A new method to prepare microparticles based on an aqueous two-phase system (atps), without organic solvents. *Journal of Colloid and Interface Science*, 599:642–649, 2021.

[128] Jianshe Chen and Eric Dickinson. Effect of surface character of filler particles on rheology of heat-set whey protein emulsion gels. *Colloids and Surfaces B: Biointerfaces*, 12(3-6):373–381, 1999.

[129] Irvin M Krieger. A dimensional approach to colloid rheology. *Transactions of the Society of Rheology*, 7(1):101–109, 1963.

[130] Donald H Napper. Steric stabilization. *Journal of colloid and interface science*, 58 (2):390–407, 1977.

[131] SF Liu, F Lafuma, and R Audebert. Rheological behavior of moderately concentrated silica suspensions in the presence of adsorbed poly (ethylene oxide). *Colloid and Polymer Science*, 272(2):196–203, 1994.

[132] Yu Saito, Yuji Hirose, and Yasufumi Otsubo. Effect of poly (ethylene oxide) on the rheological behavior of silica suspensions. *Rheologica acta*, 50(3):291–301, 2011.

[133] Huabin Liu and Hanning Xiao. Adsorption of poly (ethylene oxide) with different molecular weights on the surface of silica nanoparticles and the suspension stability. *Materials Letters*, 62(6-7):870–873, 2008.

[134] Manigandan Sabapathy, Sam David Christdoss Pushpam, Madivala G Basavaraj, and Ethayaraja Mani. Synthesis of single and multipatch particles by dip-coating method and self-assembly thereof. *Langmuir*, 31(4):1255–1261, 2015.

[135] Manigandan Sabapathy, Viswas Kollabattula, Madivala G Basavaraj, and Ethayaraja Mani. Visualization of the equilibrium position of colloidal particles at fluid–water interfaces by deposition of nanoparticles. *Nanoscale*, 7(33):13868–13876, 2015.

[136] Manigandan Sabapathy, Khalid Zubair Md, Hemant Kumar, Sashikumar Ramamirtham, Ethayaraja Mani, and Madivala G Basavaraj. Exploiting

heteroaggregation to quantify the contact angle of charged colloids at interfaces. *Langmuir*, 38(24):7433–7441, 2022.

[137] Maher Damak, Md Nasim Hyder, and Kripa K Varanasi. Enhancing droplet deposition through in-situ precipitation. *Nature Communications*, 7(1):12560, 2016.

[138] Salman Akram, Xinyue Wang, Thierry F Vandamme, Mayeul Collot, Asad Ur Rehman, Nadia Messaddeq, Yves Mély, and Nicolas Anton. Toward the formulation of stable micro and nano double emulsions through a silica coating on internal water droplets. *Langmuir*, 35(6):2313–2325, 2019.

[139] Behnam Khadem, Maya Khellaf, and Nida Sheibat-Othman. Investigating swelling-breakdown in double emulsions. *Colloids and Surfaces A: Physicochemical and Engineering Aspects*, 585:124181, 2020.

[140] Howard A Stone, Abraham D Stroock, and Armand Ajdari. Engineering flows in small devices: microfluidics toward a lab-on-a-chip. *Annu. Rev. Fluid Mech.*, 36: 381–411, 2004.

[141] Todd M Squires and Stephen R Quake. Microfluidics: Fluid physics at the nanoliter scale. *Reviews of modern physics*, 77(3):977, 2005.

[142] Osman A Basaran. Small-scale free surface flows with breakup: Drop formation and emerging applications. *American Institute of Chemical Engineers. AIChE Journal*, 48(9):1842, 2002.

[143] Axel Günther and Klavs F Jensen. Multiphase microfluidics: from flow characteristics to chemical and materials synthesis. *Lab on a Chip*, 6(12):1487–1503, 2006.

[144] Gerald Muschiolik. Multiple emulsions for food use. *Current Opinion in Colloid & Interface Science*, 12(4-5):213–220, 2007.

[145] Eric Dickinson. Double emulsions stabilized by food biopolymers. *Food Biophysics*, 6(1):1–11, 2011.

[146] María Matos, Gemma Gutiérrez, Lemuel Martínez-Rey, Olvido Iglesias, and Carmen Pazos. Encapsulation of resveratrol using food-grade concentrated double emulsions: Emulsion characterization and rheological behaviour. *Journal of Food Engineering*, 226:73–81, 2018.

[147] Junwei Wang, Simon Hahn, Esther Amstad, and Nicolas Vogel. Tailored double emulsions made simple. *Advanced Materials*, 34(5):2107338, 2022.

[148] Jie Yang, Zhengbiao Gu, Li Cheng, Zhaofeng Li, Caiming Li, Xiaofeng Ban, and Yan Hong. Preparation and stability mechanisms of double emulsions stabilized by gelatinized native starch. *Carbohydrate Polymers*, 262:117926, 2021.

[149] Ankit Kumar, Ramandeep Kaur, Vikas Kumar, Satish Kumar, Rakesh Gehlot, and Poonam Aggarwal. New insights into water-in-oil-in-water (w/o/w) double emulsions: Properties, fabrication, instability mechanism, and food applications. *Trends in Food Science & Technology*, 128:22–37, 2022.

[150] Qiushui Chen, Stefanie Utech, Dong Chen, Radivoje Prodanovic, Jin-Ming Lin, and David A Weitz. Controlled assembly of heterotypic cells in a core–shell scaffold: organ in a droplet. *Lab on a Chip*, 16(8):1346–1349, 2016.

[151] Andrew S Utada, Elise Lorenceau, Darren R Link, Peter D Kaplan, Howard A Stone, and DA Weitz. Monodisperse double emulsions generated from a microcapillary device. *Science*, 308(5721):537–541, 2005.

[152] Gang Liu, X Miao, Wei Fan, Ross Crawford, and Yin Xiao. Porous plga microspheres effectively loaded with bsa protein by electrospraying combined with phase separation in liquid nitrogen. In *Journal of Biomimetics, Biomaterials and Tissue Engineering*, volume 6, pages 1–18. Trans Tech Publ, 2010.

[153] Subeen Kim, KyuHan Kim, and Siyoung Q Choi. Controllable one-step double emulsion formation via phase inversion. *Soft Matter*, 14(7):1094–1099, 2018.

[154] Yang Song, Alban Sauret, and Ho Cheung Shum. All-aqueous multiphase microfluidics. *Biomicrofluidics*, 7(6), 2013.

[155] Eric Dickinson. Particle-based stabilization of water-in-water emulsions containing mixed biopolymers. *Trends in food science & technology*, 83:31–40, 2019.

[156] Taco Nicolai and Brent Murray. Particle stabilized water in water emulsions. *Food Hydrocolloids*, 68:157–163, 2017.

[157] Alfonso M Gañán-Calvo. Generation of steady liquid microthreads and micron-sized monodisperse sprays in gas streams. *Physical review letters*, 80(2):285, 1998.

[158] Alfonso M Ganán-Calvo and José M Gordillo. Perfectly monodisperse microbubbling by capillary flow focusing. *Physical review letters*, 87(27):274501, 2001.

[159] Alfonso Gañán-Calvo. Device and method for creating aerosols for drug delivery, 2003. US Patent 6, 595, 202.

[160] Lucía Martín-Banderas, María Flores-Mosquera, Pascual Riesco-Chueca, Alfonso Rodríguez-Gil, Ángel Cebolla, Sebastián Chávez, and Alfonso M Gañán-Calvo. Flow focusing: a versatile technology to produce size-controlled and specific-morphology microparticles. *Small*, 1(7):688–692, 2005.

[161] IT Norton and WJ Frith. Microstructure design in mixed biopolymer composites. *Food hydrocolloids*, 15(4-6):543–553, 2001.

[162] Yoshimune Nonomura, Naoto Kobayashi, and Naoki Nakagawa. Multiple pickering emulsions stabilized by microbowls. *Langmuir*, 27(8):4557–4562, 2011.

[163] BP Binks and JA Rodrigues. Types of phase inversion of silica particle stabilized emulsions containing triglyceride oil. *Langmuir*, 19(12):4905–4912, 2003.

[164] Madhvi Tiwari, Madivala G Basavaraj, and Venkateshwar Rao Dugyala. Tailoring pickering double emulsions by in situ particle surface modification. *Langmuir*, 39 (8):2911–2921, 2023.

[165] Faezeh Sabri, Wendell Raphael, Kevin Berthomier, Louis Fradette, Jason R Tavares, and Nick Virgilio. One-step processing of highly viscous multiple pickering emulsions. *Journal of colloid and interface science*, 560:536–545, 2020.

[166] Yongqiang He, Fei Wu, Xiying Sun, Ruqiang Li, Yongqin Guo, Chuanbao Li, Lu Zhang, Fubao Xing, Wei Wang, and Jianping Gao. Factors that affect pickering emulsions stabilized by graphene oxide. *ACS applied materials & interfaces*, 5(11): 4843–4855, 2013.

[167] Fatemeh Shahaliyan, Alireza Safahieh, and Hajar Abyar. Evaluation of emulsification index in marine bacteria pseudomonas sp. and bacillus sp. *Arabian Journal for Science and Engineering*, 40:1849–1854, 2015.

# Chapter A

# ABBREVIATIONS

**ATPS** Aqueous Two- Phase System
**W/W emusion** Water-in-Water emulsion
**O/W emulsion** Oil-in-Water emulsion
**W/O emulsion** Water-in-Oil emulsion
**W/W/W emulsion** Water-in-Water-Water emulsion
**CI** Creaming Index
**SEM** Scanning Electron Microscopy
**HRTEM** High Resolution Transmission Electron Microscopy
**DLS** Dynamic Light Scattering